Synthesis of Derivatives of D-ManAcA:

Aminosugar Component of *S. aureus* Capsular Polysaccharides

By

Yuriko Y. Root

Submitted in Partial Fulfillment of the Requirements

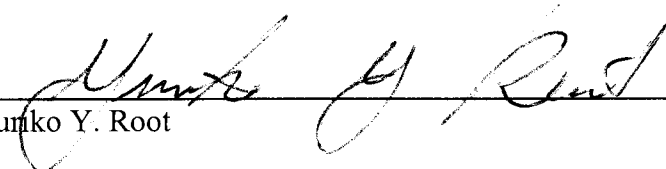for the Degree of

Master of Science

in the Chemistry Program

YOUNGSTOWN STATE UNIVERSITY

May, 2003

Synthesis of Derivatives of D-ManAcA: Aminosugar component of
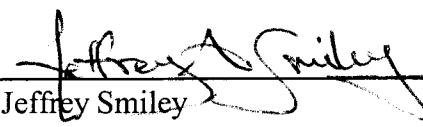# *S. aureus* Capsular Polysaccharides

Yuriko Y. Root

I hereby release this to the public. I understand that this thesis will be made available from the OhioLINK ETD Center and the Maag Library Circulation Desk for public access. I also authorize the University or other individuals to make copies of this thesis as needed for scholarly research.

Signature: _____

Yuriko Y. Root

Approvals:

_____ 4/30/03

Dr. Peter Norris   Date
Thesis Advisor

_____ 4/30/03

Dr. John Jackson   Date
Committee Member

_____ 4/30/03

Dr. Jeffrey Smiley   Date
Committee Member

_____ 5/1/03

Dr. Peter J. Kasvinsky   Date
Dean of Graduate Studies

Thesis Abstract

Convenient methods for the synthesis of amino sugar analogs of *N*-acetyl-2-amino-2-deoxy-D-mannopyranose uronic acid (D-ManAcA) were studied. The parallel synthesis method provided an advantage to the approach of multiple compound synthesis of glycomimetic analogs such as glycosyltriazoles and anomeric glycosyl amides. The starting materials, acyl-protected β-glycosyl azide compounds, were readily prepared *via* S_N2; the substitution of a glycosyl bromide with N_3. The synthesis involves 1,3-dipolar cycloadditions of azides with alkynes, which provided a variety of heterocycles, as well as the Staudinger reaction to produce phosphinimine ylides to generate a desired amide compound using a solid-phase support. According to the results obtained from the above, several cycloaddition reactions provided high yields of compounds. From the Staudinger reactions, high yields of product with several acid chlorides were obtained.

Acknowledgements

I would like to thank the YSU Department of Chemistry and the School of Graduate Studies for allowing me to pursue my MS degree, as well as Dr. John Jackson and Dr. Jeffrey Smiley for being members of my thesis committee and giving me the time and advice when I needed them. I would like to thank to Penny Miner and Bruce Levinson for getting my Mass spectral data.

Thanks to all the people in the Norris Research Group for making a long day of work in lab much more fun. I would like to thank especially Joe Lisko and Chris Meta for giving me all the help I needed at the beginning of my MS degree.

Most of my gratitude goes to Dr. Peter Norris for giving me a chance to grow as a chemist and also as an individual. I also want to thank him for always believing in me. I can't thank him enough for all of the help and things that you have done for me. You have given me not only the knowledge that I need as a chemist but also your caring support when I was in need. What I am now is largely because of you and I will always be grateful for that.

Table of Contents

1.   Synthesis of precursor compounds for D-ManNAcA glycomimetics

2.   Synthesis of glycosyl azides from D-glucopyranuronate and D-glucose

3.   1,3-Dipolar cycloadditions of glycosyl azides

4.   Conversion of glycosyl azides into amides

5.   Attempt for the synthesis of D-ManAcA amide derivative **42**

        General Procedures

List of Tables

List of Figures

Introduction

Staphylococci are spherical Gram-positive bacteria that are commonly known to live on the skin and mucous membranes of humans. Many of these bacteria are harmless to the human body due to our host defenses and they are distinguished as opportunistic pathogens. Among these bacteria, Staphylococcus aureus (S. aureus) is known to be a significant bacterium found in human infections. S. aureus is a major cause of nosocomial and community-acquired infections. It has ranked as the number one cause of the hospital-borne infections in the United States each year.[1] They are responsible for food poisoning as well as life-threatening diseases, blood stream infections (BSI) and septic shock. According to the SCOPE Surveillance Program, it is the most common etiologic agent to cause nosocomial blood stream infection in the U.S.[2] The incidence of fatal cases among children due to S. aureus infection have been also reported in the U.S.[3,4] S. aureus infections are growing to be a serious global concern; in 1997, the sentry antimicrobial surveillance program showed that S.aureus was again the most significant species isolated from skin and soft tissue infections occuring in European hospitals.[5] The study conducted by Elbashier, et al. showed that not only was S. aureus the most isolated organism in hospitals, they were also the most common microbe among Gram-positive cocci.[6] The results of studies clearly demonstrate how microbe infections can be fatal to humans and they are a major threat to the welfare of people worldwide.

Many forms of bacteria are adapting and changing their genetic makeup to resist the currently available antibiotics. The World Health Organization estimated that approximately 50,000 people die each day throughout the world from infectious diseases.[7] Antibiotic resistance in pathogenic bacteria is a serious problem in the

treatment of patients infected with such bacteria. This has been an ongoing concern for many decades for medical providers.

The discovery of penicillin in the 1940's was a major event in the history of medicine, but today about 90% of *S. aureus* isolates are resistant to penicillin.[8] Penicillin, oxacillin, and amoxicillin are all known as beta-lactam antibiotics and exert similar effects on the microbial organisms. The most important activity of beta-lactam antibiotics is the inhibition of the peptidoglycan synthesis, especially the Gram-positive organisms (due to the lack of an outer membrane). This peptidoglycan layer provides the shape of cell walls and it counteracts the effects of osmotic pressure to prevent the wall from rupturing, which results in autolysis. Therefore, to maintain a rigid cell wall structure is essential for bacteria to survive. Despite the effects of these antibiotics, they are no longer effective against some bacterial infections due to the specific defense mechanisms evolved by bacteria. Because of the emergence of beta-lactam resistant organisms, the development of antimicrobial agents that will inhibit the cell wall formation has been emphasized. The most effective antibiotic against *S. aureus* infections (vancomycin) was introduced in 1958 but the first vancomycin-resistant *S. aureus* isolates were detected in 1987.[9]

S. aureus organisms cause a diverse spectrum of infectious diseases found in hospitals and communities. The serotype 5 and 8 are the most common virulent factors among *S. aureus* strains. These bacteria possess the protecting coat called "capsule" or capsular polysaccharide (CP), and this capsule provides *S. aureus* excellent protection against lymphocytes. Very little is known about the biosynthesis of the CP, but the interruption of the capsule formation is one approach that can be taken to cripple this

bacterium. This capsule is made up of repeating units (Figure 1) of three monomer amino sugars: *N*-acetyl-2-amino-2-deoxy-D-mannopyranose uronic acid (D-ManAcA), *N*-acetyl-2-amino-2-deoxy-D-fucopyranose (D-FucNAc), and *N*-acetyl-2-amino-2-deoxy-L-fucopyranose (L-FucNAc) (Figure 2).

Serotype 5   Serotype 8
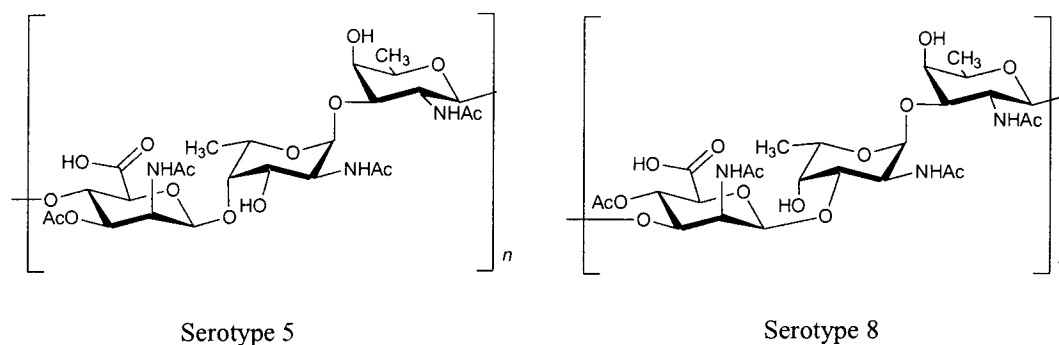
Figure 1: The repeating amino sugar units of the *S. aureus* capsular polysaccharides.

D-ManAcA   D-FucNAc   L-FucNAc
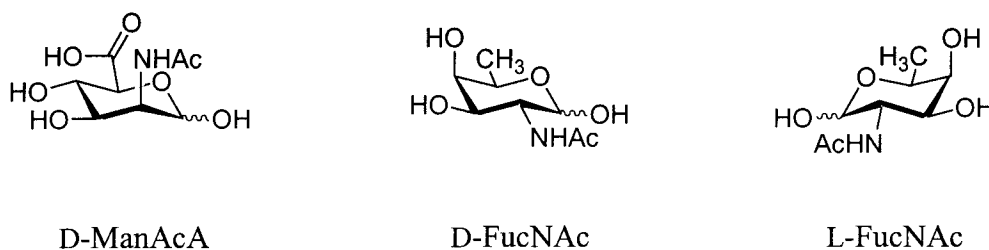
Figure 2: Amino sugar components of the *S. aureus* CP.

The biosynthesis of the capsular polysaccharide (CP) depends on a series of highly specific enzymes. The investigation of these enzymes at the molecular level becomes an important approach for the inhibition of CP formation. Studies on several pathogenic strains have revealed that the enzymes D-GlcNAc epimerase and D-ManAc dehydrogenase mediate the construction of the D-ManNAcA portion of the CP. The

epimerase is known to be involved in the synthesis of a precursor compound, which is then presumably linked with an accepting sugar by a glycosyl transferase *via* a glycosidic bond. Pathogenic strains such as *E. coli* reveal that the UDP-GlcNAc 2-epimerase is involved in an initial *anti*-elimination of UDP to generate the intermediate glucal, followed by a *syn*-addition of UDP to give the product UDP-ManNAc (Scheme 1).[10]
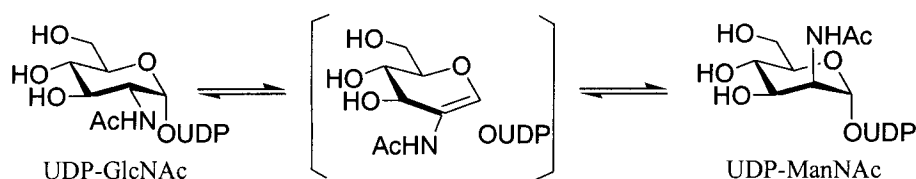
Scheme 1: Epimerization of UDP-GlcNAc to UDP-ManNAc.

UDP-ManNAc is then oxidized by a UDP-dehydrogenase to give UDP-D-ManAcA. With the aid of a transferase, this must then be linked with another amino sugar as part of the biosynthesis of CP (Scheme 2).[11]
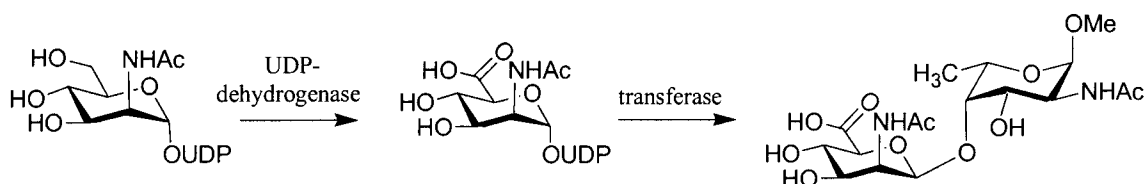
Scheme 2: Glycosyl linkage catalyzed by the transferase.

Since every enzyme catalyzes a specific modification of substrates, the synthesis of glycomimetics that are similar to those compounds found in Nature will have significant potential for inhibition at multiple stages of a CP biosynthetic pathway.

Glycomimetics can either compete for the receptor (the binding site) with the natural substrates or resemble the structures formed in an intermediate or transition state of an enzyme-catalyzed reaction. For example, a mimetic resembling the shape of the enzyme's active site, and which has appropriately positioned chemical groups, could bind to the enzyme and inhibit the biological process, i.e. a competitive inhibition. Another mimetic could also be a replacement sugar that is attached to the UDP complex and which inhibits the formation of glycosidic bond during the transition state.

One of the approaches made to synthesize potential compounds for antimicrobial agents is in iminosugars, also known as azasugars. Iminosugars, in which a nitrogen atom is in place of the ring oxygen of the cyclic form of a carbohydrate are known to inhibit glycosidases, enzymes that catalyze the hydrolysis of glycosidic bonds in oligo- and polysaccharides.[12] Such interference could block the expression or alter the structure of CP. Through extensive studies on the mechanistic transition states of reactions, many inhibitor analogs, such as iminocyclitols have been developed.[13] The derivatives of iminocyclitol can be synthesized with the use of aldolase followed by hydrogenation of azido-sugars (Figure 3).[14] This cyclic imine sugar may mimic the reducing sugar in the transition state in the glycosyltransfer reaction and inhibit transfer to an acceptor sugar (e.g. Figure 4).[15]
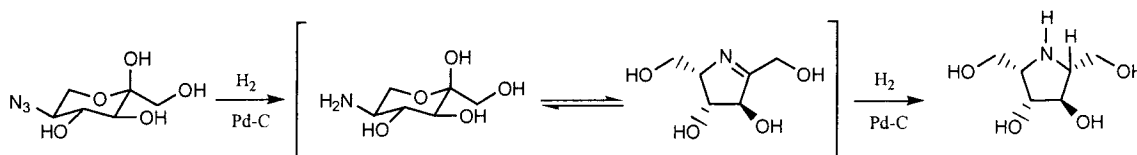
Figure 3: The hydrogenation of an azido-sugar to an iminocyclitol.
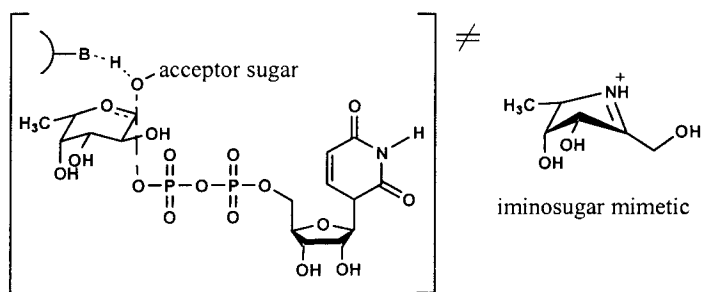
Figure 4: Transition state of transferase reaction and a possible mimetic.

Biosynthesis of disaccharides involves the transfer of a glycosyl group from, for example, a UDP-sugar complex to a hydroxy group of a monosaccharide. Different types of glycosidic bonds can be formed when replacing the anomeric hydroxyl with other atoms, such as O, N, C, or S atoms. The O-glycosides are found to be abundant in Nature compared to other types of glycosides. Many researchers have approached challenging synthesis, to construct the anomeric glycosidic bonds.
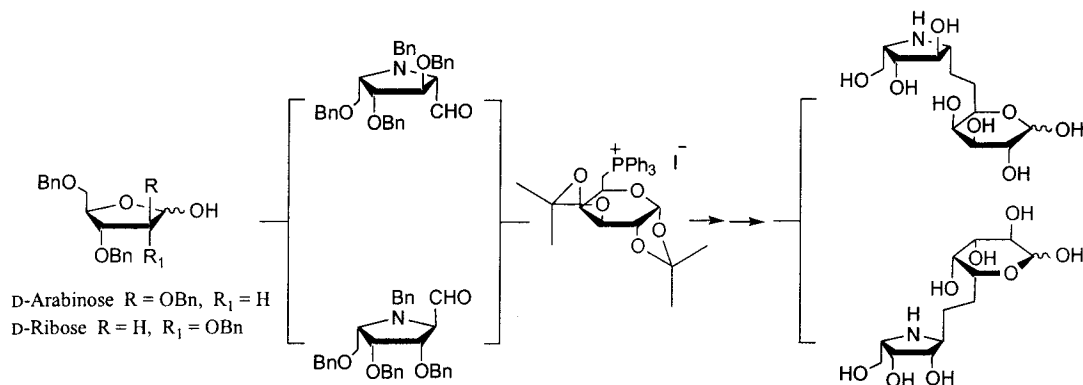
Scheme 3: Wittig-based synthesis of (1-6)- and (1-5)-linked C-disaccharides.

The synthesis of C-glycosides containing an azasugar (aza-C-disaccharides) is a new approach for novel antibacterials. Dondoni et al.[16] have introduced the formation of

(1-6)- and (1-5)-aza-*C*-disaccharides from D-arabinose and D-ribose. The first step involves the formation of aldehydes to react with ylide compounds *via* a Wittig reaction to give the product. These compounds not only are potential compounds that will inhibit the enzyme-catalyzed reaction but also will not be hydrolyzed by a hydrolase (Scheme 3).

Since many biological functions involve carbohydrates, the efforts to understand carbohydrate chemistry and to synthesize glycomimetics have increased dramatically. The history of carbohydrates can be traced back to the late 1800's, first investigated extensively by Emil Fischer. His studies have led many researchers to discover the important biological roles of these molecules and his investigations of enzymes and carbohydrate reactions laid the foundation for enzyme biochemistry. In the late 1980's, the study of carbohydrates in biological processes was given the name "glycobiology." [17]

Glycobiology basically deals with the properties of macromolecules such as glycoproteins and glycolipids and how carbohydrates are involved in recognition events. Unlike proteins and lipids, carbohydrates can exist as a highly branched or a simple single molecule except the ones that are present in the cells. Carbohydrates have the general molecular formula $C_n(H_2O)_n$, thus they were considered to be hydrates of carbon. Today, carbohydrates are defined as polyhydroxyaldehydes and polyhydroxyketones. Carbohydrates are classified under four general terms: monosaccharides, disaccharides, oligosaccharides, and polysaccharides. Examples of monosaccharides are glucose, galactose, mannose, and fructose. Glucose is the most common monosaccharide found in biological processes. The monosaccharides exist as acyclic, furanose (five-membered ring), and pyranose (six-membered ring) forms in the solution (Figure 5).
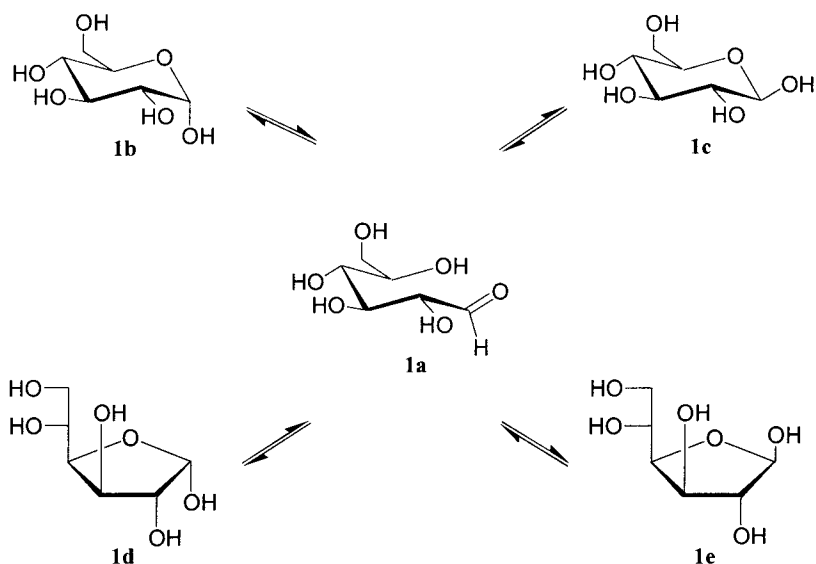
Figure 5: The configurations of D-glucose in solution.

The formation of a ring results from the attack of an oxygen atom attached to the C4 or C5 onto the carbonyl carbon of the aldehyde. Due to the sp^2 hybrization of the carbonyl carbon, an oxygen atom can attack either from the top or the bottom position, which results in the mixture of alpha (α) (Figure 5 **1b** and **1d**) or beta (β) (Figure 5 **1c** and **1e**) configurations. The α configuration contains the -OH attached to the anomeric carbon (C1) pointing down below the plane of the molecule (the axial position), and the -OH above the plane (the equatorial position) is the β configuration. All monosaccharides belong to either the D or the L series based on the -OH group attached to the stereocenter farthest removed from the carbonyl group (Figure 6). Mostly the D configuration carbohydrates are involved in biological processes although L-sugars do appear in some cases, for example in the capsular polysaccharides of *S. aureus* bacteria (L-FucNAc), as has been discussed earlier.
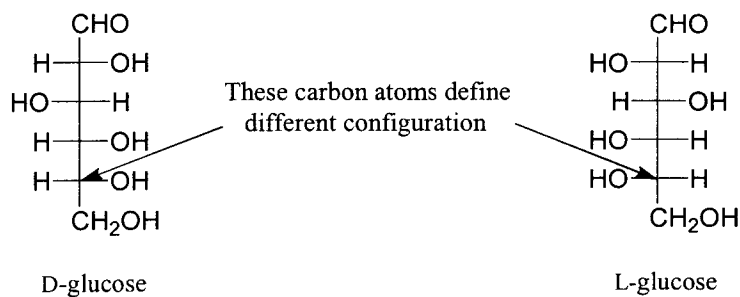
Figure 6: The D- and L-glucose configurations.

There are many natural products that mimic the sugars in which the hydroxyl group is replaced with another functional group. When the hydroxyl group attached to a carbon other than the anomeric carbon is replaced with N atom functionality it is simply called an amino sugar.

The synthesis of aminosugar analogs has been investigated in great detail because they are an important component of naturally occurring polysaccharides. One of the methods introduced for the functionalization of monosaccharides is the nucleophilic addition of an amine to a double bond to form amino sugar derivatives (Scheme 4).
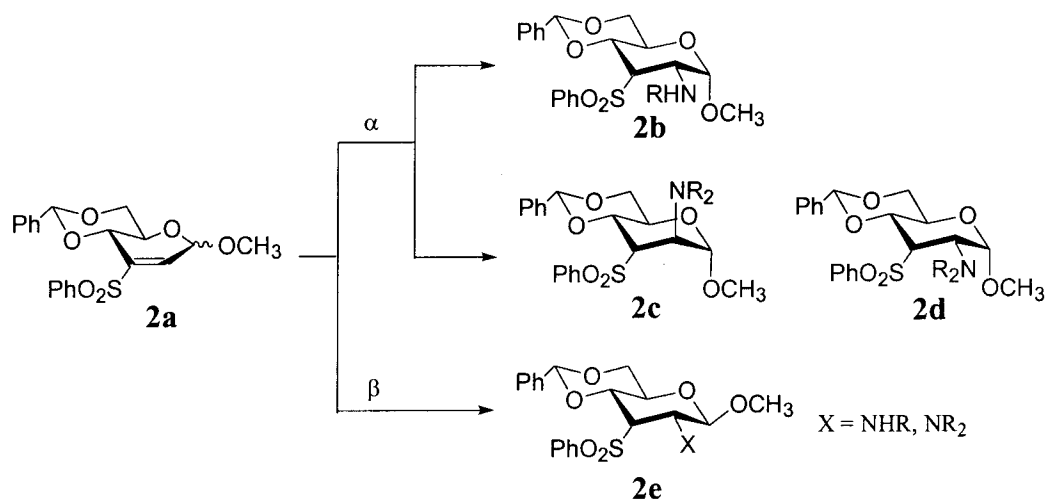
Scheme 4: Diastereoselectivity of amine conjugate addition.

The reactions of α-sulfone **2a** with a primary amine gave a single isomer (**2b**), but the mixture of isomers was obtained with a secondary amine (**2c** and **2d**). Only a single isomer (**2e**) is produced when the β-sulfone reacts with both primary and secondary amines.[18]

As another example of amino sugar synthesis, Lichtenthaler *et al.*[19] have introduced a sequence in which a 2-acetoxy-3,4-di-*O*-acetyl-D-glycal methyl ester (**3**) was reacted in a series of steps to generate the glycomimetic of *N*-acetyl-D-mannose uronic acid (Scheme 5). The β-glycoside (**4**) was reduced with an excess of $BH_3 \cdot THF$ complex in THF followed by *N*-acetylation with acetic anhydride to give the amino sugar (**5**). The reaction shows the preference of hydride attacking the C-2 from the α-side and causing it to give 1,2-*cis*-amino sugar product.
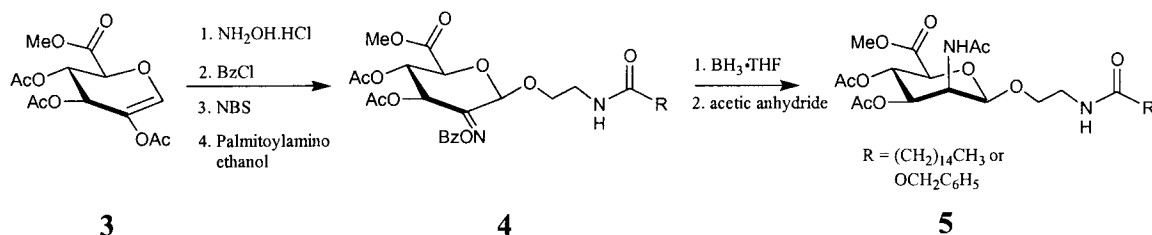
Scheme 5: Formation of amino sugar from glycal.

Stereochemistry plays a major role in the potential synthesis of bioactive compounds, especially those that are involved in enzymatic reactions, such as inhibitors or substrates. The stereospecificity is a crucial point in the enzyme-catalyzed reaction. In many laboratory syntheses a compound containing either a carbonyl or double bond will react with a nucleophile to give a racemic mixture, due to the equal probability of

nucleophiles attacking at either face. During an enzyme-catalyzed reaction, only a specific site of the substrate is held firmly to the active site of the enzyme, which means that the enzyme active site and the substrate-binding site must "match" (lock and key formation) in order to carry out the biological process. The stereochemistry at the anomeric carbon is also very important since the linkage between two monomers occurs at C-1 and C-3 or C-1 and C-4 in *S. aureus* CP biosynthetic pathways.

Using a traditional method to synthesize compounds (such as substrates) with a desirable shape, or active compounds that can form enzyme-inhibitor complex structures, is a very time-consuming process. Combinatorial methodology has become an asset to obtain various compounds or "libraries" and to identify the most promising leads for novel compound synthesis.[20] Basically, there are three ways to obtain the compounds: combinatorial, parallel, and mixture synthesis in solid-phase or solution-phase. The way the combinatorial solid-phase synthesis[21] works is that the number of products increases exponentially relative to the number of reagents used. In parallel synthesis, each reaction is performed in a series of simple steps under different conditions by adding various reagents (e.g. Figure 7). This method requires a synthesis of a highly reactive intermediate to produce a product.
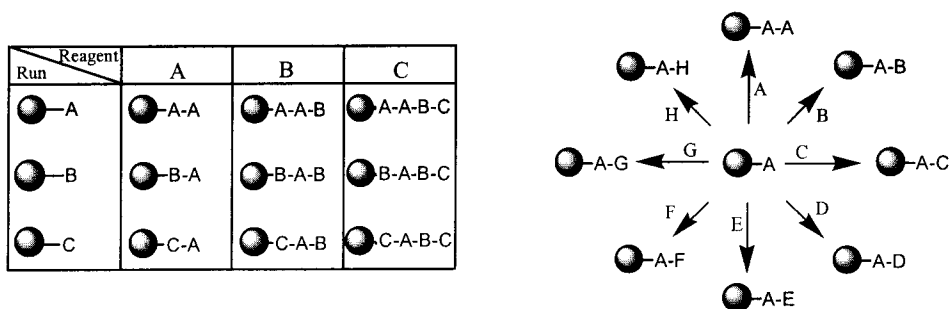
Figure 7: Parallel synthesis.

The mixture synthesis is very similar to the parallel synthesis method except all the reactions occur in one vessel. In this method, an end product with various functional groups will be obtained by introducing excess amount of reagents to the compounds with multiple reactive sites (e.g. Figure 8).[22] The first step involves the attachment of reactants to the resin. Once the reactants are attached to the resin, they will react with different types of reagents.
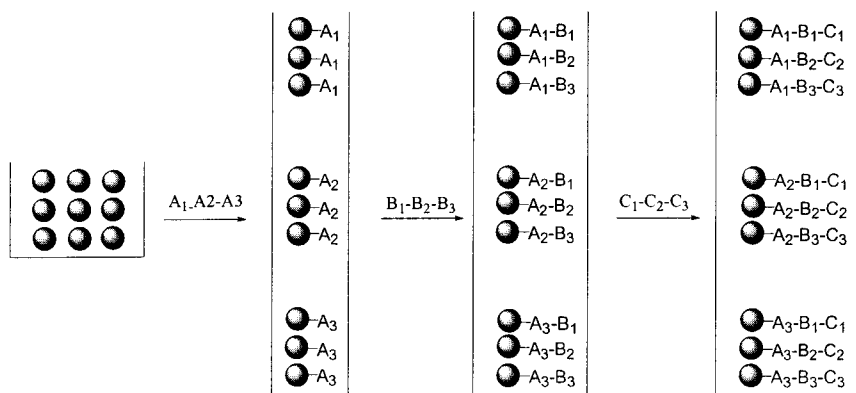
Figure 8: Mixture synthesis.

Combinatorial synthesis on solid-phase provides not only multiple compounds but also eliminates some purification steps. The purification steps involve simply filtering and washing the resin with proper solvents followed by a resin-cleavage reaction to remove the resin. This method offers many advantages, for example conducting multistep reactions, because excess reagents can be added and removed easily by washing it with a solvent at each step. Although, additional purification may be required depending on the purity of compounds.

Recently, using the solid-phase method to create multiple compounds has been widely adopted by pharmaceutical research and development companies. Yan *et al.*

demonstrated that the polymer-bound molecules in solid-phase have the ability to provide stereoselective construction of glycosidic linkages.[23]   Schuster *et al.* have reported a strategy for the formation of compounds *via* glycosidic bonds employing enzymes, but the method is still limited by the availability of enzymes.[24]   Their discoveries may introduce an effective approach towards the synthesis of glycomimetics, including those designed to mimic sugars found in the CP of *S. aureus*.

The solid phase synthesis using an enzyme directs the researchers to discover many bioactive molecules, mainly in the pharmaceutical industries. Since drug discovery relies on the ability of the chemist to access a wide range of molecular diversity, combinatorial methodology has an advantage of providing such compounds. The discovery of potential drugs may take years of research and its effective time period depends on the virulence factors expressed by the organisms, due to the ability of bacteria to evolve resistance to antibiotics. Clearly, it is necessary to discover new drugs that are effective for the treatment of infectious diseases caused by drug resistant bacteria.

Because antibiotic resistance of *S. aureus* is a major problem in the medical community, derivatives of the CP aminosugars of this bacterium were investigated in this research. Specifically, approaches to derivatives of the monomer unit D-ManAcA have been studied. Two areas of synthetic methodology that have been emphasized in the synthesis of glycomimetic derivatives are azide-alkyne cycloadditions and Staudinger reactions to form glycosyl amides. In addition, the parallel synthesis methodology was employed for multi-derivative compound synthesis. As a result of synthetic efforts, a large number of compounds were obtained and these approaches may eventually lead towards the discovery of new antimicrobial agents.

Statement of Problem

The most powerful antibiotic to treat the bacterium *Staphylococcus aureus (S. aureus)* infections, vancomycin, is becoming increasingly ineffective. Currently available treatments for *S. aureus* are known to disrupt the construction of the cell wall, however blocking synthesis of the bacterial capsular polysaccharide may provide a new point of attack. Using this concept, a potentially new direction for the treatment for *S. aureus* has been investigated.

The synthesis of glycomimetics similar to one of the amino sugars found in the CP of *S. aureus* serotypes 5 and 8 is the focus of this research. The capsule is made up of three repeating amino sugars: *N*-acetyl-2-amino-2-deoxy-D-mannopyranose uronic acid (D-ManAcA), *N*-acetyl-2-amino-2-deoxy-D-fucosamine (D-FucNAc) and *N*-acetyl-2-amino-2-deoxy-L-fucosamine (L-FucNAc).

The target of this research is to synthesize glycomimetics of D-ManAcA, an amino sugar derivative of the D-mannose parent sugar. With the aid of transferase enzymes, amino sugar monomers are linked together through 1,4-β- and 1,3-β-glycosidic bonds for type 5 an 8 respectively. Manipulation of the functional group at the anomeric carbon may give glycomimetics that disrupt the biosynthetic pathway of the CP, thus resulting in the prevention of capsule construction. Since little is known about the biosynthetic pathway of CP formation, the synthesis of glycomimetics by replacing the C-1-β-oxygen atom of D-ManAcA that is involved in the glycosidic bond formation with a carbon, nitrogen or sulfur atom will be a suitable approach to inhibit the enzyme activities. The replacement of the O atom with N-substituents has been investigated.

Results and Discussion

1. Synthesis of precursor compounds for D-ManNAcA glycomimetics

Lichtenthaler, *at al.* developed an excellent method to generate the precursor compounds of D-ManNAcA because it provided the advantage of obtaining most of the intermediate compounds in crystalline form.[19] Each step in the synthesis of the intermediates has been discussed in detail below.

The initial step involves the treatment of D-glucurono-6,3-lactone (**6**), which can be obtained inexpensively, with sodium hydroxide in methanol for one hour to produce the methyl D-glucopyranuronates **7**. After the evaporation of the mixture of **7**, it was acetylated with acetic anhydride in pyridine to protect all the hydroxyl groups. The mixture was reacted for three hours and reaction confirmed by disappearance of starting material and appearance of a new spot with a higher R_f value on the TLC plate. The crude material was purified by a simple aqueous workup using methylene chloride for extraction to provide a mixture of isomers (**8 α/β**). The compound, methyl 2,3,4,5-tetra-*O*-acetyl-β-D-glucopyranuronate (**8β**) was isolated *via* recrystallization by dissolving the mixture in hot isopropanol, which afforded 58 % of **8β** as clear crystals.[25]
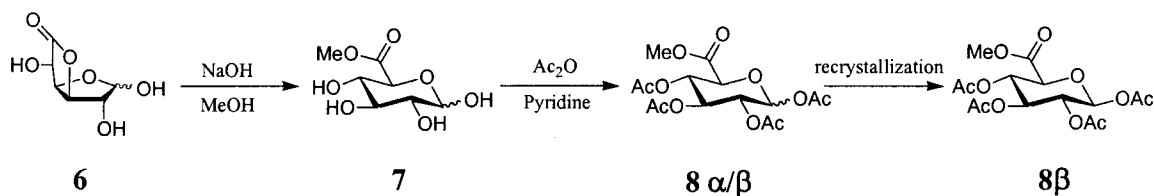
Scheme 6: Preparation of methyl 2,3,4,5-tetra-*O*-acetyl-β-D-glucopyranuronate (**8β**).

The ^{1}H NMR spectrum of **8β** showed three signals at 2.02, 2.03 and 2.11 ppm (one double intensity) that correspond to the acetyl protecting groups. Also, a single

sharp peak was observed at 3.75 ppm for the methyl attached to the oxygen atom of the ester functionality. The coupling constant of H-1 and H-2, 7.87 Hz, shows the position of these two hydrogen atoms to be neighboring atoms in an axial position and that aided the identification of the crystals as **8β**. Analysis of the ^{13}C NMR spectrum showed the signals for the carbonyl carbons of the acetyl protecting groups, and also the ester group had shifts at 169.7-170.8 ppm.
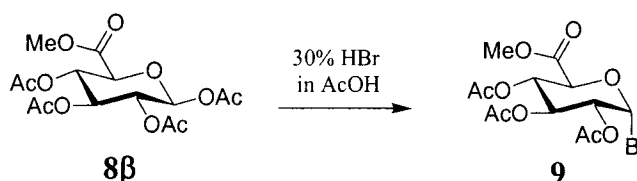
Scheme 7: Formation of methyl 2,3,4-tri-*O*-acetyl-α-D-glucopyranuronosyl bromide (**9**).

Bromide **9** was readily synthesized *via* treatment of **8β** with 30% HBr in acetic acid for three hours to give a single stereoisomer in 87% yield. There is a preference for the Br atom in the axial position due to the anomeric effect. TLC indicated a UV active spot with a lower R_f value compared to the starting material, and the ^{1}H NMR spectrum showed the loss of the C-1 acetyl protecting group signal and a downfield shift for the anomeric proton to 6.63 ppm. The remaining acetyl protecting group signals were observed at 2.05 and 2.09 ppm, with one of the signals integrating to two acetyl protecting groups. The ^{13}C NMR spectrum provided the evidence for four carbonyl shifts, in which three of them correspond to the acetyl protecting groups at 170.38-171.44 ppm. Also evident are the signals around 21 ppm illustrating the methyl groups associated with the acetyl protecting groups. The signal for the methyl group associated with the ester was further downfield due to the neighboring oxygen atom and it was seen

at 62.06 ppm. Mass spectral data shows an M^+ at 415.8 that corresponds to the calculated molecular weight 397.17 with the addition of a water molecule.
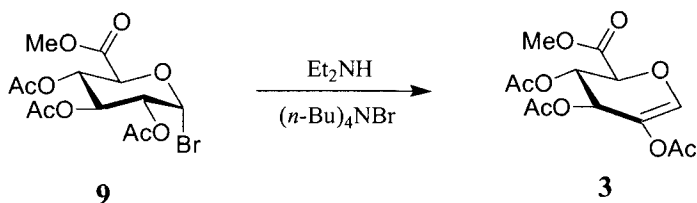
Scheme 8: The synthesis of glycal **3** *via* elimination reaction.

Because Br is a good leaving group, reaction with diethylamine and tetra-butylammonium bromide in DMF gave a glycal (**3**) *via* an elimination reaction. TLC showed a UV-active spot that burned at a slightly lower R_f value compared to the starting material. The product was purified by elution from a column of silica gel to afford **3** in 68% yield. The ^1H NMR spectrum showed the change of the C-1 proton signal of the starting material at 6.63 ppm, which now shows as a singlet at 6.83 ppm. This was due to the absence of a neighboring hydrogen atom and also introduction of the π bond between C1 and C2. Again, the signals for the methyl groups of the acetyl protecting groups were observed at 2.02, 2.11, and 2.15 ppm. Also there was a change in the shape of the signal for H-3 from a doublet of doublets to a doublet with a coupling constant $J = 2.47$ Hz. Analysis of the ^{13}C NMR spectrum showed the carbonyl carbons of the protecting groups at 170.14, 170.33 and 170.41, as well as 167.56 ppm for the carbonyl group of CO_2Me. The signal for the anomeric carbon was shifted further downfield from 87.64 to 140.11 ppm due to the π bond between C1 and C2. A similar result was also observed for C2, which was shifted from 71.09 to 128.43 ppm. The rest of the signals showed very little change when they were compared with the starting material spectrum. Mass

spectrometry provided an M^+ of 334.2, which corresponds to the calculated molecular weight 316.08 with the addition of a water molecule.
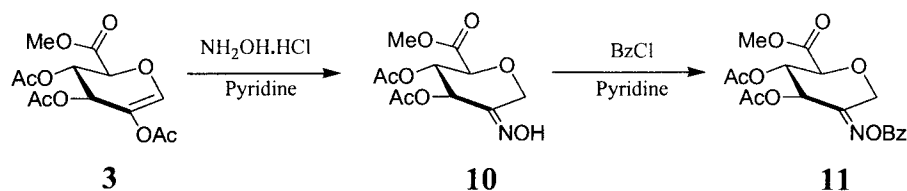
Scheme 9: *O*-Benzoyloxime of methyl 3,4-di-*O*-acetyl-1,5-anydro-D-fructuronate.

The reaction of glycal **3** with hydroxylamine hydrochloride in pyridine afforded a 65% yield of oxime **10** as a solid. The TLC showed a spot that was UV active and burned at a lower R_f value than that of the starting material. Based on the ^{1}H NMR spectrum analysis, the disappearance of a signal for the methyl group associated with an acetyl protecting group indicates the loss of one acetyl protecting group. Also shown in the spectrum is a change for the H-1 signal for the starting material, which was shifted upfield and shows as a doublet of doublets between 4.69 and 4.86 ppm with a coupling constant of 15.74 Hz. The ^{13}C NMR provided more evidence for the reaction of enol acetate **3** by showing the C1 signal shifted upfield from 140.11 to 60.37 ppm but the C2 signal remained downfield, due to the loss of the double bond at C1 and the new formation of a double bond at C2 with the N atom. The signals that appeared at 21.88 and 22.10 ppm correspond to the carbonyl group of the acetyl protecting groups and the signal at 53.8 ppm for the carbonyl group of CO_2Me. The rest of the signals appeared between 60.37 - 73.35 ppm, which corresponds to the remaining carbons of **10**. A signal for the NOH proton did not show on the ^{1}H NMR spectrum.

The benzoylation of **10** with benzoyl chloride in pyridine afforded *O*-benzoyloxime **11** in 77% yield as a yellow solid. The TLC of the reaction mixture showed a spot that was UV active and the R_f value that shows a slight difference in the polarity between the product and that of the starting material. Investigation of the ^{1}H NMR spectrum showed the appearance of signals that correspond to the benzoyl protecting group at 7.49 (*m*-Ar-H), 7.62 (*p*-Ar-H) and 8.03 (*o*-Ar-H). The C1 proton signals were shown between 4.95 and 5.03 ppm as a doublet of doublets with a coupling constant of 15.74 Hz. The signals for both H-3 and H-5 were shown as doublets at 5.70 and 4.46 ppm respectively due to the presence of one neighboring hydrogen for each (H-4). The ^{13}C NMR spectrum also provides evidence for the formation of the product by new signals for the benzene ring carbons at 128.95-130.81 ppm and also a corresponding carbonyl signal at 134.93 ppm. Electrospray Ionization (ESI) mass spectrometry shows an M^+ of 271.9, which corresponds to the loss of CO_2Ph from a molecular weight of 393.78.
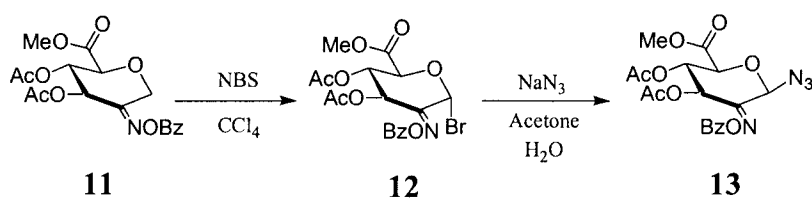
Scheme 10: Formation of azide **13**.

The first step involved in the synthesis of methyl 3,4-di-*O*-acetyl-2-(benzoyloxyimino)-1-bromo-2-deoxy-α-D-*arabino*-hexopyranuronate (**12**) was the addition of bromine *via* radical substitution of **11**. The gentle reflux of a mixture of **11** and Br_2 in CCl_4 was achieved by using a 250 W lamp as a heating source. A UV-active

spot that is slightly lower than the starting material was observed with R_f value of 0.65. Two singlets observed on the ^{1}H NMR at ~ 2.0 ppm correspond to the acetyl protecting groups at C3 and C4. Again, the methyl group associated with the ester appears at 3.80 ppm and a slight difference in the signal shifts compared to the starting material of the benzene protons are shown on the spectrum. C1 proton signals at 4.95 and 5.03 ppm had disappeared and the appearance of a new signal further downfield due to the electronegativity of the bromine atom at 7.43 ppm as singlet provided evidence of the product. The ^{13}C NMR data also supported the bromination at C1 with the change of signal from 70.27 to 73.60 ppm.

The formation of benzoyloxyimino azide **13** was achieved by reacting **12** with sodium azide in a mixture of acetone: water (5:1) as solvent. After 3 hours, TLC indicted the consumption of starting material. The product was found to be UV active and also with a lower R_f value than that of the starting material. The crude ^{1}H NMR spectrum provided the signals corresponding to the product. The disappearance of the C1 proton at 7.43 ppm and appearance of a new signal at 6.60 ppm as a singlet indicated the loss of the Br atom at C1. The synthesis of crude **13** requires ~ 3 hours to complete the reaction, however it is likely that longer reaction times may lead to decomposition. The remaining proton signals of the product **13** observed on the ^{1}H NMR spectrum showed a slight upfield shift compared to the starting material **12**.

2. Synthesis of glycosyl azides from D-glucopyranuronate and D-glucose

The structure of the primary products formed in the reaction of β-glycosyl azides (a glucuronosyl azide and a glucosyl azide were studied) from several types of reaction

were investigated in order to find suitable conditions for synthesis of derivatives of azide **13**. Preparation of glucuronate azide **14** was achieved *via* the synthesis of 2,3,4-tri-*O*-acetyl-α-D-glucopyranosyl bromide (**9**) from α-acetylated **8α**.

The first step involved in the synthetic strategy was the bromination of α-acetylated glucuronolactone **8α** with HBr, which gave thermodynamically favored compound **9** in 86% yield. The spots shown on the TLC gave a UV active spot that burned with a slightly lower R_f value compared to that of the starting material. The absence of one of the acetyl protecting group signals between 2.02-2.15 ppm in the ^{1}H NMR spectrum and the appearance of a singlet, which corresponds to the C1 proton at 6.62 ppm, indicates the bromination of **8α** at C1. The ^{13}C NMR also supported the bromination of **8α** with the disappearance of a carbonyl signal that was observed between 161-171 ppm on the starting material ^{13}C NMR.
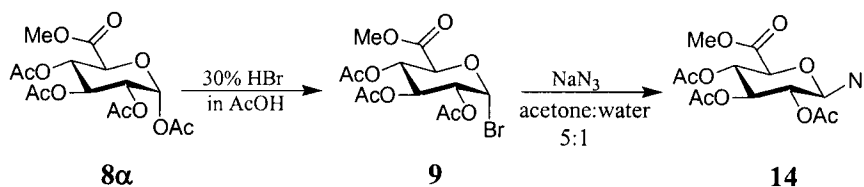
Scheme 11: Synthesis of glucopyranuronosyl azide **14**.

2,3,4-Tri-*O*-acetyl-α-D-glucopyranosyl bromide (**9**) reacts readily with NaN$_3$ to afford glucuronate azide **14** (Scheme 11) as a yellow solid. TLC showed a UV active spot burning at a higher R_f value than that of starting material. The ^{1}H NMR spectrum showed the signal shift from 6.63 ppm to 4.71 ppm with a coupling constant 8.79 Hz, due to shielding of the N$_3$ group. All the acetyl protecting group signals were observed with

the same intensity around 2.00 ppm. The carboxylic ester methyl signal was again seen at ~3.70 ppm. Comparing the ^{13}C NMR with that of the starting material, there was a slight shift observed for the anomeric carbon and one of the carbonyl carbons but the rest of the signals remained basically the same. Investigation of the mass spectral data afforded an M^+ of 377.0, which corresponds to the calculated molecular weight of 359.29 with the addition of a water molecule.
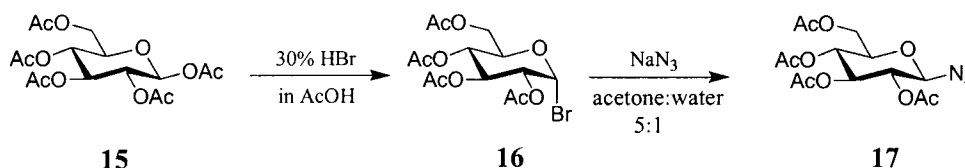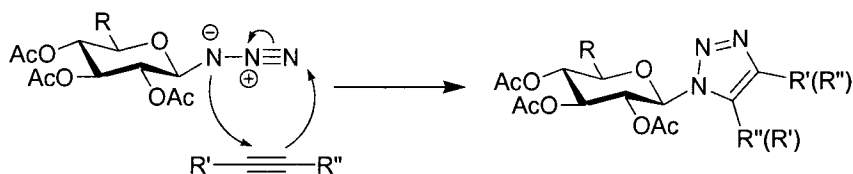

Scheme 12: Preparation of glucosyl azide **17**.

The synthesis of glycosyl bromide **16** involves exactly the same procedure as for the preparation of methyl 2,3,4-tri-*O*-acetyl-α-D-glucopyranuronosyl bromide (**9**) and the similar results were also observed (Scheme 12). Again, the α-glucosyl bromide **16** was obtained *via* S_N1 to give the thermodynamically favored product with the bromine atom in the axial position. TLC indicated the formation of a UV active spot burning at a lower R_f value than that of the starting material. ^{1}H NMR data showed the disappearance of the anomeric proton signal at 5.70 ppm and the appearance of a doublet at 6.61 ppm.

Glucosyl bromide **16** was treated with NaN₃ and readily converted to glucosyl azide **17** *via* S_N2 reaction. The byproduct was precipitated as a yellow solid, making it an easy matter to isolate **17** as a white solid in 91% yield. Again, in the nucleophilic substitution of azide, TLC showed a UV active spot with a lower R_f value than the starting material due to the loss of the Br atom. Observing the ^{1}H NMR spectrum, a signal at 6.61 ppm representing the anomeric proton of starting material had disappeared

and a new signal at 4.64 ppm had appeared. The replacement of Br atom with N_3 caused

shielding of the C1 proton and moved the signal upfield. The H-2, H-3, and H-4 proton

signals were only evidenced through the integration of the region between 4.95-5.21

ppm. The signals for the carbonyl carbons of the acetyl protecting groups were shown

between 21.64-22.13 ppm on the ^{13}C NMR spectrum.

3. 1,3-Dipolar cycloadditions of glycosyl azides.

Synthesis of glycosyl triazole heterocycles was investigated by using the Huisgen

1,3-dipolar cycloaddition.[26] The glycosyl N atom attacks alkyne carbon, which motivates

the π electrons to attack the terminal N atom to afford an aromatic 1,2,3-triazole

compound. The reaction is a simple concerted cycloaddition and the possibility of

regioisomers occurs when unsymmetrical alkynes are used in these reactions (Scheme

13).

Scheme 13: 1,3-dipolar cycloaddition of glycosyl azides to give 1,2,3-triazoles.

Glucuronosyl azide **14** and glucosyl azide **17** were reacted with six different types

of alkynes (Tables 1 and 2) to afford a variety of compounds. Using the parallel

synthesis method, the compounds were readily prepared and purified. The reaction

vessel containing diethylacetylene dicarboxylate provided the highest yield, however, no

products were isolated from reactions with diphenyl acetylene and phenyl acetylene for

both the glucurono azide and glucosyl azide. Possibly, the concerted cycloaddition reaction is blocked by a large substituent on the alkyne. When 23 hour and 72 hour reaction times were applied to both diphenyl acetylene and phenyl acetylene vessels, only the starting material was seen by TLC and by ^{1}H NMR analysis of the residue after evaporation. Interestingly, the ^{1}H NMR spectrum of the reaction vessel containing trimethylsilyl propiolate showed the disappearance of C1 proton of the azide, but methyl groups of the SiMe$_3$ group were not shown on the spectrum (this compound has not yet been investigated further).

Starting material	Alkyne	Product	% Yield	R$_f$ value
14	Diphenyl acetylene	N/R	-	-
	Phenyl acetylene	N/R	-	-
	Trimethylsilyl propiolate	N/R	-	-
	Propiolic acid	**18**	42	0.28
	Ethyl propiolate	**19**	52	0.42
	Diethylacetylene dicarboxylate	**20**	89	0.45

Table 1: Glucuronosyl azide (**14**) cycloadditions.


14   **18**
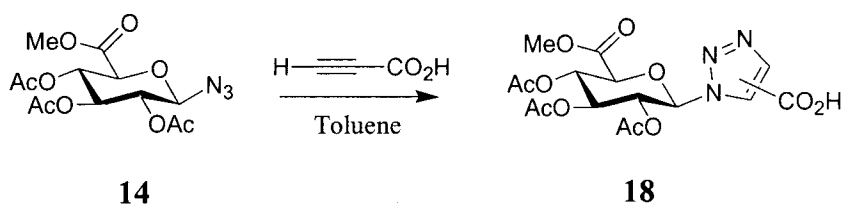
Scheme 14: 1-(methyl 2,3,4-tri-*O*-acetyl-β-D-glucopyranuronosyl)-1*H*-[1,2,3]triazol-4-(and-5)-carboxylic acids (**18**).

The reaction of glucuronosyl azide **14** with propiolic acid apparently afforded a mixture of isomers **18** due to the head-head or head-tail concerted reaction. TLC of the products showed a much lower R$_f$ than the starting material. Analysis of the ^{1}H spectrum

showed signals that correspond to both triazole isomers (at 7.74 and 7.87 ppm) and unreacted starting material although carboxylic acid protons were not observed. The ^{13}C NMR spectrum gave more evidence for the formation of isomers of **18** with two signals that correspond to the triazole carbons at 129.22 and 130.02 ppm.

Similar reaction of **14** with ethyl propiolate again gave a mixture of isomers (**19**, Scheme 15). TLC showed a UV active spot that also burned with a much lower R_f value than that of the starting material. The ^{1}H NMR spectrum showed evidence of the product by showing signals at 1.36 ppm (CO$_2$CH$_2$C$\underline{H}_3$) and 4.36 ppm (CO$_2$C$\underline{H}_2$CH$_3$). Also shown on the ^{1}H NMR spectrum are the signals for the triazole protons in the regioisomers at 8.10 and 8.44 ppm. These singlet signals indicated the presence of isomers of product **19**. Triazole carbon signals are hard to distinguish in the ^{13}C NMR spectrum due to the presence of excess ethyl propiolate, which caused the signals to overlap. The methyl and methylene carbons of the ethyl ester groups were shown at 15.51 and 62.71 ppm.

14   **19**
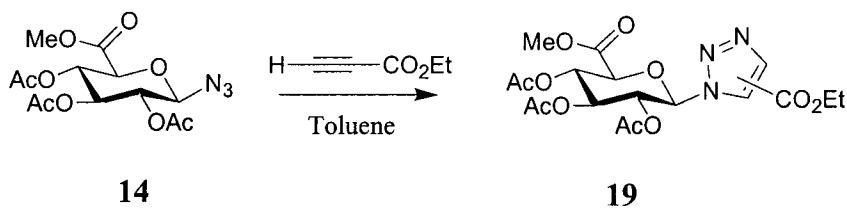
Scheme 15: 1-(methyl 2,3,4-tri-*O*-acetyl-β-D-glucopyranuronosyl)-1*H*-[1,2,3]triazol-4-(and 5-)carboxylic acid ethyl esters (**19**).


14   **20**
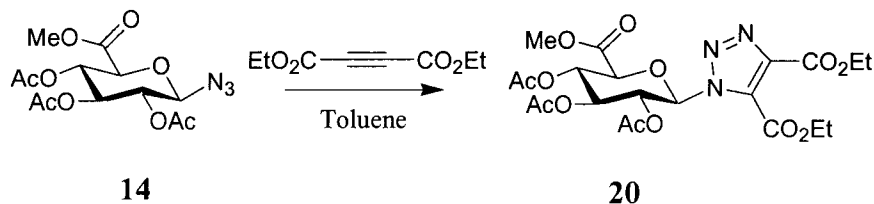
Scheme 16: 1-methyl 2,3,4-tri-*O*-acetyl-β-D-glucopyranuronosyl)-1*H*-[1,2,3]triazol-4,5-dicarboxylic acid diethyl ester (**20**).

The protocol using diethylacetylene dicarboxylate afforded a single isomer **20** as expected. Observation of the TLC results showed a UV active spot that burned at a lower R_f value than that of starting material. Investigation of the ^1H NMR spectrum showed the disappearance of a doublet at 4.71 ppm and appearance of a new signal at 6.17 ppm indicating the formation of a triazole at C1. The signals observed at 1.41 ppm ($CO_2CH_2C\underline{H}_3$) and 4.28 ppm ($CO_2C\underline{H}_2CH_3$) with a coupling constant of 7.14 Hz and a double intensity afforded the evidence for the formation of a single product (**20**). The ^{13}C NMR spectrum also provided the signals at 15.11 ppm and 15.41 ppm that correspond to the methyl group carbons ($CO_2CH_2\underline{C}H_3$) and the signals at 131.92 ppm and 141.23 ppm that correspond to the triazole carbons.

| Starting material	Alkyne	Product	% Yield	R_f value
17	Diphenyl acetylene	N/R	-	-
	Phenyl acetylene	N/R	-	-
	Trimethylsilyl propiolate	N/R	-	-
	Propiolic acid	**21**	12	0.24
	Ethyl propiolate	**22**	91	0.21
	Diethylacetylene dicarboxylate	**23**	82	0.40

Table 2: Glucosyl azide (**17**) cycloadditions.
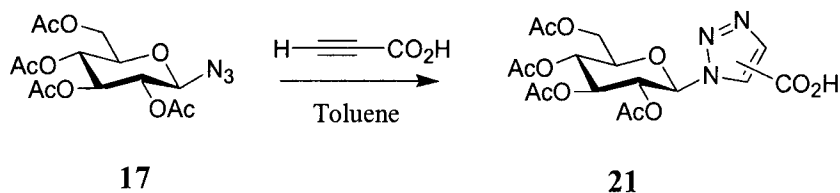
Scheme 17: 1-(2,3,4,5-tetra-*O*-acetyl- β-D-glucopyranosyl)-1*H*-[1,2,3]triazol-4-(and 5-)-carboxylic acids (**21**).
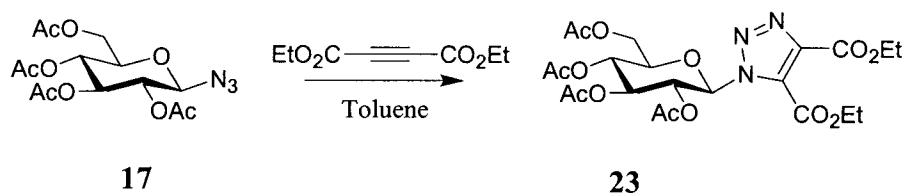
Synthesis of the triazole carboxylic acid isomers **21** (Scheme 17) was attempted *via* concerted reaction of glucosyl azide **17** with propiolic acid. The TLC of the reaction mixture again showed a UV active spot that burned with a lower R_f value than the starting material. Investigation of the ^{1}H NMR spectrum showed the appearance of the one major product, however a signal corresponding to the triazole proton was not observed. The signals for the methyl groups of the acetyl protecting groups were observed at 2.00, 2.02, 2.03 and 2.08 ppm.

The C5 proton signal for **21** was shown at 3.85 ppm, which appeared as a doublet of doublet of doublets due to the presence of neighboring C4 proton and also two C6 protons. This reaction requires further investigation.
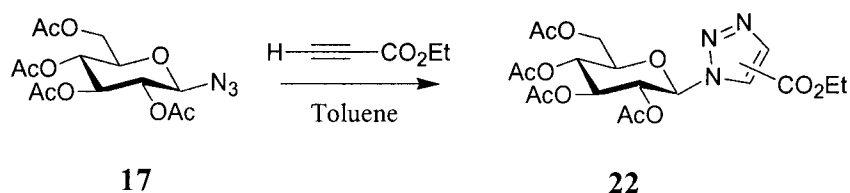
Scheme 18: 1-(2,3,4,5-tetra-*O*-acetyl-β-D-glucopyranosyl)-1*H*-[1,2,3]triazol-4-(and 5-)-carboxylic acid ethyl esters (**22**).

Compound **17** was reacted with ethyl propiolate to afford triazole isomers **22**. The investigation of TLC showed a UV active spot that burned at a lower R_f value than that of starting material. The ^{1}H NMR spectrum showed the presence of $CO_2CH_2C\underline{H}_3$ and $CO_2C\underline{H}_2CH_3$ at 1.35 ppm and 4.03 ppm respectively. The triazole protons for the isomeric products were observed downfield at 8.09 ppm and 8.38 ppm. Examination of ^{13}C NMR spectrum shows the appearance of signals at 158.61 ppm and 161.08 ppm, which correspond to carbonyl carbons of the carboxylic acid esters.

Scheme 19: 1-(2,3,4,5-tetra-*O*-acetyl-β-D-glucopyranosyl)-1*H*-[1,2,3]triazol-4,5-dicarboxylic acid diethyl ester (**23**).

The synthesis of triazole **23** involves the cycloaddition of glucosyl azide **17** with diethylacetylene dicarboxylate. TLC showed a UV active spot that also burned with a lower R_f value than that of the starting material. The ^1H NMR spectrum afforded signals for methyl and methylene protons at 1.22 ppm and 4.09 ppm respectively with a coupling constant of 7.14 Hz respectively. Three signals with one integrating to two acetyl protecting groups were shown at 2.01, 2.03 and 2.04 ppm. Also shown in the spectrum is the change in the chemical shift of the C1 proton from 4.64 ppm to 6.11 ppm, which indicates the formation of the triazole compound. The ^{13}C NMR spectrum afforded more evidence for the formation of product with acetyl protecting group signals at 169.45-171.34 ppm, carbonyl carbons of carboxylic acid esters at 158.95 and 160.58 ppm and two triazole carbons at 131.75 ppm and 141.36 ppm.

4. Conversion of glycosyl azides into amides

Formation of the amide *via* an azide reacted with triphenylphosphine was achieved using in the Staudinger reaction.[27] The reaction sequences involves the formation of a triazaphosphadiene intermediate (Scheme 20) first then followed by the loss of N_2 to afford a phosphinimine ylide (Scheme 20).
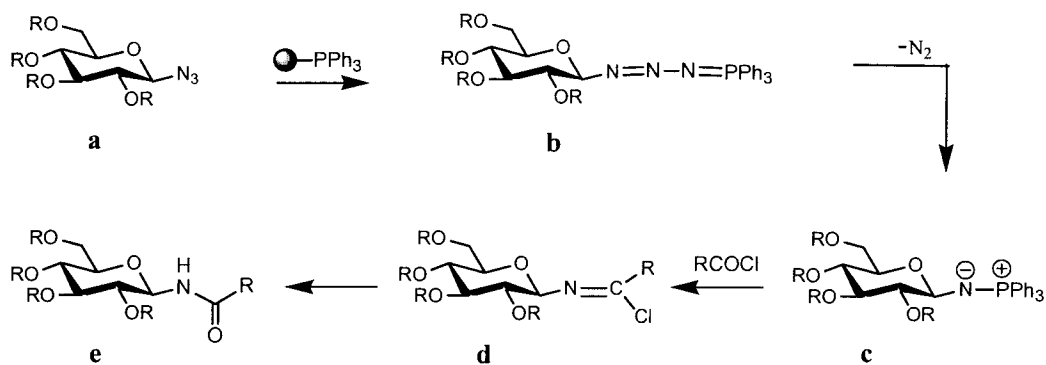
Scheme 20: Amide synthesis *via* Staudinger reactions.

The phosphinimine ylide was then reacted with an acid chloride to yield *N*-glycosyl amides (Scheme 20 **d**). Because of the ready availability of the glycosyl azides, the introduction of different substituents at C1 to provide a stereoselective synthesis of β-glycosyl amide compounds was investigated. Use of a parallel synthesizer provided fast access to a variety of amide compounds. Up to twelve different types of carboxylic acid chloride (Tables 3 and 4) were used to afford various types of amide derivatives.

The general method of adding a glycosyl azide to an acid chloride and polymer-supported triphenylphosphine (PS-PPh₃) was exemplified in the synthesis of compound **24** in high yield (Scheme 21). Mechanistically, the initial step involves the formation of an ylide, which then attacks the carbonyl carbon of *p*-nitrobenzoyl chloride to afford a chloroimine intermediate, which is then hydrolyzed to afford the amide product.
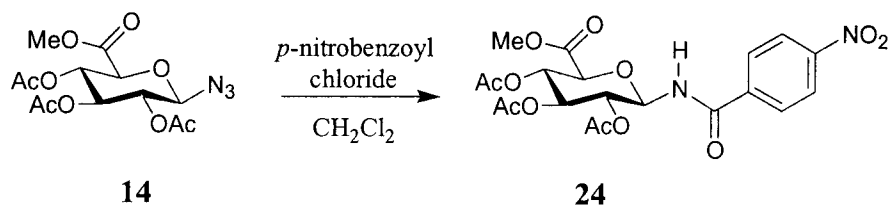

Scheme 21: *p*-Nitrobenzoic acid-(2,3,4-tri-*O*-acetyl-β-D-methyl glucopyranuronate)-amide (**24**).

The reaction afforded a high yield (87%) of **24** as yellow syrup (Table 3). Study of the TLC showed a UV active spot that burned at a lower R_f value than starting material. Investigation of the ^1H NMR spectrum indicated that the signal at 5.47 ppm is actually the overlap of two doublet of doublets and the integration value provided the evidence of this signal as two hydrogens (shown as a "quartet" signal shape). One of the signals contains a coupling constant of 8.97 Hz, which is the same value for the NH proton that appeared at 7.36 ppm, thus it was determined to be the H-1 proton. Aryl ring resonances indicating two types of protons were shown at 7.93 ppm and 8.32 ppm as doublets. Analysis of the ^{13}C NMR spectrum also provided evidence for the formation of **24** by presenting the five signals in the region 166.43-172.16 ppm, which indicates the carbonyl carbons of acetyl protecting group, ester and amide. The aryl ring carbon signals are also found between 124.87-150.94 ppm, and the signal at 54.14 ppm represents the methyl group of the carboxylic acid ester. This signal appeared further downfield compared to the methyl group of the acetyl protecting groups, and the methyl groups of acetyl protecting group signals are clustered together around 22 ppm.

Starting material	Acid Chloride	Product	% Yield	R_f value
14	*p*-nitrobenzoyl chloride	**24**	87	0.36
	2-furoyl chloride	**25**	38	0.23
	2-naphthoyl chloride	**26**	44	0.35
	benzoyl chloride	**27**	85	0.32
	1-naphthoyl chloride	**28**	64	0.33
	2-thiophenecarbonyl chloride	**29**	50	0.37

Table 3: Synthesis of amides *via* Staudinger reaction (Glucuronosyl azide **14**).
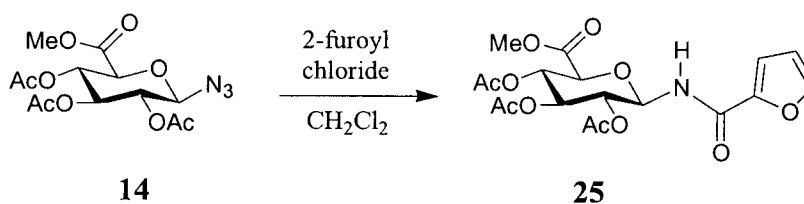
Scheme 22: Furan-2-carboxylic acid (2,3,4-tri-*O*-acetyl-β-D-methyl glucopyranuronate)-amide (**25**).

The reaction of glucuronosyl azide **14** with 2-furoyl chloride also provided an amide product (Table 3). The carbonyl carbon of the amide and the furan ring carbon signals are shown on the ^{13}C NMR spectrum at 157.57 ppm and the region 128.98-138.24 ppm respectively. There is still unreacted 2-furoyl chloride in the mixture according to the spectrum. Also there are signals representing the carbonyl carbon of the carboxylic acid ester and acetyl protecting groups in the range 162.64-172.47 ppm. Again the methyl groups of the acetyl protecting groups are shown around 21.88 ppm. The reaction progress was monitored on the TLC plate and showed the formation of a UV active spot burning at a lower R_f value than that of the starting material **14**.

As for D-glucuronosyl compounds **26-29** (Figure 9), yields of products in the 44-84% range were observed. The ^{1}H NMR spectrum of **27** showed the disappearance of the starting material H-1 doublet signal at 4.71 ppm. Determination of the location of the NH signal was difficult because of the presence of aryl ring protons, shown at ~ 6.5-8.5 ppm, which caused the signal for NH to overlap with those signals. Comparing the results obtained from compounds **25** (Scheme 22) and **29** (Figure 9; five-membered rings with O atom and S atom respectively), the presence of the more electronegative O atom on the compound **25** possibly explains a lower product yield than for amide compound **29**, which suggests a general pattern emerging as will be discussed in detail below.
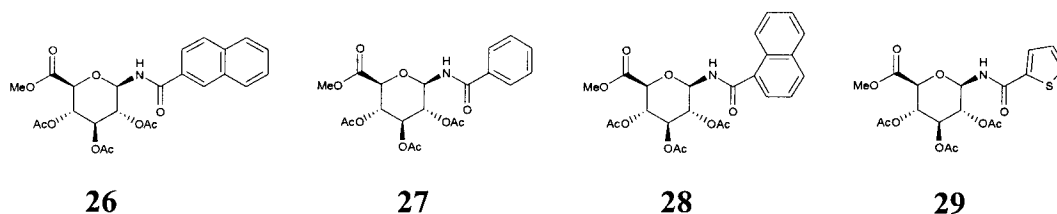
Figure 9: D-Glucuronosyl amide compounds **26-29**.

The results reported here indicate that the reaction rate depends on the electrophilicity of the acid chloride reactant. Similar to the reaction of azide **14** with *p*-nitrobenzoyl chloride, when glucosyl azide **17** was treated with *p*-nitrobenzoyl chloride in the presence of PS-PPh₃, the reaction afforded amide **30** in 93% yield (Scheme 23). Observing the product TLC indicated the formation of a UV active spot burning at a lower R_f value than the starting material.
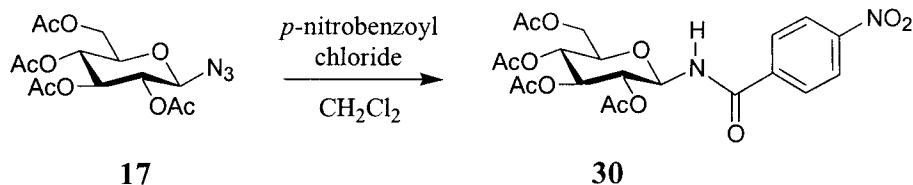
Scheme 23: *p*-Nitrobenzoic acid-(2,3,4,6-tetra-*O*-acetyl-β-D-glucopyranosyl)-amide (**30**).

Investigation of the ^{1}H NMR spectrum showed the disappearance of the doublet signal at 4.64 ppm, which corresponded to the glucosyl azide C1 proton. Appearance of a one-proton signal was observed at 7.32 ppm, indicating the attachment of NH at C1. The formation of product **30** was also evident from the ^{13}C NMR spectrum, which showed the carbonyl carbon of the amide at 166.04 ppm. The acetyl protecting group carbonyl carbon signals are shifted further downfield compared to the amide carbonyl

carbon and they are shown in the region 170.52-172.84 ppm. The methyl groups of the acetyl protecting group signals are again clustered together and appear at ~ 22 ppm. Also evidence for the formation of **30** is that its aryl carbon signals are observed in the region 124.96-139.08 ppm.

Starting material	Acid Chloride	Product	% Yield	R_f value
17	p-nitrobenzoyl chloride	**30**	93	0.31
	2-furoyl chloride	**31**	40	0.18
	2-naphthoyl chloride	**32**	72	0.30
	benzoyl chloride	**33**	55	0.28
	1-naphthoyl chloride	**34**	66	0.31
	2-thiophenecarbonyl chloride	**35**	56	0.31
	1-pyrrolidinoyl chloride	**36**	-	-
	butyryl chloride	**37**	61	0.25
	trimethylacetyl chloride	**38**	17	0.23
	4-fluorobenzoyl chloride	**39**	61	0.33
	isovaleryl chloride	**40**	61	0.30
	nicotinoyl chloride	**41**	40	0.14

Table 4: Synthesis of amides *via* Staudinger reactions using glucosyl azide **17**.

When 2-furoyl chloride was applied to the reaction mixture with glucosyl azide **17**, it afforded a decreased product yield compared to the reaction with p-nitrobenzoyl chloride (Table 4). The results may be explained by comparing the substituents on both acid chlorides. The NO_2 substituent is an electron-withdrawing group whereas the furan ring has the resonance form that can stabilize the partial positive charge of the carbonyl carbon. As a result, the p-nitrobenzoyl chloride possesses a more electrophilic carbonyl

carbon and it is more likely to be attacked faster by a nucleophile. Even though the electrophilicity of the furoyl chloride carbonyl carbon is probably lower, the reaction still afforded amide **31** in 40% yield.
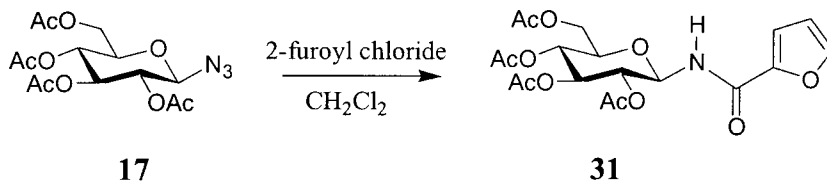

Scheme 24: Furan-2-carboxylic acid-(2,3,4,6-tetra-*O*-acetyl-β-D-glucopyranosyl)-amide (**31**).

The ^{1}H NMR of the reaction residue does not indicate the presence of the starting material, which might be expected to account for the missing 60% of material from this reaction. The 40% yield was probably due to the attachment of the starting material to the polymer-supported triphenylphosphine to a form phosphinimine ylide, which was removed with polymer at the gravity filtration step without having reacted with acid chloride. This also explains the presence of excess acid chloride in the mixture, even though the excess amine polymer was used to try to remove it. The ^{1}H NMR spectrum also showed the evidence of product by indicating a doublet signal at 7.23 ppm with a coupling constant 9.34 Hz that corresponds to the NH atom and the furan proton signals at the range 6.61-7.71 ppm. The signal corresponding to the carbonyl carbon of the amide was seen at 162.85 ppm in the ^{13}C spectrum. The reaction progress was monitored by TLC and showed a UV active spot that burned at a lower R_f value than **17** after a six-hour reaction time.

Importantly, the formation of the amide being affected by the structure of the acid chloride was clearly observed from the synthesis of compound **38** (Scheme 25). After

azide **17** was reacted with polymer-supported triphenylphosphine, the inductive effect of trimethyl substituent apparently plays a significant rule on the nucleophile's access the carbonyl carbon of trimethylacetyl chloride. Not only does inductive electron donation probably affect the activity of the electrophile, there is also the steric hindrance caused by three methyl groups. This was evident from the product yield of only 17%. When comparing acid chloride substituents that are similar in structure, the yields are in the middle range. For example, compounds **32, 33, 34, 35** and **37** (Figure 10) were formed in the range 50-70%yield.
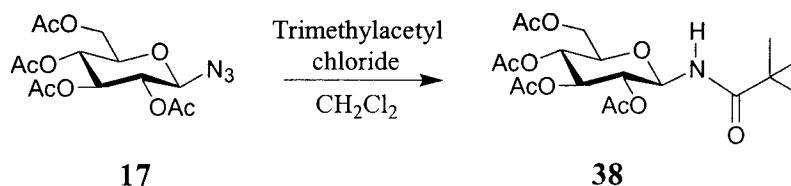
Scheme 25: Trimethyl acetic acid-(2,3,4,6-tetra-*O*-acetyl-β-D-glucopyranosyl)-amide (**38**).
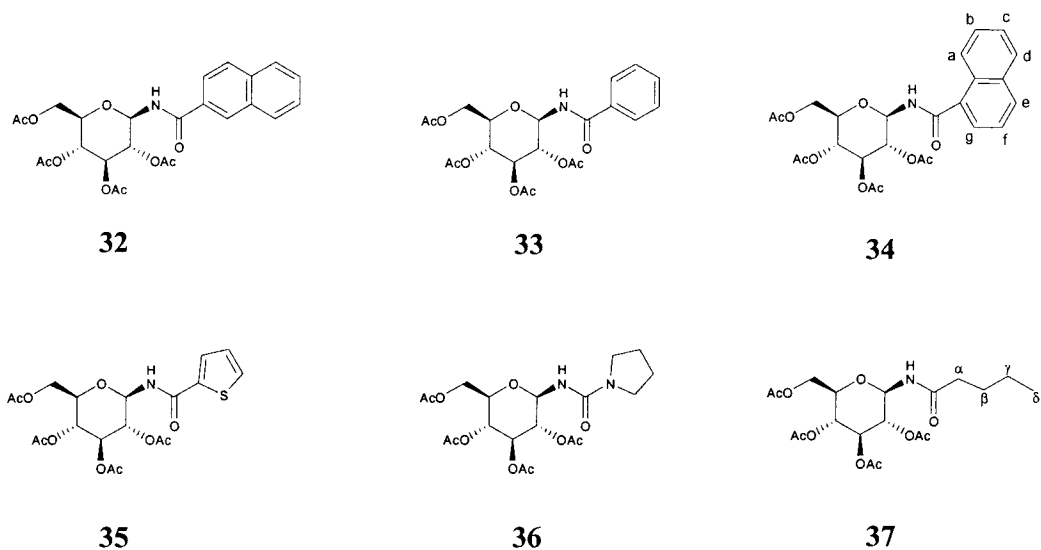
Figure 10: D-Glucosyl amide compounds **32-37**.

Neither the ^{1}H NMR nor ^{13}C NMR spectrum indicated the formation of product 36 during an attempted reaction of glucosyl azide 17 with 1-pyrrolidinoyl chloride. The presence of a lone pair of electrons on the neighboring N atom may stabilize the partial positive of that carbon and cause it to become less electrophilic, thus decreasing the rate of reaction of the phosphonium ylide with that carbon. The transformations of 17 to the amide products 39-41 (Figure 11) were carried out and resulted in a range of product yields. The results obtained from above suggested the same reasoning to explain the electrophilicity of the acid chloride carbonyl carbon. For compound 39, the reaction rate of the ylide with 4-flourobenzoyl chloride is decreased by the electron-withdrawing fluorine atom at the *para* position of the benzene ring.
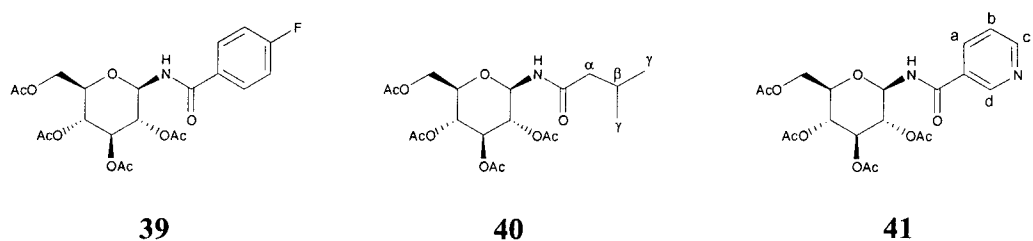
Figure 11: D-Glucosyl amide compounds 39-41.

Compound 40 afforded much higher yield compared to the trimethylacetyl derivative 38 (Scheme 25). The difference between these two compounds is the presence of a methylene group at the alpha position in compound 40, and in addition to steric effects, the inductive effect felt by the carbonyl carbon is less for isovaleroyl chloride. The low yield observed for compound 41 (from nicotinoyl chloride) may be due to the interference of the basic pyridine ring, which needs to be investigated further.

After briefly reviewing the nature of the acid chloride substituent, the formation of the chloroimine intermediate apparently depends on the electrophilicity of the carbonyl

carbon of the acid chloride and also the accessibility of the nucleophile to that carbonyl carbon. In summary, two starting materials, a glucuronosyl and a glucosyl azide, which only differ at the C5 functional group, provided similar results in this study. Thus, a Staudinger-based route to amide synthesis takes place at the C1 of the sugar and the sugar C-5 substituent has little effect on the reaction. Beta stereochemistry is retained in this method even though the reactivity of acid chloride is affected by its substituent. Improvement of the reaction was suggested from the presence of starting material observed on the ^{1}H NMR spectra of several product residues, which suggested that use of polymer-supported reagents require longer reaction time than with PPh_3 itself. Also, due to the loss of starting material attaching to the polymer reagent, the reactive reagents must be selected carefully to achieve optimum results.

5. Attempt for the synthesis of D-ManAcA amide derivative 42.

Based on the results obtained from the reaction of glucuronosyl and glucosyl azides (14 and 17 respectively) with p-nitrobenzoyl chloride, which afforded a high yield of product in both cases, p-nitrobenzoyl chloride was chosen as the reagent for the possible synthesis of benzoyloxyimino amide 42 (Scheme 26). Upon the successful synthesis of benzoyloxyimino azide 13, the amide synthesis was attempted to possibly achieve the desired product 42 using the conditions developed previously. Azide 13 was dissolved in CH_2Cl_2, p-nitrobenzoyl chloride was added followed by PS-PPh_3, and the mixture was stirred and refluxed overnight.
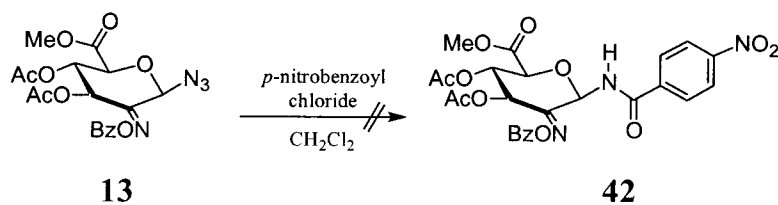
Scheme 26: Attempted Staudinger reaction for the formation of amide **42**.

Using assumptions from the work with glucuronosyl azide **14** and glucosyl azide **17**, an excess of acid chloride was used along with an extended reaction time. Even with this careful approach, the synthesis of D-ManAcA derivative compound, amide **42** could not be obtained as expected, the ^{1}H NMR spectrum of the crude reaction mixture showing multiple products suggesting that azide **13** may decompose under the reaction conditions.

Experimental

General Procedures

The reaction progress was monitored by thin layer chromatography (TLC) with UV light detection since most of the reaction materials are UV active. The TLC plate was treated with a 5% sulfuric acid/ethanol solution to burn the reaction material to provide the indication of the carbohydrate product. Isolation of the product was done by recrystallization and flash chromatography performed with 32-63 μm, 60-Å silica gel. A Bruker Esquire-HP 1100 mass spectrometer was used for low-resolution MS. A Varian Gemini 2000 NMR system was used for ^{1}H and ^{13}C NMR spectroscopy at 400 MHz and 100 MHz respectively, using CDCl$_3$ or D$_6$-DMSO as solvents. Proton and carbon chemical shifts (δ) are recorded in parts per million (ppm). Splitting patterns of multiplets are labeled as follows: s (singlet), d (doublet), dd (doublet of doublets), ddd (doublet of doublet of doublets), t (triplet), q (quartet), and m (multiplet) with coupling constants (J) measured in Hz. X-ray diffraction was also used to determine the solid-state crystal structure of one of the compounds used herein.

Preparation of methyl D-glucopyranuronate (7) from D-glucurono-6,3-lactone (6).[19]

In a 500 mL round-bottom flask equipped with a septum and magnetic stir bar, NaOH (0.02 g, 0.5 mmol) was dissolved in MeOH (250 mL) at room temperature. D-Glucurono-6,3-lactone (6) (4.0 g, 22.7 mmol) was added in 50 mg portions to the mixture and allowed to stir at room temperature for 1 hour to convert the furanose into the pyranose (7).

Preparation of methyl 2,3,4,5-tetra-*O*-acetyl-β-D-glucopyranuronate (8β) from D-glucuronolactone pyranose (7) *via* crystallization of methyl 2,3,4,5-tetra-*O*-acetyl-α/β-D-glucopyranuronate (8).

After concentration of the mixture from the previous experiment *in vacuo* the residue (16 g, 90.9 mmol) **7** was dissolved in dry pyridine (60 mL) and then cooled to 0 °C. Acetic anhydride (60 mL) was slowly added to the mixture, and the solution was allowed to stir at room temperature for 4 hours or until TLC (100% ethyl acetate, product R_f = 0.69) showed consumption of starting material. The mixture was then poured over ice water (300 mL) and the organic product was extracted with methylene chloride (3 x 50 mL). The combined extracts were dried over anhydrous magnesium sulfate, filtered and reduced. In a 500 mL round-bottom flask, the anomers **8 α/β** (33 g, mixture of α/β) were dissolved in isopropanol (200 mL) at 80 °C. The solution was then poured into a 500 mL beaker to encourage the growth of crystals at room temperature to afford 19.8 g of **8β** (58%). The concentration of filtrate gave 12.7 g of a syrup that was mainly **8α** (37%).

^{1}H NMR (CDCl$_3$): δ 2.02, 2.03, 2.11 (4s with one double intensity, 12H total, 4 x COCH$_3$), δ 3.75 (s, 3H, OCH$_3$), 4.17 (d, 1H, H-5, J = 9.52 Hz), 5.13 (dd, 1H, H-2, J = 8.42, 8.42 Hz), 5.23 (dd, 1H, H-4, J = 9.52, 9.52 Hz), 5.30 (dd, 1H, H-3, J = 9.15, 9.15 Hz), 5.75 (d, 1H, H-1, J = 7.87 Hz).

^{13}C NMR (CDCl$_3$): 21.85, 54.20, 70.00, 71.19, 72.84, 74.01, 92.34, 167.68, 169.71, 170.06, 170.31, 170.77.

m/z calculated: 376.0   *m/z* found: 394.0 (+H$_2$O).

Preparation of methyl 3,4,5-tri-*O*-acetyl-α-D-glucopyranosyl bromide (9) from methyl 2,3,4,5-tetra-*O*-acetyl-β-D-glucopyranuronate (8β).

In a 50 mL round-bottom flask equipped with a septum and magnetic stir bar, methyl 2,3,4,5-tetra-*O*-acetyl-β-D-glucopyranuronate (**8β**) (3.0 g, 8.0 mmol) was dissolved in 30% HBr in acetic acid (12 mL). The mixture was stirred at room temperature until TLC (100% ethyl acetate, product R_f = 0.81) showed consumption of starting material (~4 hours). The residue after evaporation *in vacuo* was dissolved in chloroform (60 mL) and washed with cold saturated sodium bicarbonate (20 mL) and water (20 mL). The aqueous layers were extracted with methylene chloride and the organic extracts were dried over anhydrous magnesium sulfate. The extracts were filtered and reduced to afford 2.8 g (7.0 mmol) of **9** as a brown syrup (87%).

^{1}H NMR (CDCl₃): δ 2.05, 2.09 (3s with one double intensity, 9H total, 3 x COCH₃), 3.75 (s, 3H, OCH₃), 4.57 (d, 1H, H-5, J = 10.25 Hz), 4.84 (dd, 1H, H-2, J = 4.02, 4.21 Hz), 5.23 (dd, 1H, H-3, J = 9.89, 9.89 Hz), 5.60 (dd, 1H, H-4, J = 9.70, 9.70 Hz), 6.63 (d, 1H, H-1, J = 4.03 Hz).

^{13}C NMR (CDCl₃): δ 21.89, 62.06, 68.24, 71.25, 71.70, 73.17, 87.64, 170.38, 170.72, 170.78, 171.44.

m/z calculated: 397.17   *m/z* found (ESI): 415.8 (+H₂O).

Formation of methyl 3,4,5-tri-*O*-acetyl-2,6-anhydro-D-*lyxo*-hex-5-enonate (3) from methyl 3,4,5-tri-*O*-acetyl-α-D-glucopyranosyl bromide (9).

To an ice-cooled stirred solution of methyl 3,4,5-tri-*O*-acetyl-α-D-glucopyranosyl bromide (5.8 g, 14.7 mmol) and tetrabutylammonium bromide (4.7 g, 14.7 mmol) in

DMF (120 mL) in a 250 mL round-bottom flask equipped with septa and a magnetic stir bar, was added diethylamine (2.3 mL, 22 mmol) dropwise. The mixture was stirred at room temperature until TLC (100% ethyl acetate, product R_f = 0.74) showed consumption of starting material (~20 hours) and then neutralized with an acidic resin (IRC-50). The reaction mixture was filtered to remove the acidic resin and then partitioned between ice water (15 mL) and methylene chloride (15 mL). The organic phase was washed with 1 M HCl (50 mL), saturated sodium bicarbonate (50 mL) and water (50 mL). The organic product was extracted with methylene chloride and the combined extracts were dried over magnesium sulfate. Evaporation of the solvent gave a residue (3.79 g), which was purified by elution from a column of silica gel (2:1 hexane: ethyl acetate). The major fraction was concentrated to give 3.2 g (68%) of glycal **3** as a black syrup.

^{1}H NMR (CDCl$_3$): δ 2.02, 2.11, 2.15 (3s, 9H total, 3 x COCH$_3$), 3.81 (s, 3H, OCH$_3$), 4.84 (d, 1H, H-5, J = 2.20 Hz), 5.39 (d, 1H, H-3, J = 2.47 Hz), 5.47 (dd, 1H, H-4, J = 2.38, 2.38 Hz), 6.83 (s, 1H, H-1).

^{13}C NMR (CDCl$_3$): δ 21.94, 22.07, 22.10, 53.84, 61.51, 69.17, 73.44, 128.43, 140.11, 167.56, 170.14, 170.33, 170.41.

m/z calculated: 316.08   *m/z* found (ESI): 257.0 (-CO$_2$CH$_3$).

Preparation of the oxime of methyl 3,4-di-*O*-acetyl-1,5-anhydro-D-fructuronate (10) from methyl 3,4,5-tri-*O*-acetyl-2,6-anhydro-D-*lyxo*-hex-5-enonate (3).

Methyl 3,4,5-tri-*O*-acetyl-2,6-anhydro-D-*lyxo*-hex-5-enonate **(3)** (5.5 g, 17.4 mmol) was dissolved in dry pyridine (120 mL) containing hydroxylamine hydrochloride

(7.3 g, 100 mmol) and placed in a 250 mL round-bottom flask equipped with a septum and magnetic stir bar. The solution was stirred at room temperature for 20 hours when TLC (100% ethyl acetate, product $R_f = 0.65$) showed consumption of starting material. After concentration of the mixture the residue was diluted with dichloromethane (400 mL). The solution was then washed with 1 M HCl (200 mL), saturated Na_2SO_4 (200 mL), and water (3 x 200 mL). The combined organic extracts were dried over anhydrous magnesium sulfate, filtered and reduced to give 3.25 g of **10** as a yellow solid (65%).

^{1}H NMR (CDCl$_3$): δ 2.07, 2.12 (2s, 6H total, 2 x COCH$_3$), 3.81 (s, 3H, OCH$_3$), 4.34 (d, 1H, H-5, $J = 4.21$ Hz), 4.69, 4.86 (dd, 2H, H-1, $J = 15.74$, 15.74 Hz), 5.44 (dd, 1H, H-4, $J = 4.67$, 4.67 Hz), 5.47 (d, 1H, H-3, $J = 4.76$ Hz).

^{13}C NMR (CDCl$_3$): δ 21.88, 22.10, 53.80, 60.37, 69.34, 70.88, 75.35, 150.21, 169.50, 169.93, 170.41.

m/z calculated: 289.02 m/z found: 230.1 (-CO$_2$CH$_3$).

Formation of the *O*-benzoyloxime of methyl 3,4-di-*O*-acetyl-1,5-anhydro-D-fructuronate (11) by addition of benzoyl chloride to methyl 3,4-di-*O*-acetyl-1,5-anhydro-D-fructuronate oxime (10).

A 25 mL round-bottom flask containing methyl 3,4-di-*O*-acetyl-1,5-anhydro-D-fructuronate **(10)** (0.30 g, 1.0 mmol) dissolved in dry pyridine (10 mL) was equipped with a septum and magnetic stir bar. Benzoyl chloride (1.2 mL, 10 mmol) was added dropwise *via* syringe to the ice-cooled stirred solution. The reaction mixture was allowed to stir for 4 hours or until TLC (100% ethyl acetate, product $R_f = 0.51$) showed consumption of starting material. The solution was poured over ice-water (20 mL) and

extracted with methylene chloride (3 x 5 mL). The organic layers were combined, washed with 1M HCl (10 mL), 5% aqueous NaHCO$_3$ (10 mL), and water (3 x 10 mL), dried over MgSO$_4$, and evaporated to give 0.32 g of 11 as a yellow solid (77%).

^{1}H NMR (CDCl$_3$): δ 2.10, 2.14 (2s, 6H, 2 x COCH$_3$), 3.84 (s, 3H, OCH$_3$), 4.46 (d, 1H, H-5, J = 3.48 Hz), 4.95, 5.03 (dd, 2H, H-1, J = 15.74, 15.74 Hz), 5.58 (dd, 1H, H-4, J = 4.12, 4.12 Hz), 5.70 (d, 1H, H-3, J = 4.58 Hz), 7.49 (t, 2H, m-Ar-H), 7.62 (t, 1H, p-Ar-H), 8.03 (d, 2H, o-Ar-H, J = 8.51 Hz).

^{13}C NMR (CDCl$_3$): δ 21.85, 22.07, 53.88, 60.68, 68.86, 70.27, 74.92, 128.95, 129.71, 130.67, 130.81, 134.93, 158.49, 163.70, 169.23, 171.26.

m/z calculated: 393.3 m/z found (ESI): 271.9 (-CO$_2$Ph).

Preparation of methyl 3,4-di-*O*-acetyl-2-(benzoyloxyimino)-1-bromo-2-deoxy-α-D-*arabino*-hexopyranuronate (12) by radical substitution of 11.

In a 50 mL round-bottom flask, a solution of benzoyloxime 11 (1.1 g, 2.8 mmol) and *N*-bromosuccinimide (0.57 g, 3.2 mmol) in tetrachloromethane (25 mL) was irradiated with a 250 W lamp under gentle reflux for 30 minutes. The solution was cooled to 0 °C to encourage the formation of precipitate to remove the succinimide byproduct. After removing the precipitate *via* gravity filter, the filtrate was evaporated under vacuum. The residue was partitioned between methylene chloride (5.0 mL) and water (10 mL). The aqueous layer was extracted with methylene chloride (3 x 3.0 mL) to ensure the extraction of organic material. Combined organic layers were washed with water (5.0 mL), and again, the aqueous layer was extracted with methylene chloride (3 x

3.0 mL) to ensure the collection of organic material. The organic layers were combined, dried over $MgSO_4$, and evaporated under vacuum to yield 1.3 g of **12** (96%).

^{1}H NMR ($CDCl_3$): δ 2.12, 2.21 (2s, 6H total, 2 x $COCH_3$), 3.80 (s, 3H, OCH_3), 4.67 (d, 1H, H-5, J = 9.34 Hz), 5.48 (dd, 1H, H-4, J = 9.52, 9.52 Hz), 6.24 (d, 1H, H-3, J = 9.52 Hz), 7.43 (s, 1H, H-1), 7.51 (m, 2H, m-Ar-H), 7.64 (m, 1H, p-Ar-H), 8.04 (m, 2H, o-Ar-H).

^{13}C NMR ($CDCl_3$): δ 21.78, 67.90, 68.10, 69.43, 73.60, 95.47, 128.548, 129.71, 130.73, 130.95, 155.52, 162.71, 166.95, 170.25.

m/z calculated: 472.24 m/z found: 490.99 (+H_2O).

Preparation of methyl 3,4-di-*O*-acetyl-2-(benzoyloxyimino) azide 13 by a stereospecific S_N2 displacement of α-glycosyl bromide 12.

In a 25 mL round-bottom flask, sodium azide (0.09 g, 1.39 mmol) was added to a mixture of α-glycosyl bromide (0.13 g, 0.28 mmol) and acetone : water (5 : 1, 10 mL : 2 mL). The mixture was gently refluxed for 3 hours or until TLC (1:1, hexane : ethyl acetate, product R_f = 0.47) showed consumption of starting material. The reaction mixture was poured over water (20 mL) and extracted with methylene chloride (3 x 10 mL). The organic layers were combined, dried over $MgSO_4$, and concentrated to give **13** (56%) as brown syrup.

^{1}H NMR ($CDCl_3$): δ 2.06, 2.10 (2s, 6H total, 2 x $COCH_3$), 3.77 (s, 3H, OCH_3), 4.58 (d, 1H, H-5, J = 9.34 Hz), 5.29 (dd, 1H, H-4, J = 9.34, 9.34 Hz), 5.73 (d, 1H, H-3, J = 9.25 Hz), 6.60 (s, 1H, H-1), 7.45 (m, 2H, m-Ar-H), 7.61 (m, 1H, p-Ar-H), 8.35 (m, 1H, o-Ar-H).

Preparation of methyl 2,3,4-tri-*O*-acetyl-α-D-glucopyranuronosyl bromide (9) from methyl 2,3,4,5-tetra-*O*-acetyl-α-D-glucopyranuronate (8α).

In a 50 mL round-bottom flask equipped with a septum and magnetic stir bar, methyl 2,3,4,5-tetra-*O*-acetyl-β-D-glucopyranuronate (8α) (3.0 g, 8.0 mmol) was dissolved in 30% HBr in acetic acid (12 mL). The mixture was stirred at room temperature until TLC (100% ethyl acetate, product R_f = 0.81) showed consumption of starting material (~4 hours). The residue left after evaporation *in vacuo* was dissolved in chloroform (6 mL) and washed with cold saturated sodium bicarbonate (20 mL) and water (20 mL). The aqueous layers were extracted with methylene chloride (3 x 5 mL) and the organic extracts were dried over anhydrous magnesium sulfate. The extracts were filtered and reduced to afford 2.8 g (7.0 mmol) of 9 as brown syrup (86%).

Synthesis of glucuronosyl azide 14 from methyl 2,3,4-tri-*O*-acetyl-α-D-glucopyranosyl bromide 9.

In a 100 mL round-bottom flask equipped with a septum inlet and magnetic stir bar, 5 equivalents of sodium azide (2.16 g, 33.24 mmol) was added to a solution of bromide 9 (2.64 g, 6.65 mmol) in acetone : water (5:1, 30.0 mL : 6.0 mL). The mixture was refluxed for 3 hours when TLC (1:1, hexane : ethyl acetate, product R_f = 0.65) showed consumption of the starting material. Upon completion of the reaction, the mixture was reduced to a dark yellow residue, which was dissolved in water (50 mL) and extracted with methylene chloride (3 x 10 mL). The combined organic extracts were dried over anhydrous $MgSO_4$, filtered and reduced to give glucuronosyl azide 14 as a yellow solid (54%).

^{1}H NMR (CDCl$_3$): δ 2.02, 2.03, 2.08 (3s, 9H total, 3 x COCH$_3$), 3.77 (s, 3H, OCH$_3$), 4.11 (d, 1H, H-5, J = 8.60 Hz), 4.71 (d, 1H, H-1, J = 8.79 Hz), 4.96 (dd, 1H, H-2, J = 8.79, 8.79 Hz), 5.26 (m, 1H, H-3, H-4).

^{13}C NMR (CDCl$_3$): δ 21.81, 54.25, 70.33, 71.89, 73.11, 75.27, 89.10, 167.42, 170.03, 170.19, 170.85.

m/z calculated: 359.29   *m/z* found (ESI): 377.0 (+H$_2$O).

Preparation of 2,3,4,6-tetra-*O*-acetyl-β-D-glucopyranosyl bromide (16) from 1,2,3,4,6-penta-*O*-acetyl-β-D-glucose (15).

In a 100 mL round-bottom flask equipped with a septum and magnetic stir bar, penta-*O*-acetyl-β-D-glucose (15) (6.30 g, 16.14 mmol) was dissolved in 30% HBr in acetic acid (24.0 mL). The solution was stirred at room temperature for 4 hours when TLC (1:1, hexane : ethyl acetate, product R$_f$ = 0.52) showed consumption of starting material. The residue left after evaporation *in vacuo* was dissolved in chloroform (200 mL) and washed with cold saturated sodium bicarbonate (150 mL) and water (150 mL). The combined aqueous layers were extracted with methylene chloride (3 x 50 mL) and the organic extracts were dried over anhydrous magnesium filtrate, dried over MgSO$_4$, and concentrated to afford 16 as brown syrup.

^{1}H NMR (CDCl$_3$): δ 2.03, 2.05, 2.09, 2.10 (4s, 12H total, 4 x COCH$_3$) 4.13 (d, 1H, H-2, J = 12.6 Hz), 4.13 (m, 1H, H-6), 4.31 (m, 2H, H-5, H-6') 4.83 (dd, 2H, H-6, J = 4.10, 9.98 Hz), 5.16 (dd, 1H, H-3, J = 9.89, 9.89 Hz), 5.55 (dd, 1H, H-4, J = 9.70, 9.70 Hz), 6.61 (d, 1H, H-1, J = 4.0 Hz).

^{13}C NMR (CDCl$_3$): δ 21.76, 21.82, 21.91, 21.98, 22.02, 62.06, 71.25, 71.70, 73.23, 87.64, 170.38, 170.72, 170.78, 171.44.

m/z calculated: 412.95   *m/z* found: 430.03 (+H$_2$O).

Preparation of glucosyl azide 17 by reacting α-glycosyl bromide 16 with sodium azide *via* S$_N$2 reaction.

Sodium azide (1.3 g, 20.4 mmol) was added to a 100 mL round-bottom flask containing α-glucosyl bromide **16** (6.5 g, 15.7 mmol), which was dissolved in acetone : water (5 : 1, 60 mL : 12 mL). The mixture was gently refluxed for 3 hours until TLC (1 : 1, hexane : ethyl acetate, product R$_f$ = 0.45) showed consumption of starting material. The mixture was washed with water (50 mL) and extracted with methylene chloride (3 x 25 mL). The combined organic layers were dried over MgSO$_4$ and reduced to give **17** (91%) as a white solid.

^{1}H NMR (CDCl$_3$): δ 2.01, 2.03, 2.07, 2.10 (4s, 12H total, 4 x COCH$_3$), 3.79 (ddd, 1H, H-5, *J* = 2.29, 4.76, 9.52 Hz), 4.16, (dd, 1H, H-6, *J* = 2.38, 12.45 Hz), 4.27 (dd, 1H, H-6', *J* = 4.76, 12.45 Hz), 4.64 (d, 1H, H-1, *J* = 8.97 Hz), 4.95, 5.10, 5.21 (m, 3H, H-2, H-3, H-4).

^{13}C NMR (CDCl$_3$): δ 21.64, 21.88, 21.91, 22.13, 62.77, 68.92, 71.70, 73.76, 75.06, 88.95, 170.12, 170.22, 171.12, 171.52.

m/z calculated: 373.11   *m/z* found: 390.8 (+H$_2$O).

Synthesis of carbohydrate-derived triazoles *via* cycloadditions on glucuronosyl and glucosyl azides (14 and 17 respectively).

Six 15 x 150 mm test tubes, each of which contained azide compound (100 mg: glucuronic acid azide, 0.28 mmol; glucosyl azide, 0.27 mmol) that was dissolved in toluene (5.0 mL) were placed on the parallel synthesizer rack. To each test tube, different types of alkynes (1.3 equivalents) were added. The mixtures were refluxed at 110 °C for six hours. The solvents were evaporated *in vacuo* and the products were purified by elution from a column of silica gel. The major fractions were concentrated to obtain the products.

Alkynes	Alkynes
Diphenyl acetylene	Propiolic acid
Phenyl acetylene	Ethyl propiolate
Trimethylsilyl propiolate	Diethylacetylene dicarboxylate

Table 5: Alkyne reagents.

1-(methyl 2,3,4-tri-*O*-acetyl-β-D-glucopyranuronosyl)-1*H*-[1,2,3]triazol-4-(and 5-) carboxylic acids (18).
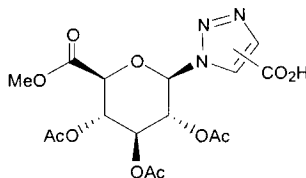
^{1}H NMR (CDCl$_3$): δ 1.86, 2.04, 2.13, 2.15, (s, 9H total for isomers, 3 x COCH$_3$), 3.74 (s, 3H, OCH$_3$), 4.33 (d, 1H, H-5), 5.36 (dd, 1H, H-2), 5.48 (dd, 2H, H-3, H-4), 5.83 (d, 1H, H-1), 7.74, 7.87 (s, 1H, triazole isomers).

^{13}C NMR (CDCl$_3$): δ 21.62, 54.48, 69.23, 70.10, 71.11, 72.96, 74.13, 75.98, 82.73, 86.40, 93.25, 99.65, 129.22, 130.02, 167.07, 167.61, 169.65, 169.83, 170.00, 170.27, 170.66, 170.78, 170.97.

m/z calculated: 445.38   *m/z* found: 428.03 (- H$_2$O).

1-(methyl 2,3,4-tri-*O*-acetyl-β-D-glucopyranuronosyl)-1*H*-[1,2,3]triazol-4-(and 5-) carboxylic acid ethyl esters (19).
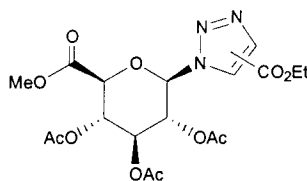
^{1}H NMR (CDCl$_3$): δ 1.36 (t, 3H, CO$_2$CH$_2$CH$_3$ for isomers), 1.85, 2.01, 2.03 (3s, 9H total, 3 x COCH$_3$), 3.72 (s, 3H, OCH$_3$), 4.36 (q, 2H, CO$_2$CH$_2$CH$_3$ for isomers), 5.25 (d, 1H, H-

5), 5.34 (dd, 1H, H-2), 5.46 (dd, 2H, H-3, H-4), 5.99 (d, 1H, H-1, J = 8.97 Hz), 8.10, 8.44

(s, 1H, triazole isomers).

^{13}C NMR (CDCl$_3$): δ 15.51, 21.80, 54.39, 69.96, 71.30, 72.72, 75.91, 86.61, 126.27,

130.09, 161.04, 166.97, 169.77, 170.25, 170.62.

m/z calculated: 473.16   *m/z* found: 458.03 (- H$_2$O).

1-(methyl 2,3,4-tri-*O*-acetyl-β-D-glucopyranuronosyl)-1*H*-[1,2,3]triazol-4,5-dicarbo-xylic acid diethyl ester (20).
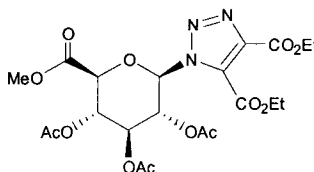
^{1}H NMR (CDCl$_3$): δ 1.31 (t, 3H, CO$_2$CH$_2$C$\underline{H}_3$, J = 7.14 Hz), 2.04, 2.05 (2s, 3H, 3 x

COCH$_3$), 3.72 (s, 3H, OCH$_3$), 4.25 (d, 1H, H-5), 4.28 (2q, 2H, 2 x CO$_2$C$\underline{H}_2$CH$_3$, J = 7.14

Hz), 5.31, 5.45 (dd, 1H, H-3, H-4, J = 9.52, 9.70 Hz), 5.97 (dd, 1H, H-2, J = 9.34, 9.34

Hz), 6.17 (d, 1H, H-1, J = 9.34 Hz).

^{13}C NMR (CDCl$_3$): δ 15.11, 15.41, 21.70, 54.31, 69.69, 70.60, 73.12, 75.94, 86.26,

131.92, 141.23, 159.06, 160.48, 166.82, 169.43, 170.17, 170.93.

m/z calculated: 529.15   *m/z* found: 317.0 (-C$_8$H$_{10}$N$_3$O$_4$).

1-(2,3,4,5-tetra-*O*-acetyl- β-D-glucopyranosyl)-1*H*-[1,2,3]triazol-4-(and 5-)carboxylic acids (21).
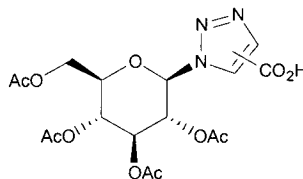
¹H NMR (CDCl₃): δ 2.00 (m, 3H each, 8 x COCH₃), 3.04, 3.08 (2s, 1H, triazole isomers), 3.85, 4.01 (ddd, isomers, H-5), 4.09, 4.25 (dd, 4H, H-6), 5.13 (m, H-2, H-4), 5.24 (t, 1H, H-3, *J* = 9.25 Hz), 5.75 (d, 1H, H-1, *J* = 8.06 Hz).

¹³C NMR (CDCl₃): δ 21.71, 65.58, 68.85, 71.37, 73.71, 76.18, 86.62, 122.97-151.35, 169.91, 170.23, 170.84, 171.39.

m/z calculated: 459.15   *m/z* found: 472.05.

1-(2,3,4,5-tetra-*O*-acetyl-β-D-glucopyranosyl)-1*H*-[1,2,3]triazol-4-(and 5-) carboxylic acid ethyl esters (22).
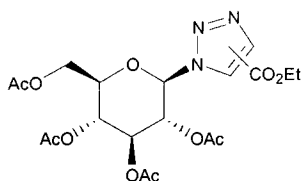
¹H NMR (CDCl₃): δ 1.35 (t, 3H, CO₂CH₂C<u>H</u>₃, *J* = 7.23 Hz), 1.97-2.03 (4s, 12H total, 4 x COCH₃), 4.03 (q, 2H, CO₂C<u>H</u>₂CH₃), 4.24 (dd, 2H, H-6), 4.37 (ddd, 1H, H-5), 5.21 (dd, 1H, H-2), 5.39 (dd, 1H, H-4), 6.08 (dd, 1H, H-3), 6.36 (d, 1H, H-1, *J* = 9.52 Hz), 8.09, 8.38 (s, 1H, triazole isomers).

^{13}C NMR (CDCl$_3$): δ 16.75, 25.05, 62.72, 63.34, 68.68, 71.57, 73.47, 76.35, 86.95, 139.25, 141.82, 158.61, 161.08, 169.82, 170.23, 170.746, 171.35.

m/z calculated: 471.10   *m/z* found: 331.03 (-C$_8$H$_{10}$N$_3$O$_4$).

1-(2,3,4,5-tetra-*O*-acetyl-β-D-glucopyranosyl)-1*H*-[1,2,3]triazol-4,5-dicarboxylic acid diethyl ester (23).
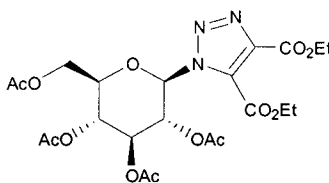
^{1}H NMR (CDCl$_3$): δ 1.22 (t, 3H, CO$_2$CH$_2$C$\underline{H}_3$, *J* = 7.14 Hz), 2.01, 2.03, 2.04 (3s, 12H total, 4 x COCH$_3$), 4.09 (q, 2H, CO$_2$C$\underline{H}_2$CH$_3$, *J* = 7.14 Hz), 3.95 (m, 1H, H-5), 4.25 (m, 2H, H-6, H-6'), 5.22 (dd, 1H, *J* = 9.79, 9.79 Hz), 5.38 (dd, 1H, H-3, *J* = 9.43, 9.43 Hz), 5.94 (dd, 1H, H-4, *J* = 9.43, 9.43 Hz), 6.11 (d, 1H, H-1, *J* = 9.34 Hz).

^{13}C NMR (CDCl$_3$): δ 15.36, 21.87, 61.57, 62.50, 63.25, 64.41, 68.41, 70.73, 74.06, 76.25, 86.47, 131.75, 141.36, 158.95, 160.58, 169.45, 170.12, 171.10, 171.34.

m/z calculated: 543.17   *m/z* found: 331.03 (-C$_8$H$_{10}$N$_3$O$_4$).

Synthesis of amides: Staudinger reactions

Formation of glycosyl amides from *N*-glycosyl azides (glucuronosyl and glucosyl azides 14 and 17)

In each of 12 test tubes was placed azide compound (100 mg: glucuronosyl azide **14**, 0.28 mmol; or glucosyl azide **17**, 0.27 mmol) dissolved in dry methylene chloride (5.0 mL). Polymer-supported triphenylphosphine (116 mg, 0.35 mmol) was added to each tube and the mixture was allowed to release the nitrogen gas. Once the nitrogen gas had been released, twelve different types of acid halides were added. The mixtures were refluxed at 40 °C for six hours. The mixture was gravity filtered into another test tube to remove polymer-supported triphenyphosphine oxide. Polymer-bound tris (2-aminoethyl) amine (100 mg, 0.44 mmol) was added to each test tube and the mixture allowed to stir for two hours at room temperature. Polymer was removed *via* gravity filtration and the filtrate was concentrated *in vacuo*.

Acid chloride	Acid chloride
p-nitrobenzoyl chloride	1-pyrrolidinoyl chloride
2-furoyl chloride	butyryl chloride
2-naphthoyl chloride	trimethylacetyl chloride
benzoyl chloride	4-fluorobenzoyl chloride
1-naphthoyl chloride	isovaleryl chloride
2-thiophenecarbonyl chloride	nicotinoyl chloride

Table 6: Acid chloride reagents used.

***p*-Nitrobenzoic acid-(methyl 2,3,4-tri-*O*-acetyl-β-D-glucopyranuronosyl)-amide (24).**
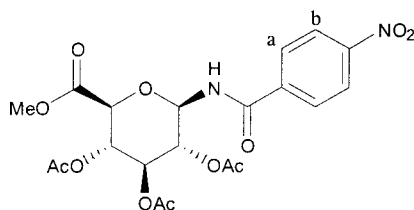
^{1}H NMR (CDCl$_3$): δ 2.05, 2.06, 2.06 (3s, 9H, 3 x COCH$_3$), 3.73 (s, 3H, OCH$_3$), 4.25 (d, 1H, H-5, J = 10.07 Hz), 5.09 (dd, 1H, H-4, J = 9.61, 9.70 Hz), 5.18 (dd, 1H, H-3, J = 9.61, 9.61 Hz), 5.47 (dd, overlapping, 2H, H-1, H-2, J = 8.97, 9.70 Hz), 7.36 (d, 1H, NH, J = 8.97 Hz), 7.93 (d, 2H, Ar-Ha, J = 9.09 Hz), 8.32 (d, 2H, Ar-Hb, J = 9.10 Hz).

^{13}C NMR (CDCl$_3$): δ 21.81, 54.14, 70.58, 71.42, 71.80, 72.81, 77.78, 79.58, 124.87, 129.72, 139.05, 150.94, 166.43, 168.13, 170.52, 170.65, 172.16.

m/z calculated: 482.12   *m/z* found: 483.18 (+ H$^+$).

Furan-2-carboxylic acid (methyl 2,3,4-tri-*O*-acetyl-β-D-glucopyranuronosyl)-amide (25).
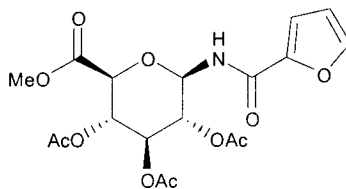
^{1}H NMR (CDCl$_3$): δ 1.95-2.14 (s, 9H total, 3 x COCH$_3$), 3.73 (s, 3H, OCH$_3$), 4.58 (d, 1H, H-5, J = 4.58 Hz), 5.20-5.42 (m, 4H, H-1, H-2, H-3, H-4), 6.16-7.57 (signals corresponding to NH and furan protons).

^{13}C NMR (CDCl$_3$): δ 21.82, 54.12, 70.58, 70.77, 71.12, 72.99, 74.99, 78.85, 113.39, 129.51, 135.09, 146.06, 159.08, 168.05, 170.47, 170.65, 171.72.

Unreacted 2-furoyl chloride was observed: ^{13}C NMR (CDCl$_3$): 113.27, 117.08, 122.83, 122.75, 153.81.

m/z calculated: 427.11   *m/z* found: 428.14 (+ H$^+$).

2-Naphthoic acid-(methyl 2,3,4-tri-*O*-acetyl-β-D-glucopyranuronosyl)-amide (26).
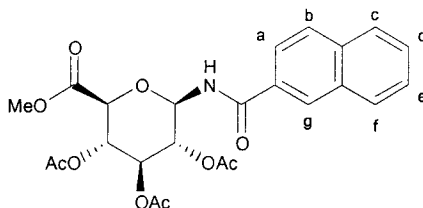
^{1}H NMR (CDCl$_3$): δ 2.06, 2.09 (2s, 9H total, 3 x COCH$_3$), 3.76 (s, 3H, OCH$_3$), 4.28 (d, 1H, H-5, J = 10.07 Hz), 5.09 (dd, 1H, H-4, J = 9.02, 9.66 Hz), 5.21 (dd, 1H, H-1, J = 9.38, 9.38 Hz), 5.49 (dd, 1H, H-2, J = 9.52, 9.52 Hz), 5.62 (dd, 1H, H-3, J = 9.61, 9.61 Hz), 6.83 (d, 1H, NH, J = 9.70 Hz), 7.46 (m, 2H, Ar-Hc, ,Ar-Hf, J = 7.69 Hz), 7.55 (m, 2H, Ar-Hd, Ar-He), 7.87 (m, 1H, Ar-Hg, J = 6.77 Hz), 7.96 (m, 1H, Ar-Hd, J = 8.24 Hz), 8.34 (m, 1H, Ar-Ha, J = 8.15 Hz).

^{13}C NMR (CDCl$_3$): δ 21.69, 54.12, 70.69, 71.46, 71.84, 72.94, 75.03, 73.79, 124.40, 127.88, 128.62-130.35 (multiple signals), 130.77, 133.43, 136.09, 168.16, 168.25, 170.53, 170.69, 172.30.

Benzoic acid-(methyl 2,3,4-tri-*O*-acetyl-β-D-glucopyranuronosyl)-amide (27).
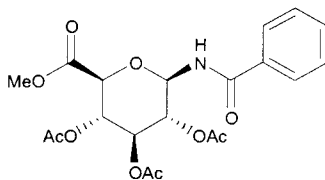
^{1}H NMR (CDCl$_3$): δ 1.95, 1.96, 1.98 (s, 9H total, 3 x COCH$_3$), 3.62 (s, 3H, OCH$_3$), 4.19

(d, 1H, H-5, J = 10.07 Hz), 5.07 (m, 2H, H-3, H-5), 5.40 (dd, 1H, H-2, J = 9.62 Hz), 5.47

(dd, 1H, H-1, J = 9.43 Hz), 7.33-7.71 (m, 6H, Ar-H, NH).

^{13}C NMR (CDCl$_3$): δ 21.82, 54.14, 70.91, 71.56, 72.82, 75.17, 79.84, 128.18, 129.78,

133.51, 168.02, 168.08, 170.47, 170.56, 172.38.

m/z calculated: 437.13   *m/z* found: 438.26 (+H$^+$).

1-Naphthoic acid-(methyl 2,3,4-tri-*O*-acetyl-β-D-glucopyranuronosyl)-amide (28).
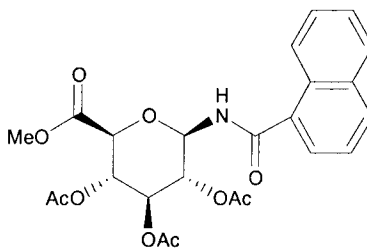
^{1}H NMR (CDCl$_3$): δ 2.06, 2.09 (s, 3H, 3 x COCH$_3$), 3.76 (s, 3H, OCH$_3$), 4.28 (d, 1H, H-

5, J = 10.07 Hz), 5.09 (dd, 1H, H-3, J = 9.52, 9.70 Hz), 5.21 (dd, 1H, H-4, J = 9.34, 10.07

Hz), 5.49 (dd, 1H, H-2, J = 9.52, 9.70 Hz), 5.62 (dd, 1H, H-1, J = 9.52, 9.70 Hz), 6.82 (d,

1H, NH, J = 9.70 Hz), 7.44-8.35 (m, 7H, Ar-H).

Thiophene-2-carboxylic acid-(methyl 2,3,4-tri-*O*-acetyl-β-D-glucopyranuronosyl)-amide (29).
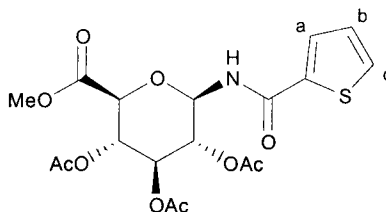
^{1}H NMR (CDCl$_3$): δ 2.04, 2.05, 2.06 (3s, 9H total, 3 x OCH$_3$), 3.74 (s, 3H, OCH$_3$), 4.23 (d, 1H, H-5, J = 10.07 Hz), 5.06 (dd, 1H, H-4, J = 9.70, 9.70 Hz), 5.19 (dd, 1H, H-1, J = 9.70, 9.70 Hz), 5.41 (dd, 1H, H-2, J = 8.24, 8.24 Hz), 5.45 (dd, 1H, H-3, J = 8.51, 9.63 Hz), 6.97 (d, 1H, NH, J = 8.79 Hz), 7.09 (dd, 1H, Hb, J = 3.30, 3.84 Hz), 7.48 (d, 1H, Hc, J = 3.85 Hz), 7.54 (d, 1H, Ha, J = 3.84 Hz).

^{13}C NMR (CDCl$_3$): δ 21.88, 54.08, 70.88, 81.49, 72.79, 75.00, 75.08, 79.78, 128.98-138.24 (thiophenecarbonyl chloride), 157.57, 162.64, 167.98, 170.58, 172.47.

p-Nitrobenzoic acid-(2,3,4,6-tetra-*O*-acetyl-β-D-glucopyranosyl)-amide (30).
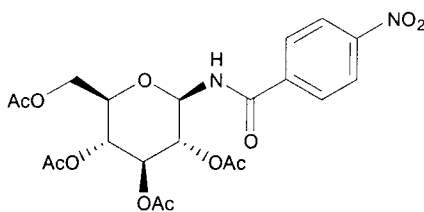
^{1}H NMR (CDCl$_3$): δ 2.03, 2.04, 2.05 (3s, 12H total, 4 x COCH$_3$), 3.91 (ddd, 1H, H-5), 4.09, 4.31 (dd, 2H, H-6, J = 12.45, 12.54 Hz), 5.05 (m, 2H, H-3, H-4), 5.39 (dd, 1H, H-2, J = 9.70, 8.97 Hz), 7.32 (d, 1H, NH, J = 8.79 Hz), 7.92 (d, 1H, H-1, J = 8.79 Hz), 8.30 (m, 4H, Ar-H).

^{13}C NMR (CDCl$_3$): δ 21.97, 62.63, 69.18, 72.09, 73.41, 74.87, 80.06, 124.96, 129.40, 129.60, 139.08, 151.05, 166.04, 170.77, 171.52, 172.84.

m/z calculated: 497.15   *m/z* found: 438.0 (-CO$_2$CH$_3$).

Furan-2-carboxylic acid-(2,3,4,6-tetra-*O*-acetyl-β-D-glucopyranosyl)-amide (31).
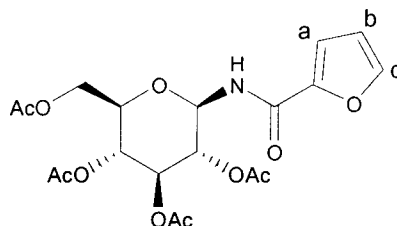
^{1}H NMR (CDCl$_3$): δ 2.02, 2.03, 2.04, 2.07 (4s, 12H total, 4 x COCH$_3$), 3.88 (ddd, 1H, H-5, J = 2.11, 4.89, 10.16 Hz), 4.09, 4.32 (dd, 2H, H-6, J = 12.45, 12.45 Hz), 5.06 (dd, 1H, H-3, J = 9.06, 9.06 Hz), 5.10 (dd, 1H, H-4, J = 9.34, 9.70 Hz), 5.36 (dd, 1H, H-2, J = 9.52, 9.52 Hz), 5.40 (dd, 1H, H-1, J = 9.34, 9.52 Hz), 6.61 (dd, 1H, Hb, J = 1.83, 3.48 Hz), 7.23 (d, 1H, NH, J = 9.34 Hz), 7.41 (m, 1H, Ha), 7.71 (d, 1H, Hc, J = 1.83 Hz).

^{13}C NMR (CDCl$_3$): δ 21.94, 62.79, 69.12, 71.50, 73.99, 74.76, 79.16, 113.53, 113.78, 144.79, 147.59, 162.85, 170.47, 170.80, 171.54, 171.86.

m/z calculated: 441.13   *m/z* found: 442.19 (+H$^+$).

2-Naphthoic acid-(2,3,4,6-tetra-*O*-acetyl-β-D-glucopyranosyl)-amide (32).
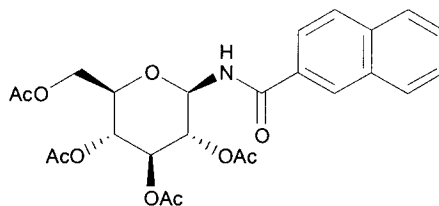
^{1}H NMR (CDCl$_3$): δ: 2.05, 2.06, 2.08 (3s, 12H total, 4 x COCH$_3$), 3.95 (ddd, 1H, H-5, J = 2.06, 4.17, 10.12 Hz), 4.14 (m, 2H, H-6, H-6'), 5.14 (m, 2H, H-3, H-4), 5.44 (dd, 1H, H-2, J = 9.52, 9.52 Hz), 5.55 (dd, 1H, H-1, J = 9.34, 9.34 Hz), 7.31 (d, 1H, NH, J = 9.15 Hz), 7.53-8.04 (m, 7H, Ar-H).

^{13}C NMR (CDCl$_3$): δ 21.93, 62.79, 69.36, 72.15, 73.76, 74.79, 80.16, 128.85, 163.67, 169.34, 170.68, 171.77, 172.54.

Benzoic acid-(2,3,4,6-tetra-*O*-acetyl-β-D-glucopyranosyl)-amide (33).
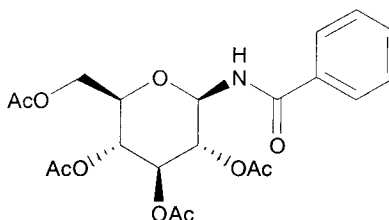
^{1}H NMR (CDCl$_3$): δ: 2.04, 3.04, 2.07 (3s, 12H total, 4 x COCH$_3$), 3.91 (ddd, 1H, H-5, J = 2.06, 4.16, 10.11 Hz), 4.10 (m, 2H, H-6, H-6'), 5.07 (dd, 1H, H-3, J = 9.70, 9.70 Hz), 5.11 (dd, 1H, H-4, J = 9.98, 9.98 Hz), 5.40 (dd, 1H, H-2, J = 9.52, 9.52 Hz), 5.46 (dd, 1H, H-1, J = 9.34, 9.34 Hz), 7.11 (d, 1H, NH, J = 9.34 Hz), 7.42-7.77 (m, 5H, Ar-H).

^{13}C NMR (CDCl$_3$): δ 21.98, 62.76, 69.39, 71.97, 73.72, 74.75, 80.08, 128.25, 129.86, 131.01, 131.56, 163.26, 170.50, 170.78, 171.52, 171.79.

m/z calculated: 452.15   *m/z* found: 331.0 (-C$_7$N$_6$NO).

1-Naphthoic acid-(2,3,4,6-tetra-*O*-acetyl-β-D-glucopyranosyl)-amide (34).
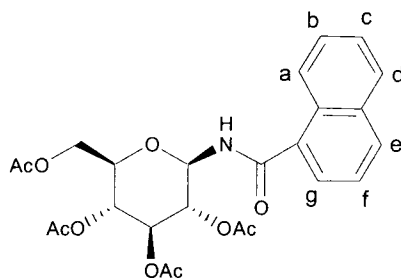
^{1}H NMR (CDCl$_3$): δ 2.06, 2.07, 2.10 (3s, 12H total, 4 x COCH$_3$), 3.97 (ddd, 1H, H-5, *J* =

2.15, 4.26, 10.18 Hz), 4.18 (m, 2H, H-6, H-6'), 5.08 (dd, 1H, H-2, *J* = 9.52, 9.70 Hz),

5.15 (dd, 1H, H-4, *J* = 9.70, 9.70 Hz), 5.44 (dd, 1H, H-3, *J* = 9.34, 9.70 Hz), 5.61 (dd,

1H, H-1, *J* = 9.52, 9.52 Hz), 6.82 (d, 1H, NH, *J* = 9.52 Hz), 7.58, 7.69, 7.93 (3m, 3H, Ar-

Hb, Ar-Hc, Ar-Hf), 8.13, 8.40, 8.77, 9.15 (4 m, 4H, Ar-Ha, Ar-Hd, Ar-He, Ar-Hg).

^{13}C NMR (CDCl$_3$): δ 21.96, 62.85, 69.26, 71.82, 73.94, 74.93, 79.62, 131.01, 136.59-

125.43, 163.87, 170.53, 170.87, 171.60, 171.96.

Thiophene-2-carboxylic acid-(2,3,4,6-tetra-*O*-acetyl-β-D-glucosyl)-amide (35).
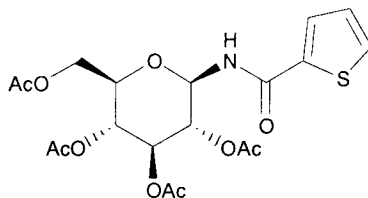
^{1}H NMR (CDCl$_3$): δ 1.95, 2.01, 2.09 (3s, 12H, 4 x COCH$_3$), 3.89 (ddd, 1H, H-5, J = 2.33, 4.81, 10.11 Hz), 4.17 (m, 2H, H-6, H-6'), 5.03 (dd, 1H, H-2, J = 9.52, 9.70 Hz), 5.11 (dd, 1H, H-4, J = 7.87, 9.89 Hz), 5.22 (m, 2H, H-1, H-3), 6.96 (d, 1H, NH, J = 9.34 Hz).

Butyric acid-(2,3,4,6-tetra-O-acetyl-β-D-glucopyranosyl)-amide (37).
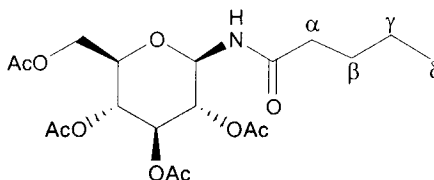
^{1}H NMR (CDCl$_3$): δ 0.89 (t, 3H, Hδ), 1.62 (m, 1H, Hγ), 1.99, 2.01, 2.02, 2.05 (4s, 12H total, 4 x COCH$_3$), 2.15 (m, 1H, Hβ), 2.31 (t, 1H, Hα), 3.81 (ddd, 1H, H-5, J = 2.15, 4.35, 10.12 Hz), 4.05 (m, 2H, H-6, H-6'), 4.90 (dd, 1H, H-2, J = 9.52, 9.52 Hz), 5.04 (dd, 1H, H-4, J = 9.52, 10.07 Hz), 5.27 (m, 2H, H-1, H-3), 6.29 (d, 1H, NH, J = 9.34 Hz).

^{13}C NMR (CDCl$_3$): δ 14.81, 19.87, 21.91, 39.72, 62.76, 69.23, 71.71, 73.79, 74.65, 79.11, 170.47, 170.75, 171.52, 171.96, 174.13.

Trimethyl acetic acid-(2,3,4,6-tetra-O-acetyl-β-D-glucopyranosyl)-amide (38).
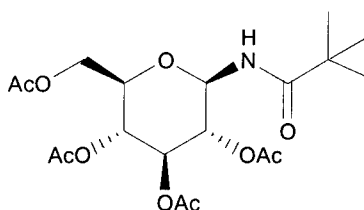
^{1}H NMR (CDCl$_3$): δ 1.26 (s, 9H, 3 x CH$_3$), 2.06, 2.08 (2s, 12H total, 4 x COCH$_3$), 3.81 (m, 1H, H-5), 4.49 (m, 2H, H-6, H-6'), 4.96 (m, 1H, H-2), 5.12 (m, 1H, H-4), 5.22 (m, 1H, H-3), 5.53 (m, 1H, H-1), 6.27 (d, 1H, NH, J = 9.30 Hz).

Small signals corresponding to the starting azide **17** were also observed in the ^{1}H spectrum.

4-Fluoro benzoic acid-(2,3,4,6-tetra-*O*-acetyl-β-D-glucopyranosyl)-amide (39).
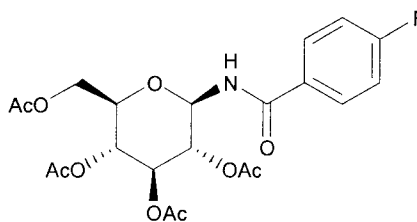
^{1}H NMR (CDCl$_3$): δ 2.04, 2.06 (4s, 12H, 4 x OCH$_3$), 3.91 (ddd, 1H, H-5, J = 10.11, 4.39, 2.06 Hz), 4.10, 4.33 (dd, 2H, H-6, H-6', J = 12.54 Hz), 5.04, 5.11, 5.40 (4 x dd, 4H, H-1, H-2, H-3, H-4), 7.12 (d, 1H, NH, J = 8.42 Hz), 7.05-8.18 (m, 4H, Ar-H).

Isovaleric acid-(2,3,4,6-tetra-*O*-acetyl-β-D-glucopyranosyl)-amide (40).
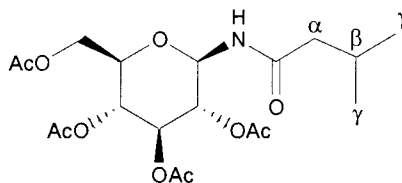
^{1}H NMR (CDCl$_3$): δ 0.89 (m, 1H, Hβ), 0.96 (d, 2H, Hα, J = 6.59 Hz), 2.01, 2.05, 2.07 (3s, 12H total, 4 x COCH$_3$), 2.20 (d, 6H, 2 x CH$_3$γ, J = 7.32 Hz), 3.81 (ddd, 1H, H-5, J = 2.11, 4.30, 10.07 Hz), 4.05 (m, 2H, H-6, H-6'), 4.90 (dd, 1H, H-2, J = 9.52, 9.70 Hz),

5.04 (dd, 1H, H-4, J = 9.52, 9.89 Hz), 5.28 (m, 2H, H-1, H-3), 6.31 (d, 1H, NH, J = 9.34 Hz).

^{13}C NMR (CDCl$_3$): δ 21.93, 23.36, 27.19, 47.16, 62.76, 69.27, 71.62, 73.79, 74.70, 79.17, 170.50, 170.78, 171.54, 171.98, 173.65.

Nicotinic acid-(2,3,4,6-tetra-O-acetyl-β-D-glucopyranosyl)-amide (41).
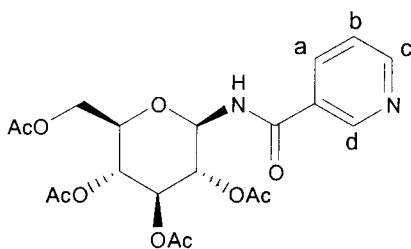
^{1}H NMR (CDCl$_3$): δ 2.04, 2.06 (2s, 12H, 4 x COCH$_3$), 3.90 (ddd, 1H, H-5), 4.11, 4.31 (m, 2H, H-6, H-6'), 5.12 (dd, 2H, H-2, H-4), 5.37 (dd, 1H, H-3, J = 9.34, 9.52 Hz), 5.44 (dd, 1H, H-1, J = 8.97, 9.52 Hz), 7.81 (d, 1H, NH, J = 8.10 Hz), 7.55, 8.28, 8.81, 9.16 (m, 4H, Ar-Ha-d).

^{13}C NMR (CDCl$_3$): δ 20.79, 61.61, 68.09, 68.09, 70.82, 72.58, 73.65, 78.87, 124.00, 129.67, 136.60, 147.04, 151.12, 164.58, 169.32, 169.65, 170.36, 171.22.

Attempted preparation of *p*-nitrobenzoic acid-[methyl 3,4-di-*O*-acetyl-2-(benzoyl-oxyimino)]-amide (42).
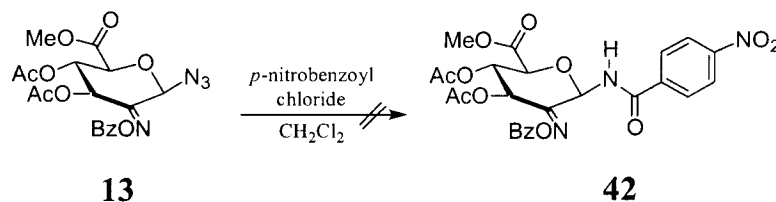
In a 25 mL round-bottom flask equipped with a septum and magnetic stir bar, polymer-supported triphenylphosphine (60 mg, 0.18 mmol) was added to a solution of methyl 3,4-di-*O*-acetyl-2-(benzoyloxyimino) azide **13** (50 mg, 0.12 mmol) in methylene chloride (10 mL) and allowed to stir to initiate the evolution of nitrogen gas. To this mixture, 2 equivalents of *p*-nitrobenzoyl chloride (44.5 mg, 0.24 mmol) were added and the mixture was allowed to stir at room temperature for 24 hours (TLC product Rf = 0.26). The mixture was gravity filtered into a round-bottom flask to remove polymer-supported tripenylphosphine oxide. Polymer-bound tris (2-aminoethyl) amine (50 mg, 0.22 mmol) was added to the mixture and the mixture was allowed to stir at room temperature for 3 hours. The amine polymer was then removed *via* gravity filtration and the filtrate was concentrated *in vacuo*. The ^{1}H NMR spectrum of the crude residue did not show the presence of any signals that could belong to compound **42**.

References:

1. http://www.eurekalert.org/pub_releases/2002-03/ru-sdc030102.php

2. Marshall, S. A.; Wilke, W. W.; Pfaller, M. A.; Jones, R. N. *"Staphylococcus aureus* and Coagulase-Negative *Staphylococci* from Blood Stream Infections: Frequency of Occurrence, Antimicrobial Susceptibility, and Molecular (mec*A*) Characterization of Oxacillin Resistance in the SCOPE Program," *Diagnostic Microbiol. and Infectious Disease.* **1998**, *30*, 205-214.

3. Quan, L.; Zhu, B.; Ishida, K.; Taniguchi, M.; Oritani, S.; Kamikodai, Y.; Fujita, M.; Masaki, Q.; Maeda, H. "Sudden Infant Death Attributed to Peracute Pulmonary Infection: Two Autopsy Cases," *Legal Medicine.* **2000**, *2*, 79-83.

4. http://www.cdc.gov/epo/mmwr/preview/mmwrhtml/mm4832a2.htm

5. Jones, M.E.; Shimitz, F. J.; Fluit, A. C.; Acar, J.; Gupta, R.; Verhoef, J. "Frequency of Occurrence and Antimicrobial Susceptibility of Bacterial Pathogens Associated with Skin and Soft Tissue Infections During 1997 from an International Surveillance Programme," *Eur. J. Clin. Microbiol. Infec. Immun. Dis.* **1999**, *18*, 403-408.

6. Elbashier, A. M.; Malik, A. G.; Khot, P. "Blood Stream Infections: Micro-organisms, Risk Factors and Mortality Rate in Qatif Central Hospital," *Ann. Saudi Medicine.* **1998**, *18*, No. 2.

7. Yoshikawa, T. "Antimicrobial Resistance and Aging: Beginning of the End of the Antibiotic Era?" *J. Am. Geriatrics. Soc.* **2002**, *50*, 226-229.

8. Simor, A. E. "Containing Methicillin-Resistant *S. aureus*," *Postgrad. Med.* **2001**, *110* (4), 43-48.

9. Jeljaszewicz, J.; Mlynarczyk, G.; Mlynarczyk, A. "Antibiotic resistance in Gram-positive cocci," *Int. J. Antimicrobial. Agents.* **2000**, *16*, 473-478.

10. Morgan, P. M.; Sala, R. F.; Tanner, E. "Eliminations in the Reactions Catalyzed by UDP-*N*-Acetylglucosamine 2-Epimerase," *J. Am. Chem. Soc.* **1997**, 10269-10277.

11. Chou, W.C.; Hinderlich, S.; Reutter, W.; Tanner, M. E. "Sialic Acid Biosynthesis: Stereochemistry and Mechanism of the Reaction Catalyzed by the Mammalian UDP-*N*-Acetylglucosamine 2-Epimerase," *J. Am. Chem. Soc.* **2003**, *125*, 2455-2461.

12. Berges, D. A.; Zhang, N.; Hong, L. "Bicyclic Azasugars Containing a Glycosidic Heteroatom II: D-Lyxose Analogues," *Tetrahedron,* **1999**, *55*, 14251-14260.

13. Wong, C. H.; Halcomb, R. L.; Ichikawa, Y.; Kajimoto, T. "Enzymes in Organic Synthesis: Application to the Problems of Carbohydrate Recognition. Part 2." *Angew. Chem. Int. Ed. Engl.* **1995**, *34*, 521.

14. Moris-Varas, F.; Quan, X. H.; Wong, C. H. "Enzymatic/Chemical Synthesis and Biological Evaluation of Seven-Membered Iminocyclitols," *J. Am. Chem. Soc.* **1996**, *118*, 7647-7652.

15. Takayama, S.; Martin, R.; Wu, J.; Laslo, K. Siuzdak, G.; Wong, C-H. "Chemoenzymatic Preparation of Novel Cyclic Imine Sugars and Rapid Biological Activity Evaluation Using Electrospray Mass Spectrometry and Kinetic Analysis," *J. Am. Chem. Soc.* **1997**, *119*, 8146-8151.

16. Dondoni, A.; Giovannini, P. P.; Marra, A. "Convergent Synthesis of Pyrrolidine-based (1-6)- and (1-5)-aza-*C*-disaccharides," *Tetrahedron Lett.* **2000**, *41*, 6195-6199.

17. "Essentials of Glycobiology" Varki, A.; Cummings, R.; Esko, J.; Freeze, H.; Hart, G.; Marth, J. Spring Harbor Laboratory Press, Cold Spring Harbor, New York, 1999, 653 pp.; ISBN 0-879-69-559-5, ISBN 0-87969-560-9.

18. Ravindran, B.; Sakthivel, K.; Suresh, C. G.; Pathak, T. "Diastereoselective Addition of Amines to Vinyl Sulfone Modified Carbohydrates: A Highly Flexible Methodology for the Synthesis of New Classes of Deoxyaminosugars," *J. Org. Chem.* **2000**, *65*, 2637-2641.

19. Lichtenthaler, F. W.; Kaji, E.; Osa, Y.; Takahashi, K.; Hirooka, M.; Zen, S. "Facile Preparation and Utilization of a Novel β-D-ManNAcA-Donor: Methyl 2-Benzoyl-oxyimino-1-bromo-2-deoxy-α-D-*arabino*-hexopyranuronate," *Bull. Chem. Soc. Jpn.* **1994**, *67*, 1130-1140.

20. St. Hilaire, P. M.; Meldal, M. "Glycopeptide and Oligosaccharide Libraries," *Angew. Chem. Int. Ed.* **2000**, 39, 1162-1179.

21. Furka, A.; Sebestyen, F.; Asgedom, M.; Dibo, G. "General Method for Rapid Synthesis of Multicomponent Peptide Mixtures," *Int. J. Peptide Protein Res.* **1991**, *37*, 487-493.

22. http://www.nyu.edu/classes/ytchang/book/e007.html

23. a) Yan, L.; Taylor, C. M.; Goodnow, R.; Kahne, D. *J. Am. Chem. Soc.* **1994**, *116*, 6953-6954.

    b) Wang, Y.; Halcomb, R. L.; *Chem. Lett.* **1995**, 273-274.

24. a) Schuster, M.; Schuster, M.; Wang, P.; Paulson, J. C.; Wang, C. H. "Solid-Phase Chemical-Enzymatic Synthesis of Glycopeptides and Oligosaccharides," *J. Am. Chem. Soc.* **1994**, *116*, 1135-1136.

b) Halcomb, R. L.; Huang, H. "Solution- and Solid-Phase Synthesis of Inhibitors of *H. pylori* Attachment and E-Selectin-Mediated Leukocyte Adhesion," *J. Am. Chem. Soc.* **1994**, *116*, 11315-11322.

25. Wagner, T. R.; Root, Y. Y.; Norris, P. "X-Ray Crystal Structure of Methyl 1,2,3,4-Tetra-*O*-acetyl-β-D-glucopyranuronate," *Carbohydr. Res.* **2002**, *337*, 2343-2346.

26. a) Kolb, H.C.; Finn, M.G.; Sharpless, K.B. "Click Chemistry: Diverse Chemical Function From a Few Good Reactions," *Angew. Chem. Int. Ed.*, **2001**, *40*, 2004-2021.

b) Demko, Z.P.; Sharpless, K.B. "A Click Chemistry Approach to Tetrazoles by Huisgen 1,3-Dipolar Cycloaddition: Synthesis of 5-Acyltetrazoles from Azides and Acyl Cyanides," *Angew. Chem. Int. Ed.*, **2002**, *41*, 2113-2116.

b) Demko, Z.P.; Sharpless, K.B. "A Click Chemistry Approach to Tetrazoles by Huisgen 1,3-Dipolar Cycloaddition: Synthesis of 5-Sulfonyltetrazoles from Azides and Sulfonyl Cyanides," *Angew. Chem. Int. Ed.*, **2002**, *41*, 2110-2113.

27. Boullanger, P.; Maunier, V.; Lafont, D. "Syntheses of Amphiphilic Glycosylamides From Glycosyl Azides Without Transient Reduction to Glycosyl Amines," *Carbohydr. Res.*, **2000**, *324*, 97-106.

Appendix
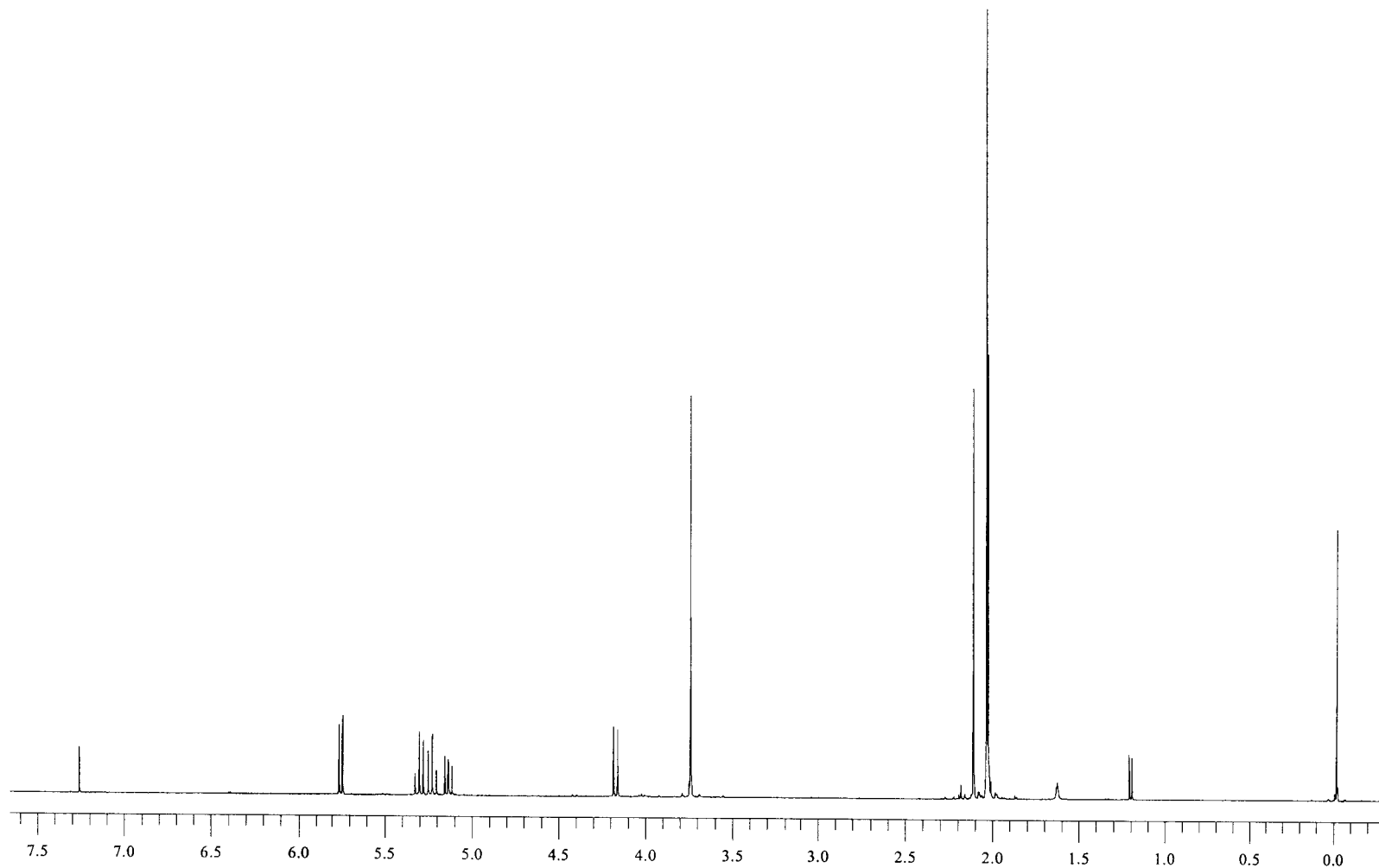
Figure 12: 400 MHz ^{1}H NMR spectrum of methyl glucuronate β-acetate **8β**.
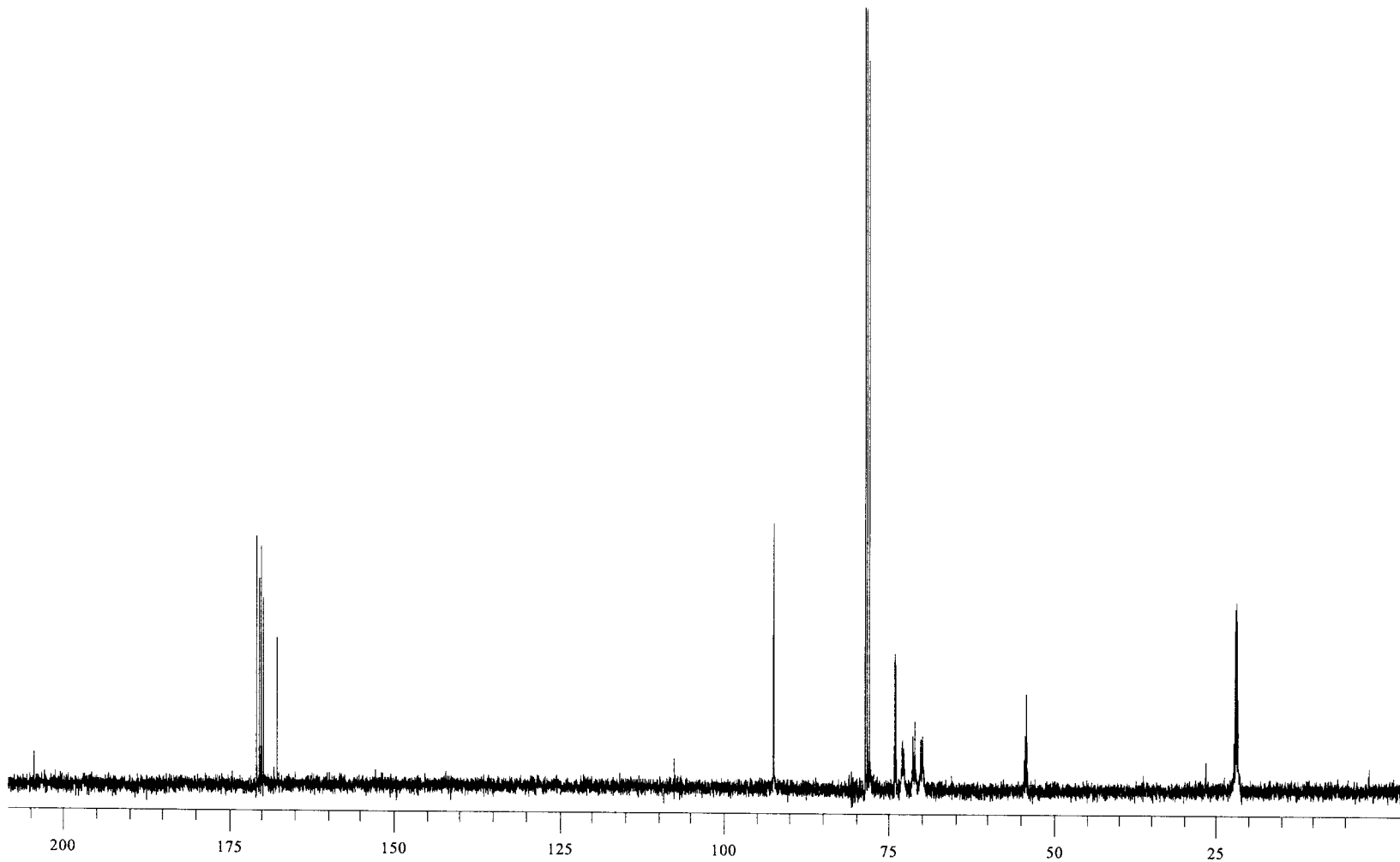
Figure 13: 100 MHz ^{13}C NMR spectrum of methyl glucuronate β-acetate **8β**.

Display Report
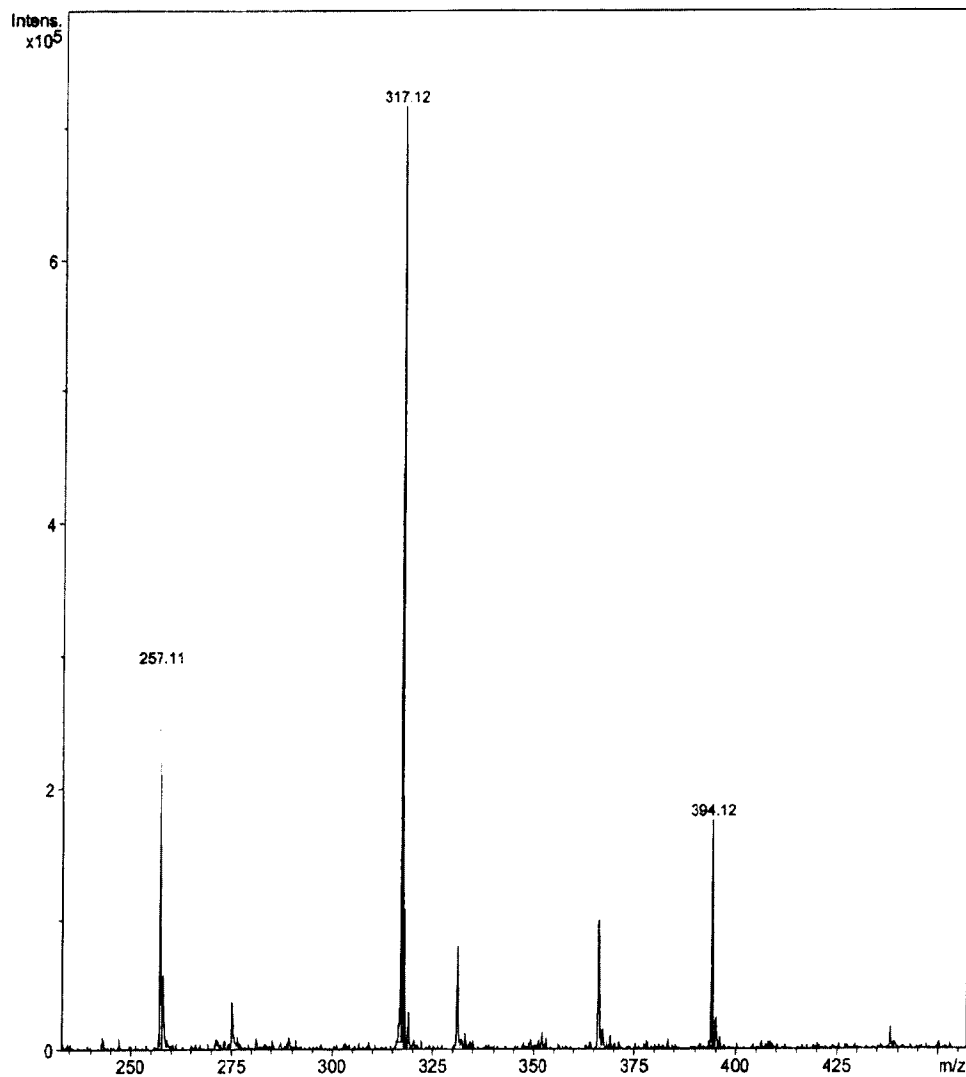
Figure 14: Mass spectrum of methyl glucuronate β-acetate 8β.
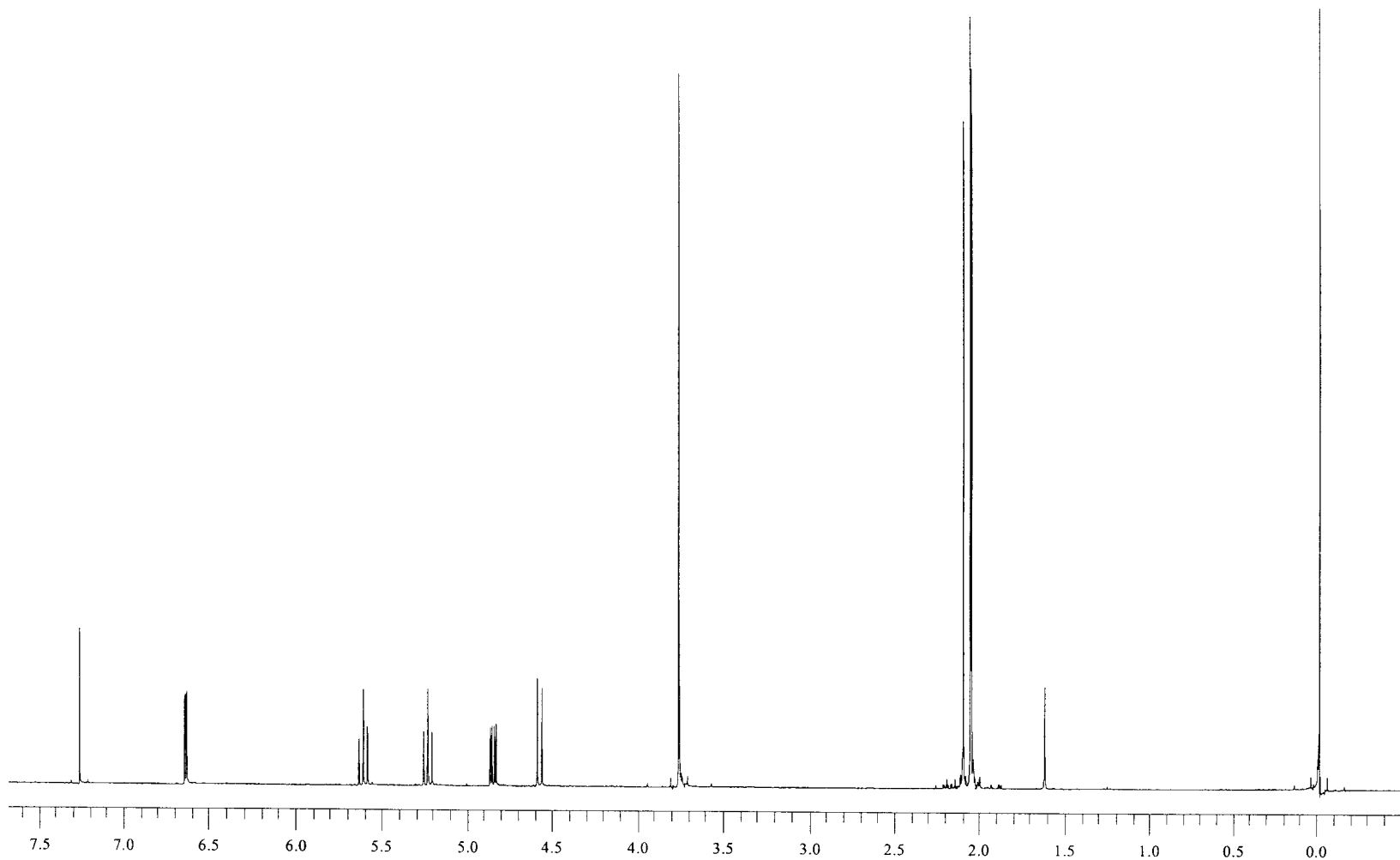
Figure 15: 400 MHz ^{1}H NMR spectrum of methyl glucuronate α–bromide **9**.
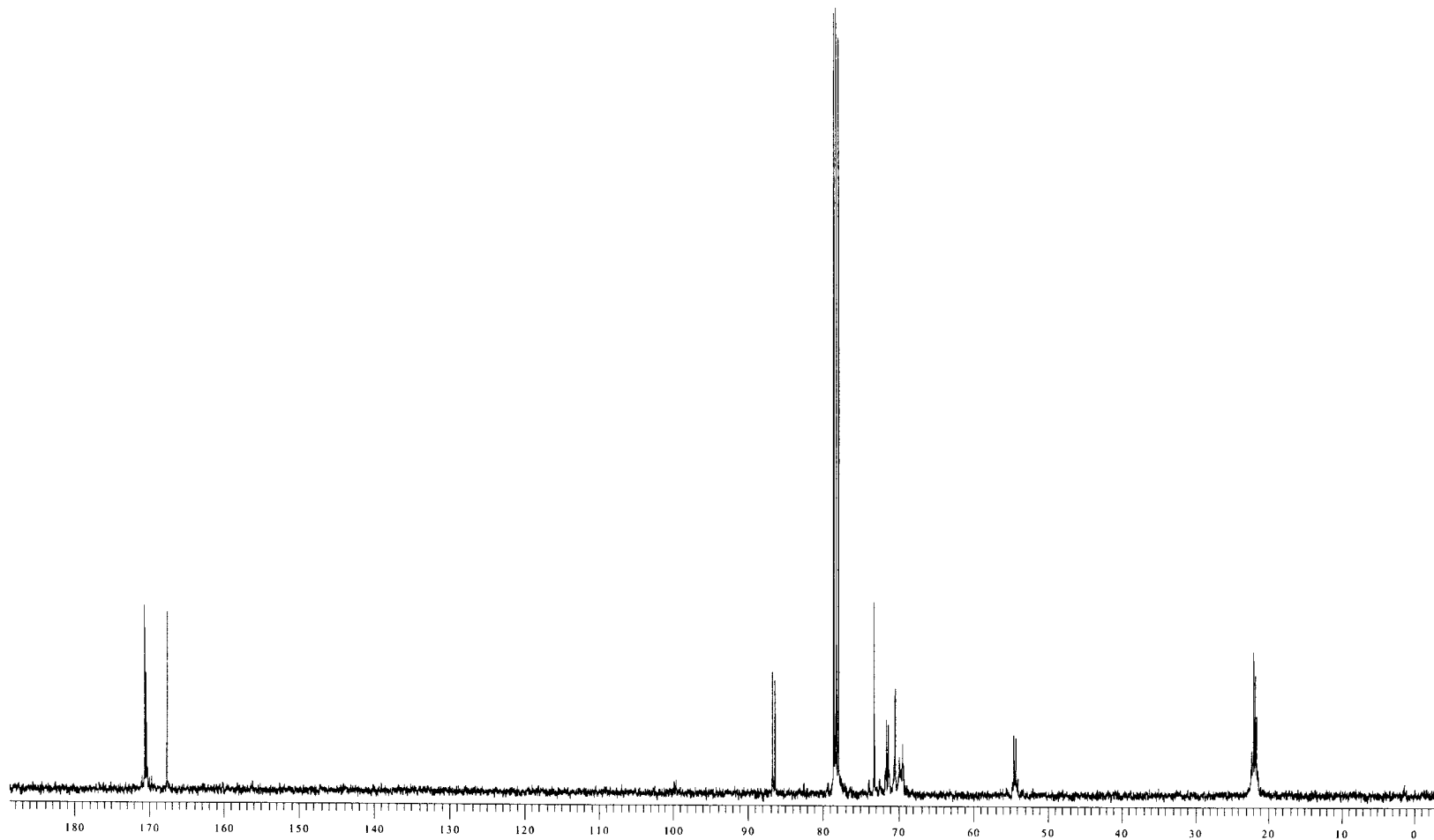
Figure 16: 100 MHz ^{13}C NMR spectrum of methyl glucuronate α–bromide **9**.
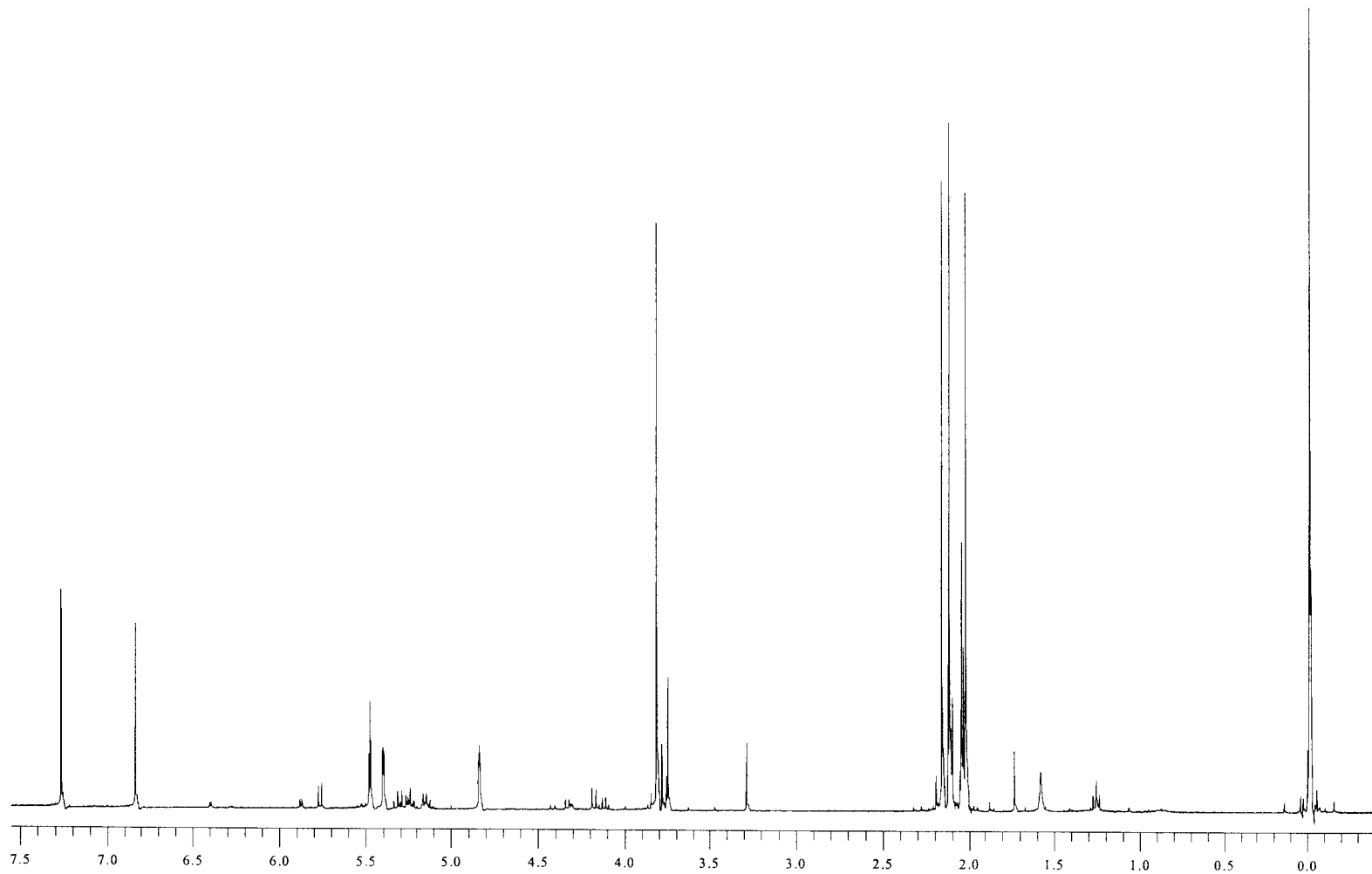
Figure 17: 400 MHz ^{1}H NMR spectrum of glycal **3**.
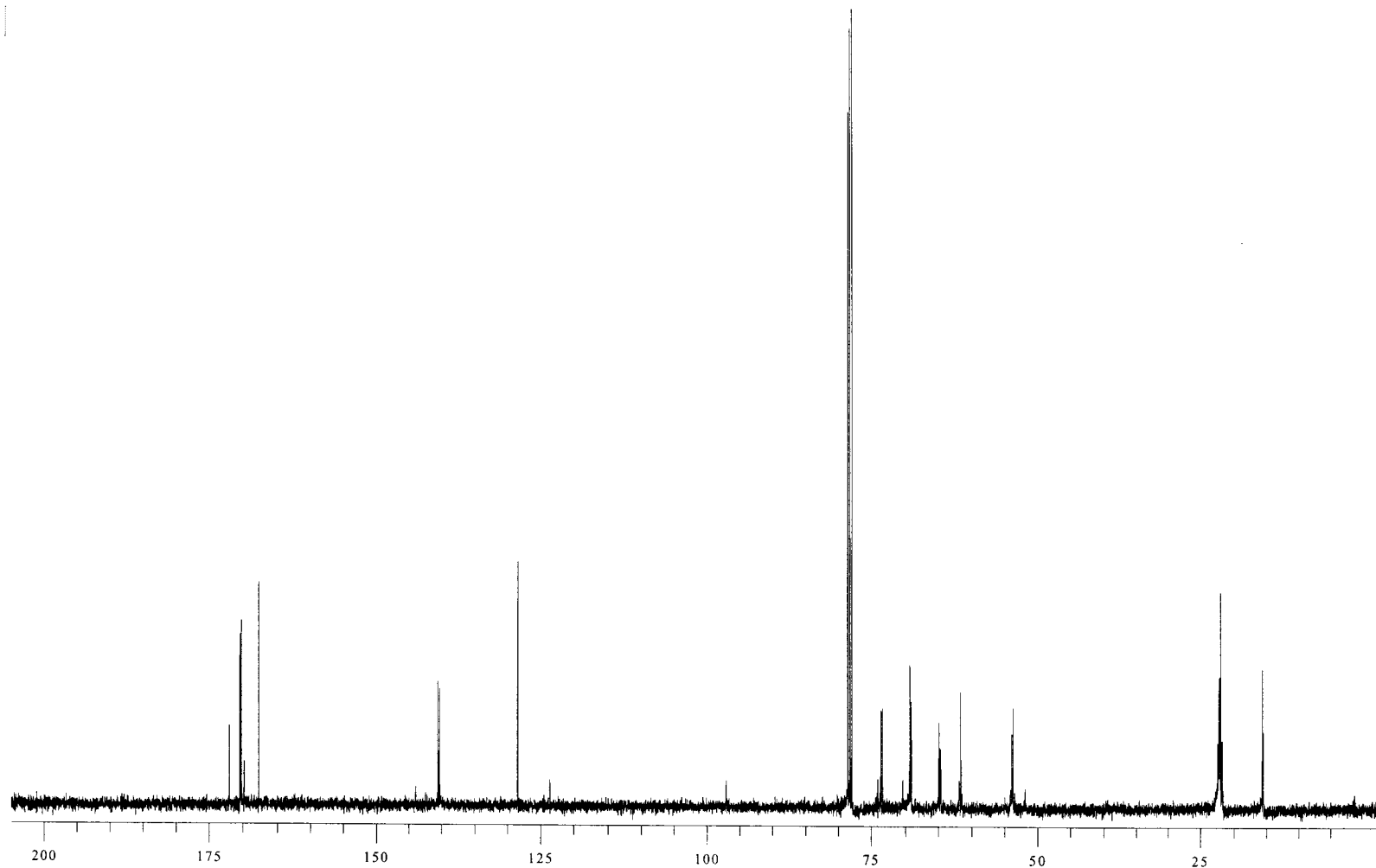
Figure 18: 100 MHz ^{13}C NMR spectrum of glycal **3**.

Display Report
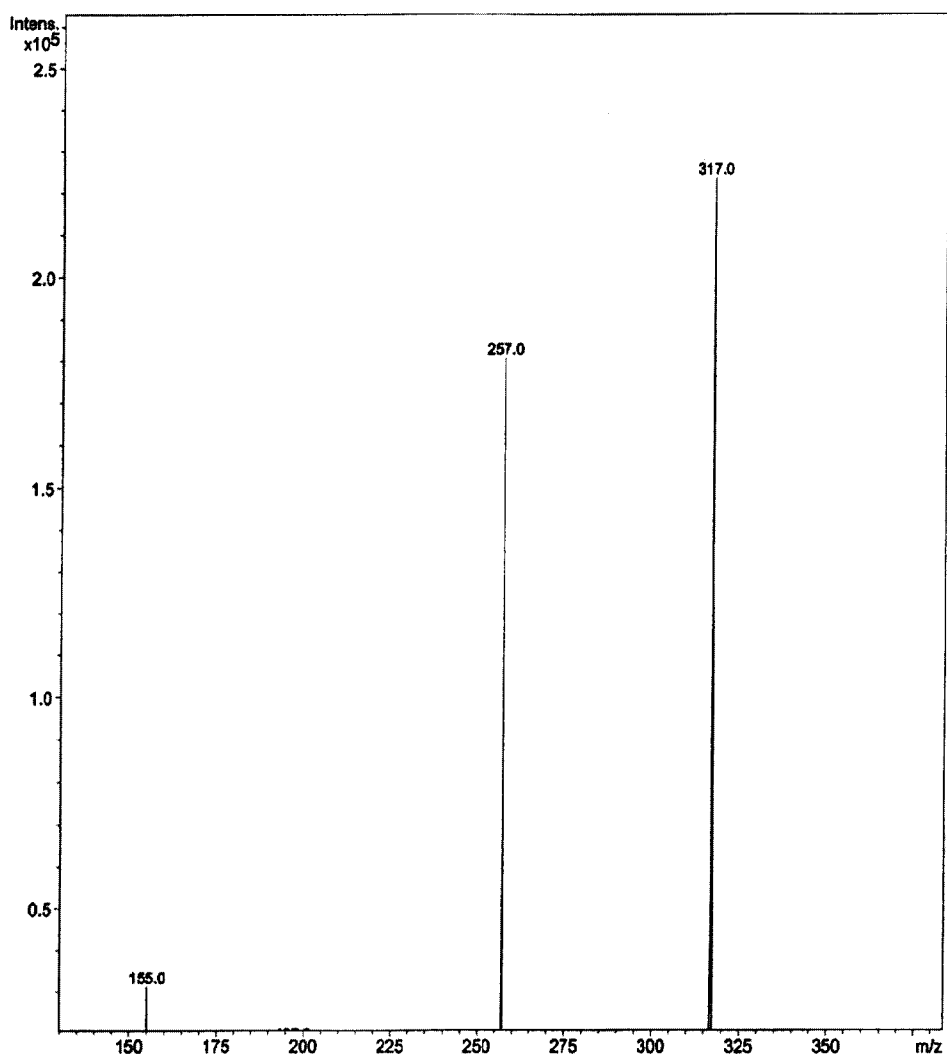
Figure 19: Mass spectrum of glycal 3.
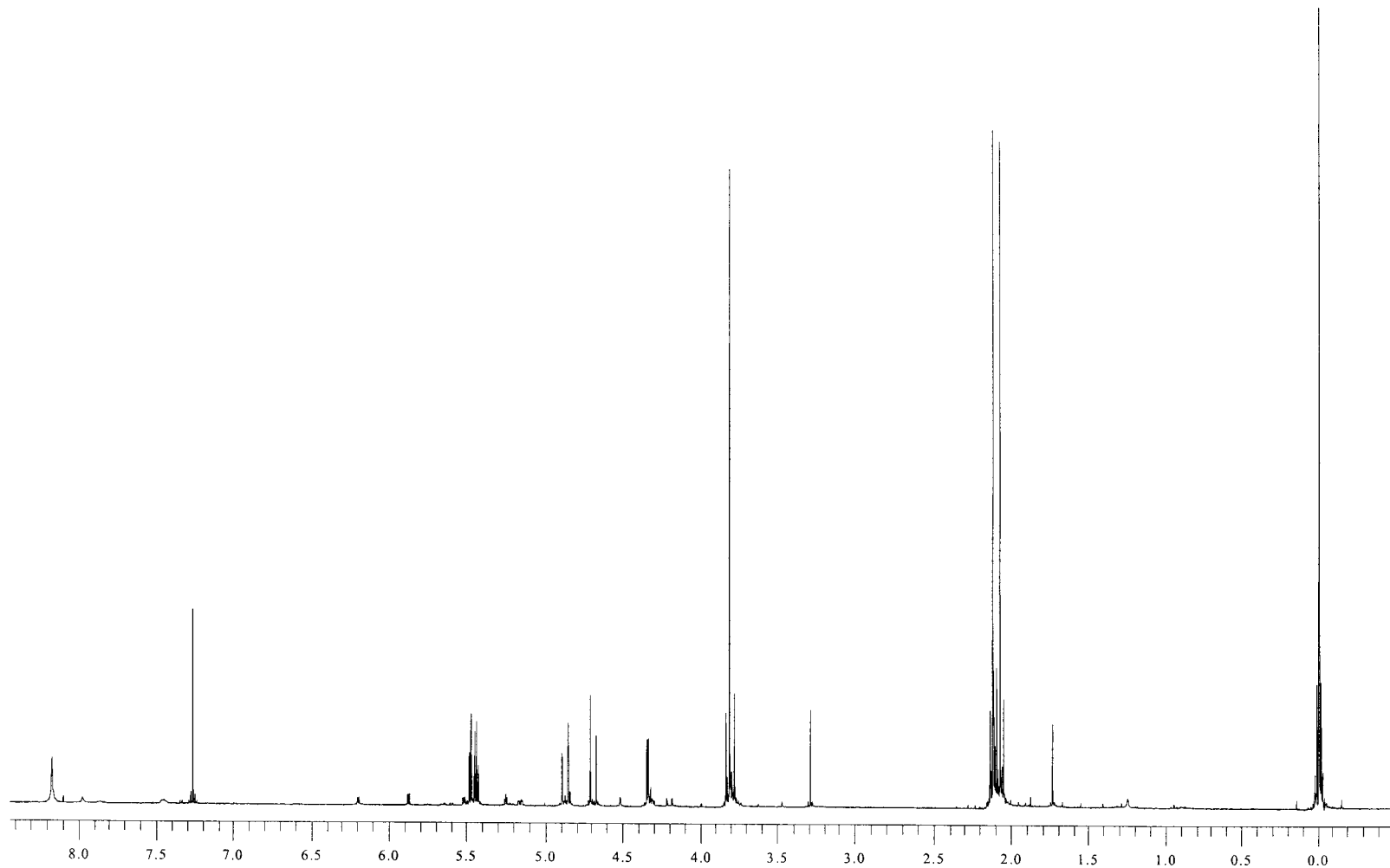
Figure 20: 400 MHz ^{1}H NMR spectrum of oxime **10**.
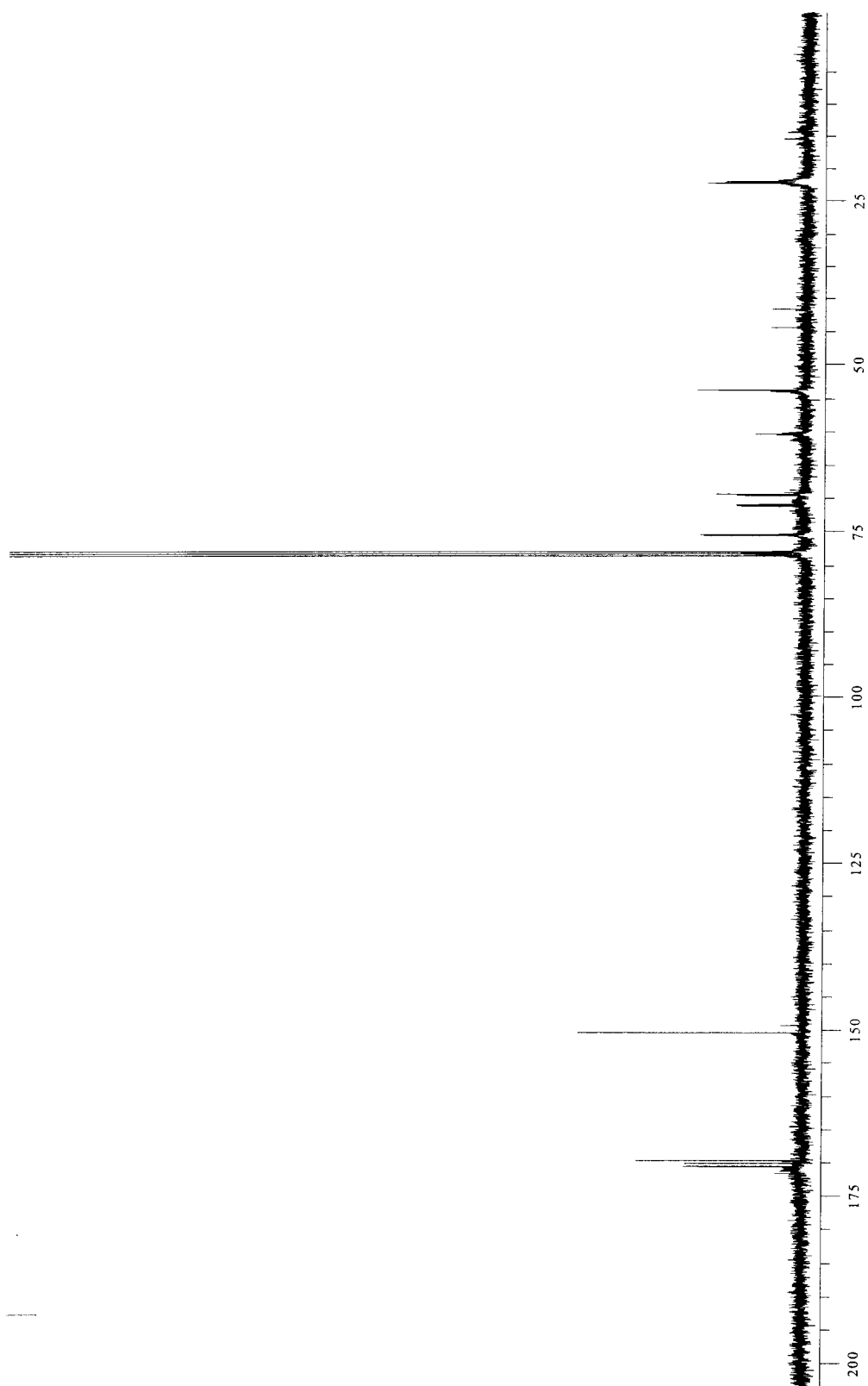
Figure 21: 100 MHz ^{13}C NMR spectrum of oxime **10**.

Display Report

Intens.
x10⁵

271.87

393.78

Figure 22: Mass spectrum of oxime 10.
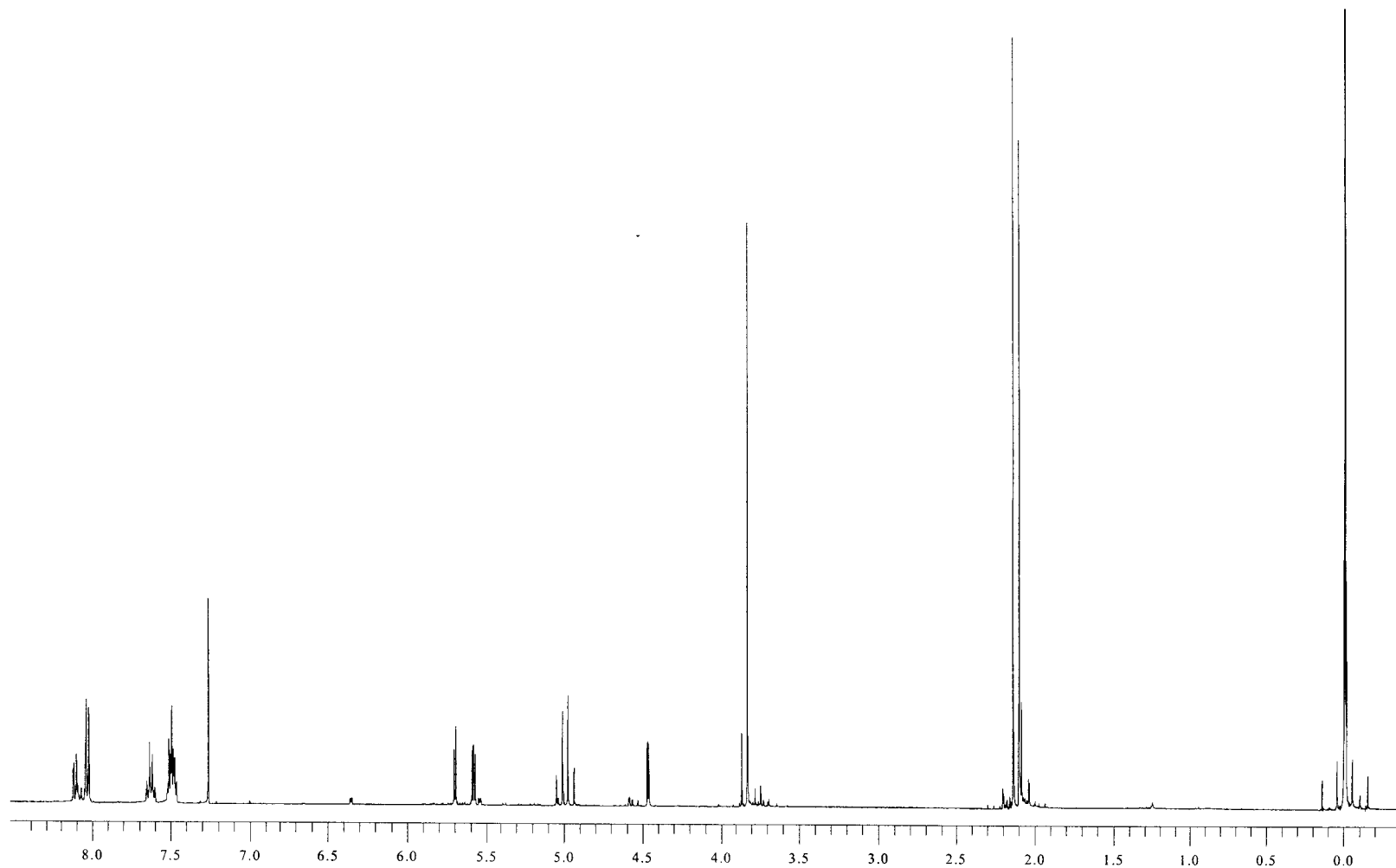
Figure 23: 400 MHz ^{1}H NMR spectrum of benzoyloxime **11**.
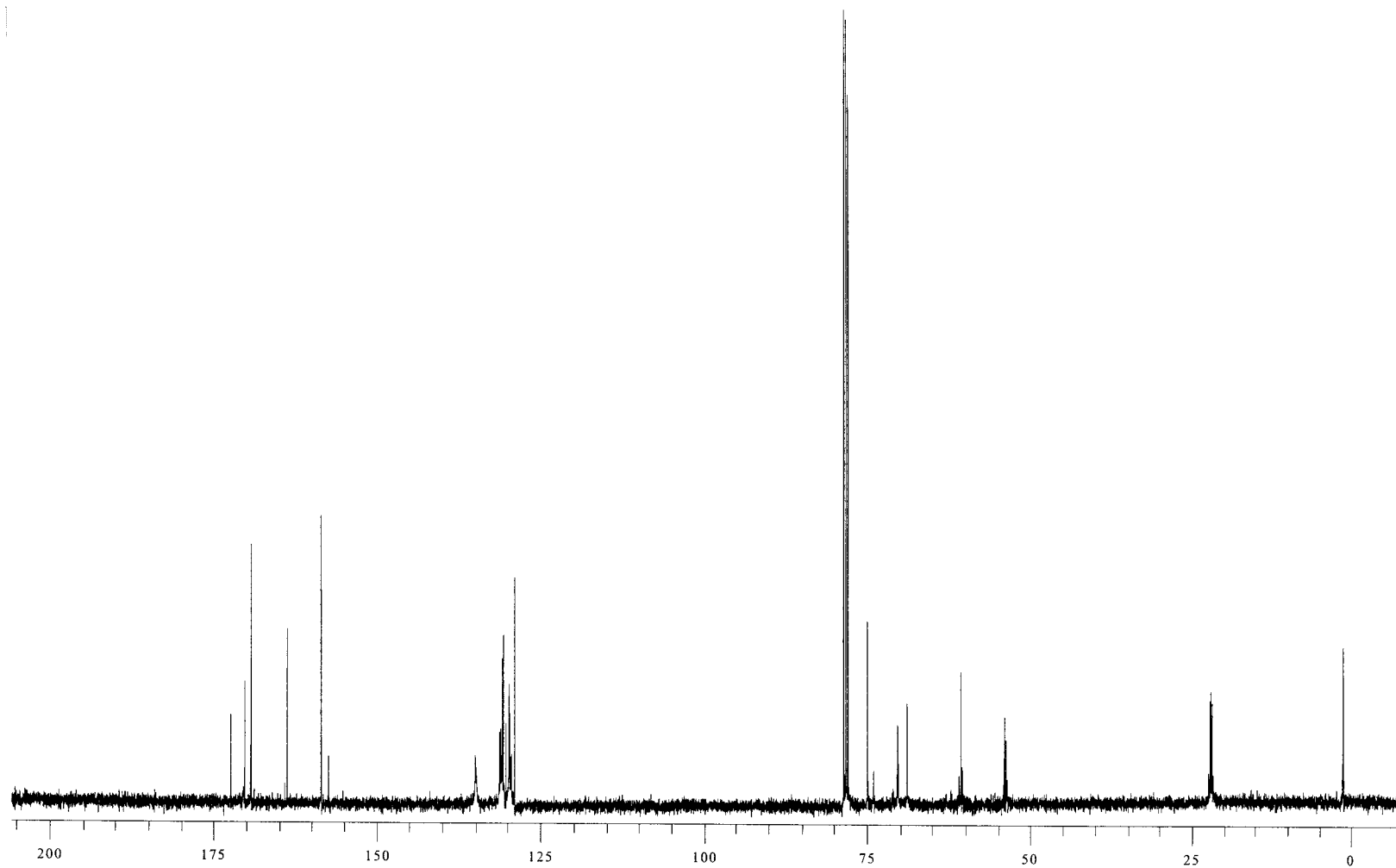
Figure 24: 100 MHz ^{13}C NMR spectrum of benzoyloxime **11**.

Display Report

Analysis Info:
File: D:\DATA\YURI\YR210510.D   Printed: Tue Feb 11 10:36:40 2003
Date acquired:
Instrument: Operator :
Task   :
Method   :   Sample   :

Acquisition Parameter:
Source   :   Polarity :
Mode   :
CapExit   :   Skim 1   :
Scan Range: Trap Drive:
Accum.time: Summation :
MS/MS   : 411.1 u
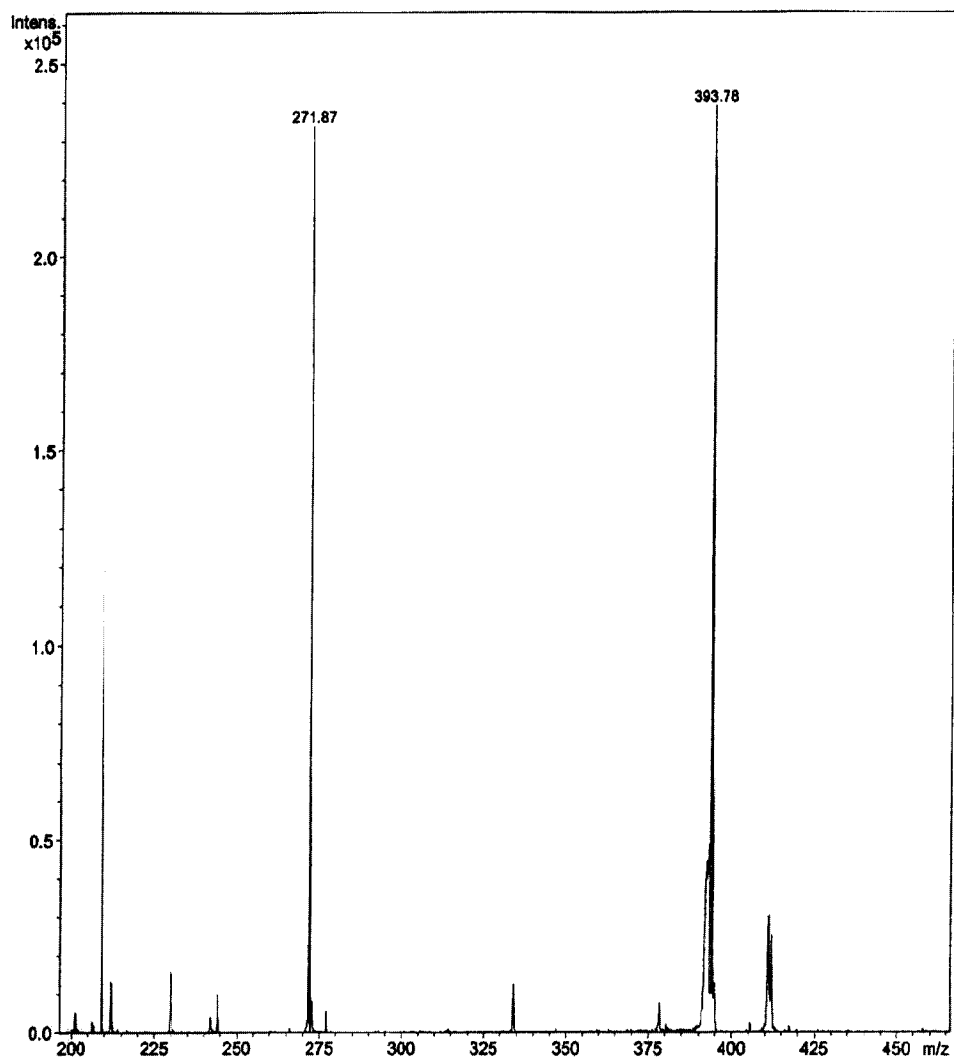
Figure 25: Mass spectrum of benzoyloxime 11.
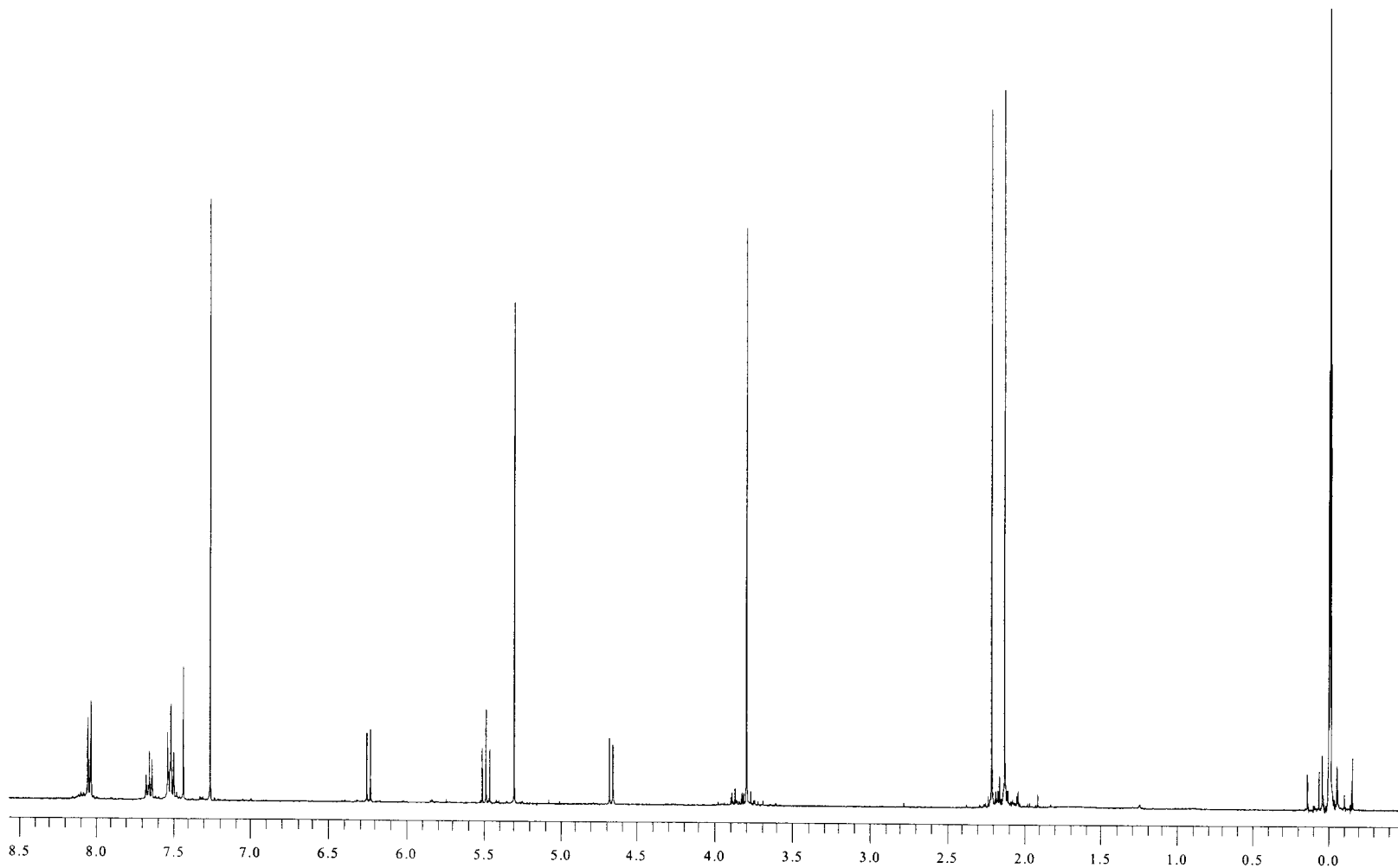
Figure 26: 400 MHz ^{1}H NMR spectrum of benzoyloxime bromide **12**.

Display Report

Analysis Info:
File: D:\DATA\YURI\5-077001.D   Printed: Fri Apr 25 12:04:07 2003
Date acquired:
Instrument: Operator :
Task   :
Method   :   Sample   :

Acquisition Parameter:
Source   :   Polarity :
Mode   :
CapExit   :   Skim 1   :
Scan Range: Trap Drive:
Accum.time: Summation :
MS/MS   :
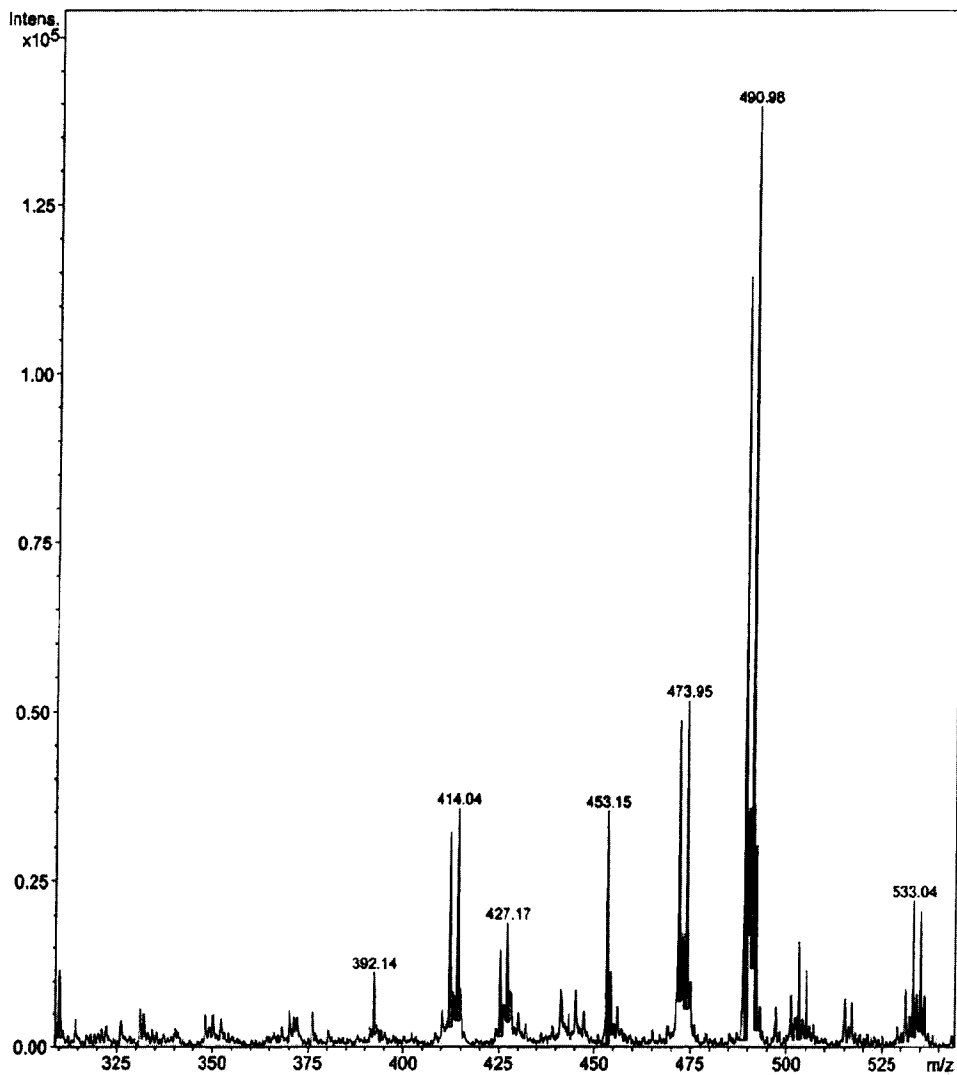
Figure 27: Mass spectrum of benzoyloxime bromide 12.
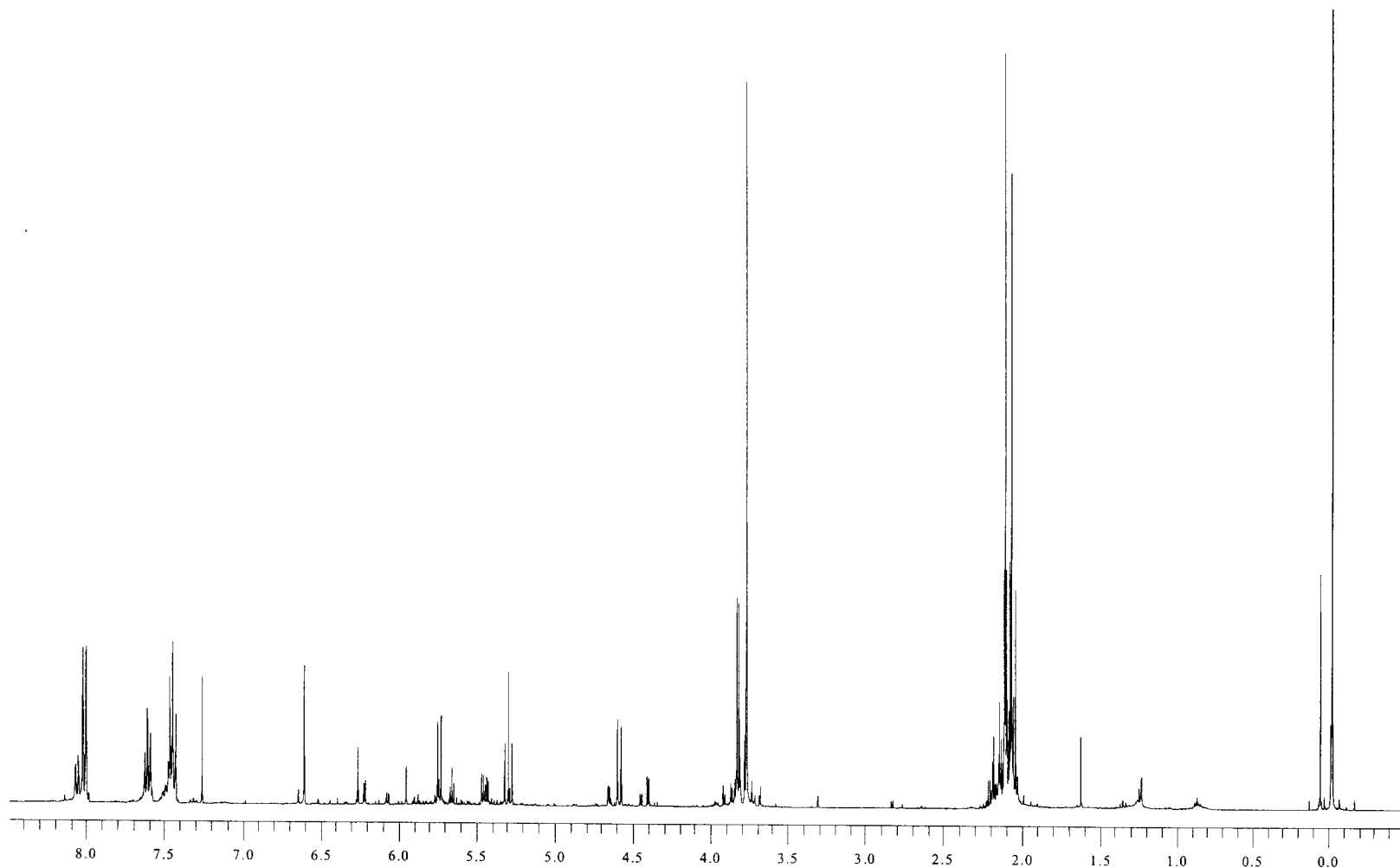
Figure 28: 400 MHz ^{1}H NMR spectrum of benzoyloxime azide **13**.
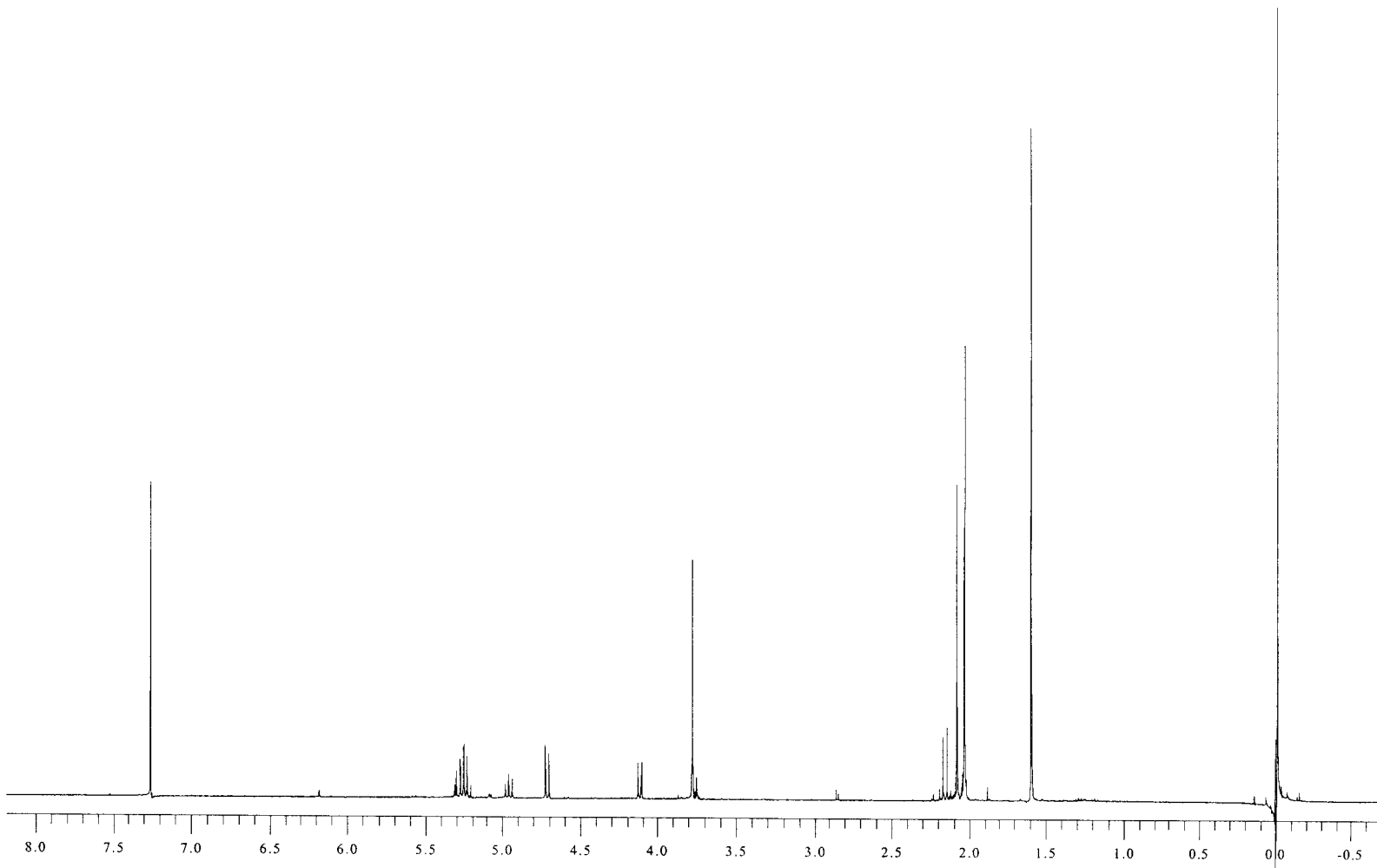
Figure 29: 400 MHz ^{1}H NMR spectrum of methyl glucuronate azide **14.**
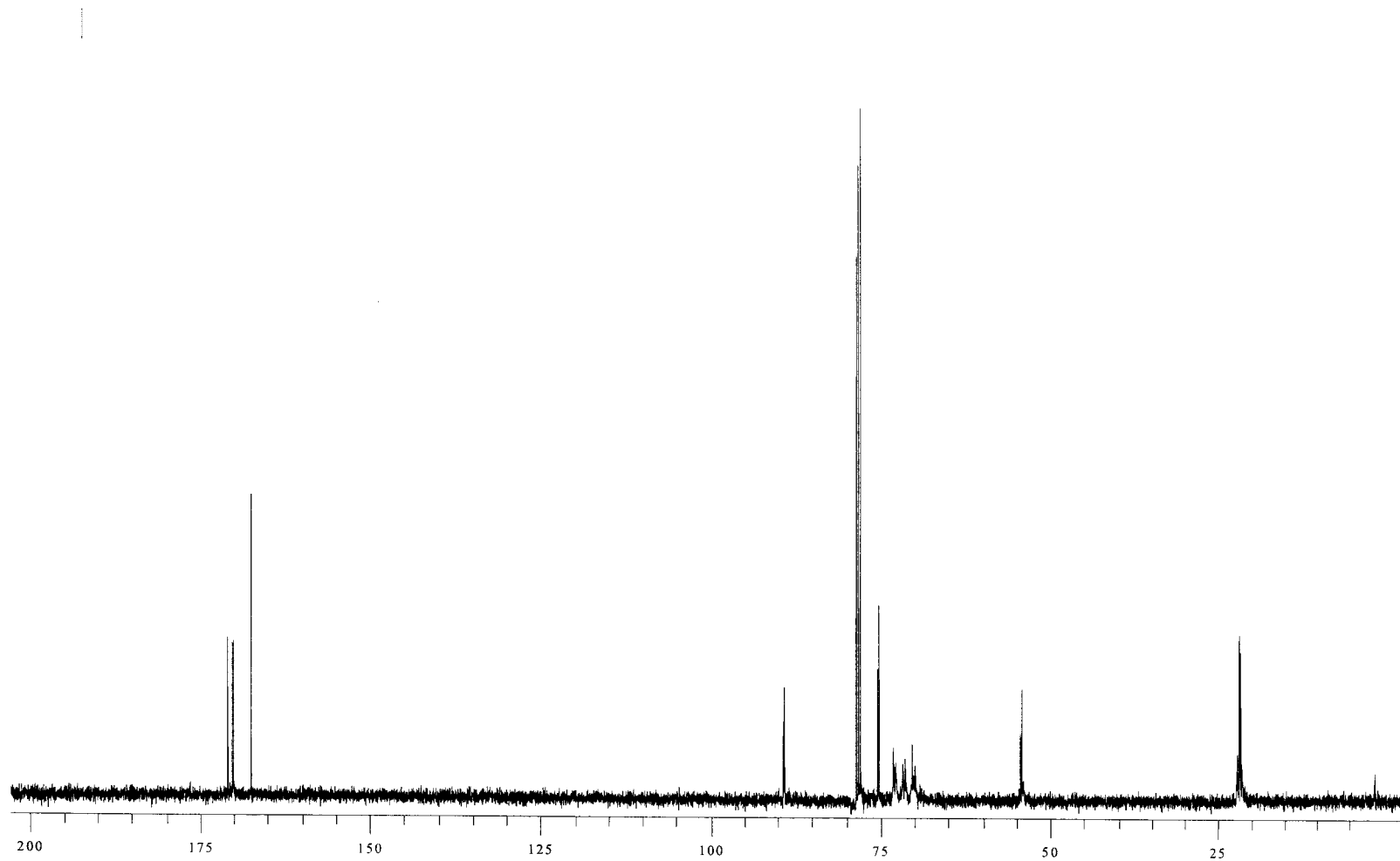
Figure 30: 100 MHz ^{13}C NMR spectrum of methyl glucuronate azide **14**.

Display Report

Analysis Info:
File: D:\DATA\YURI\YR300901.D
Date acquired:
Instrument:
Task   :
Method   :

Printed: Thu Apr 24 14:56:23 2003

Operator :

Sample   :

Acquisition Parameter:
Source   :
Mode   :
CapExit   :
Scan Range:
Accum.time:
MS/MS   :

Polarity :

Skim 1   :
Trap Drive:
Summation :
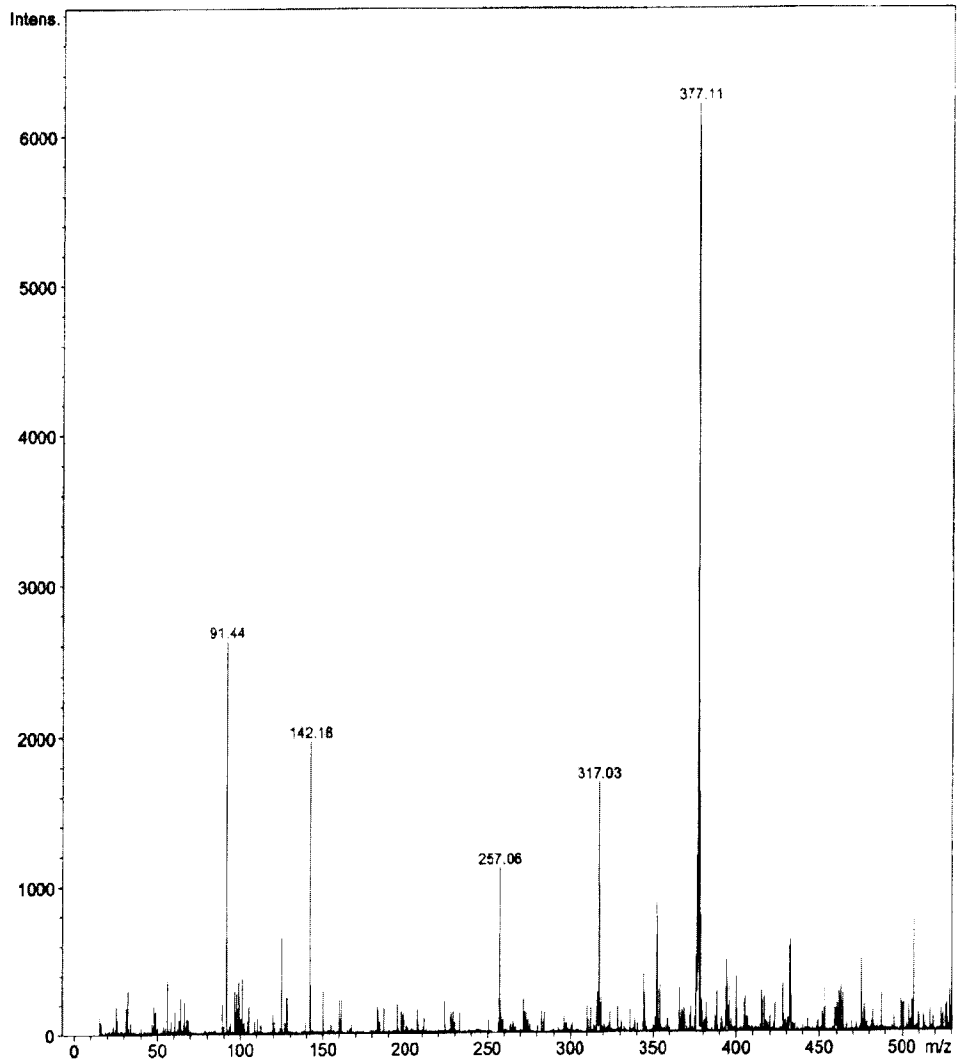
Figure 31: Mass spectrum of methyl glucuronosyl azide **14.**
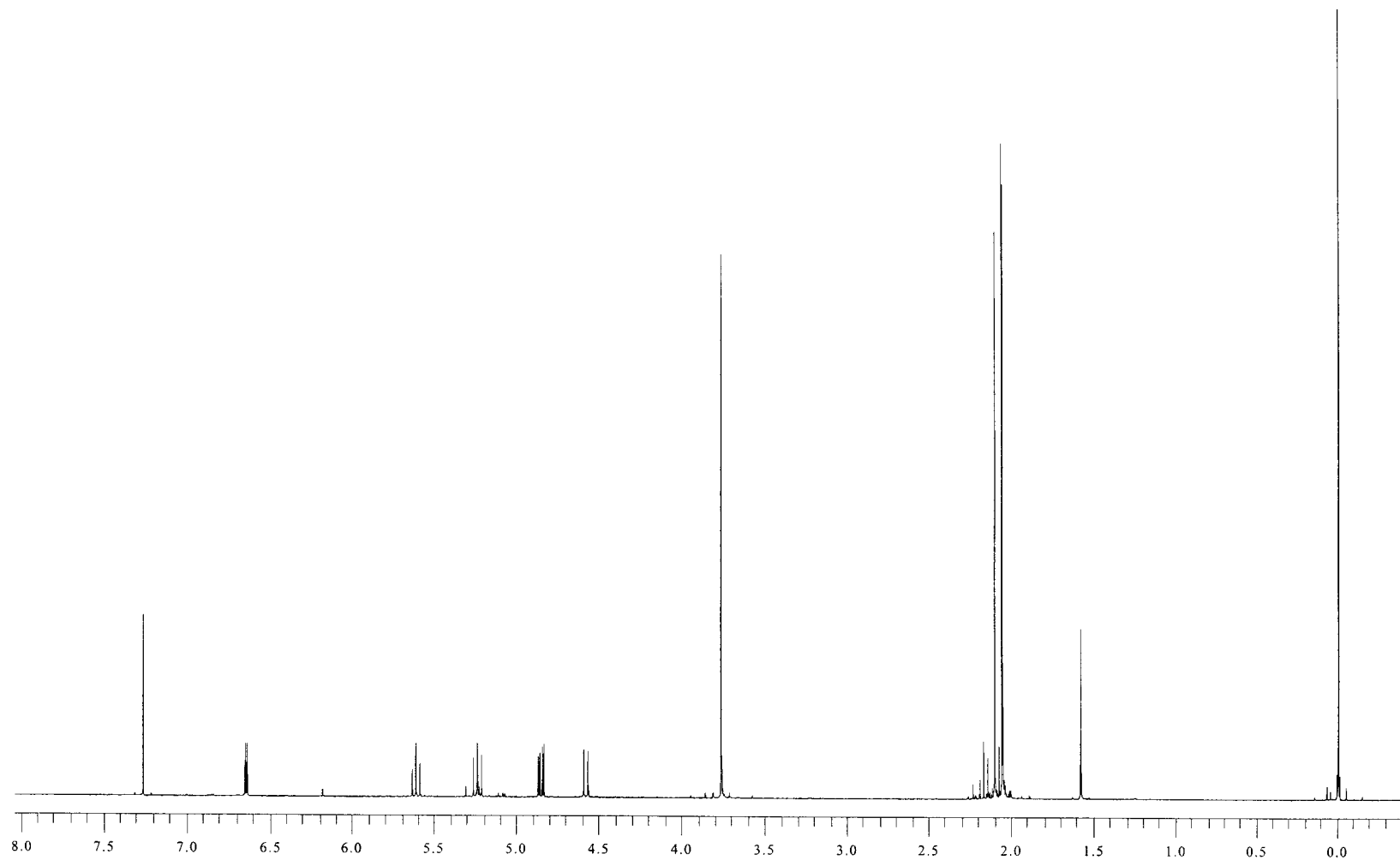
Figure 32: 400 MHz ^{1}H NMR spectrum of α-glucosyl bromide **16**.
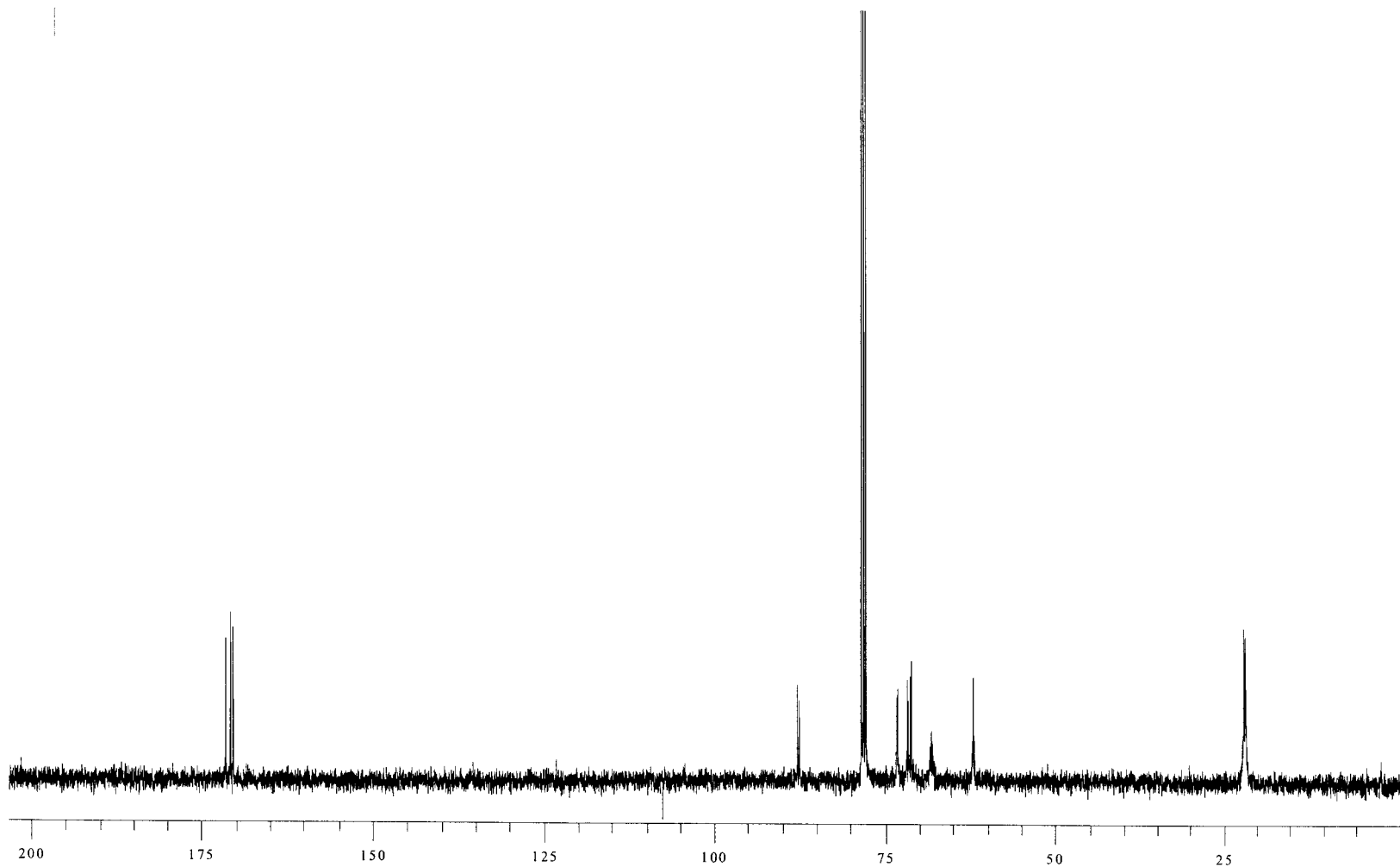
Figure 33: 100 MHz ^{13}C NMR spectrum of α-glucosyl bromide **16**.
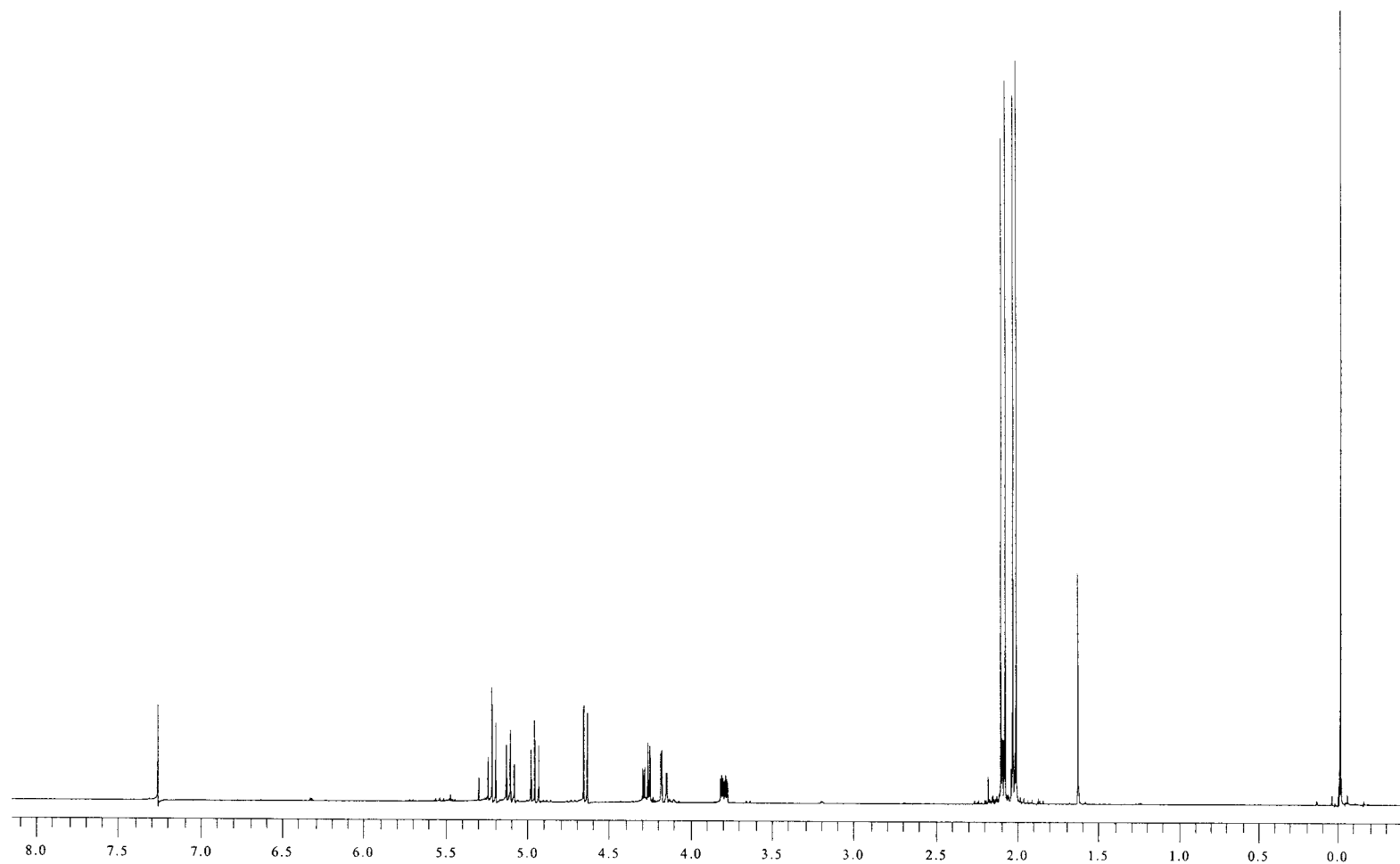
Figure 34: 400 MHz ^{1}H NMR spectrum of β-glucosyl azide **17**.
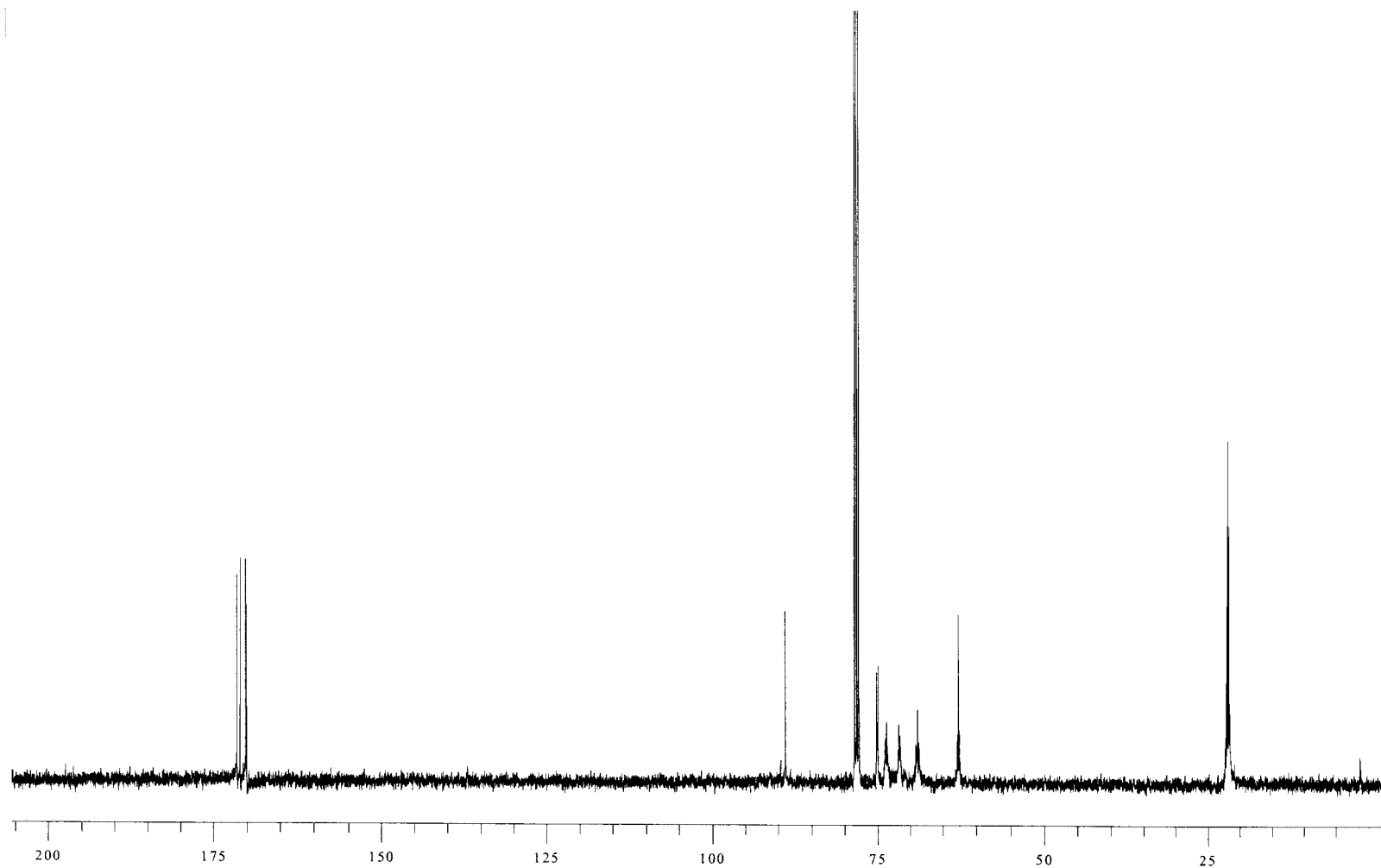
Figure 35: 100 MHz ^{13}C NMR spectrum of β-glucosyl azide **17**.

Display Report
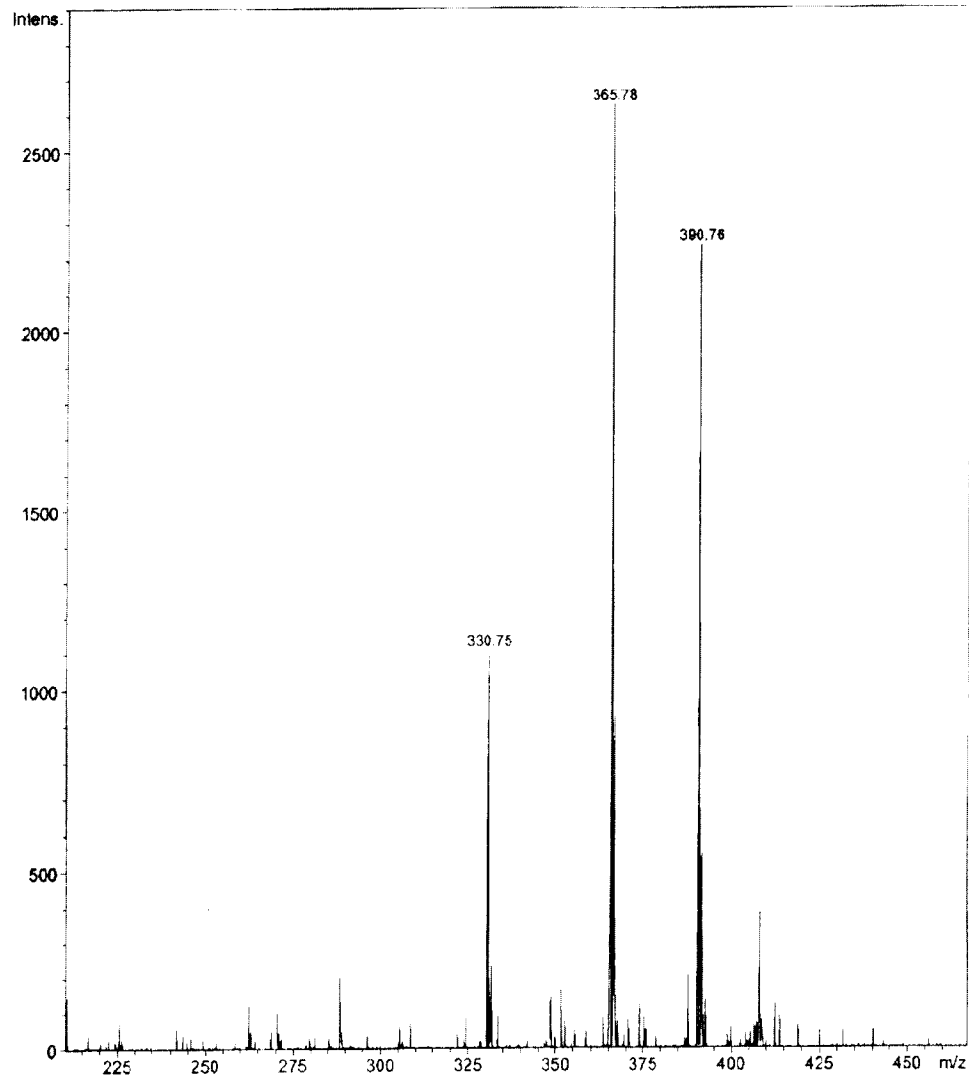
Figure 36: Mass spectrum of β-glucosyl azide 17.
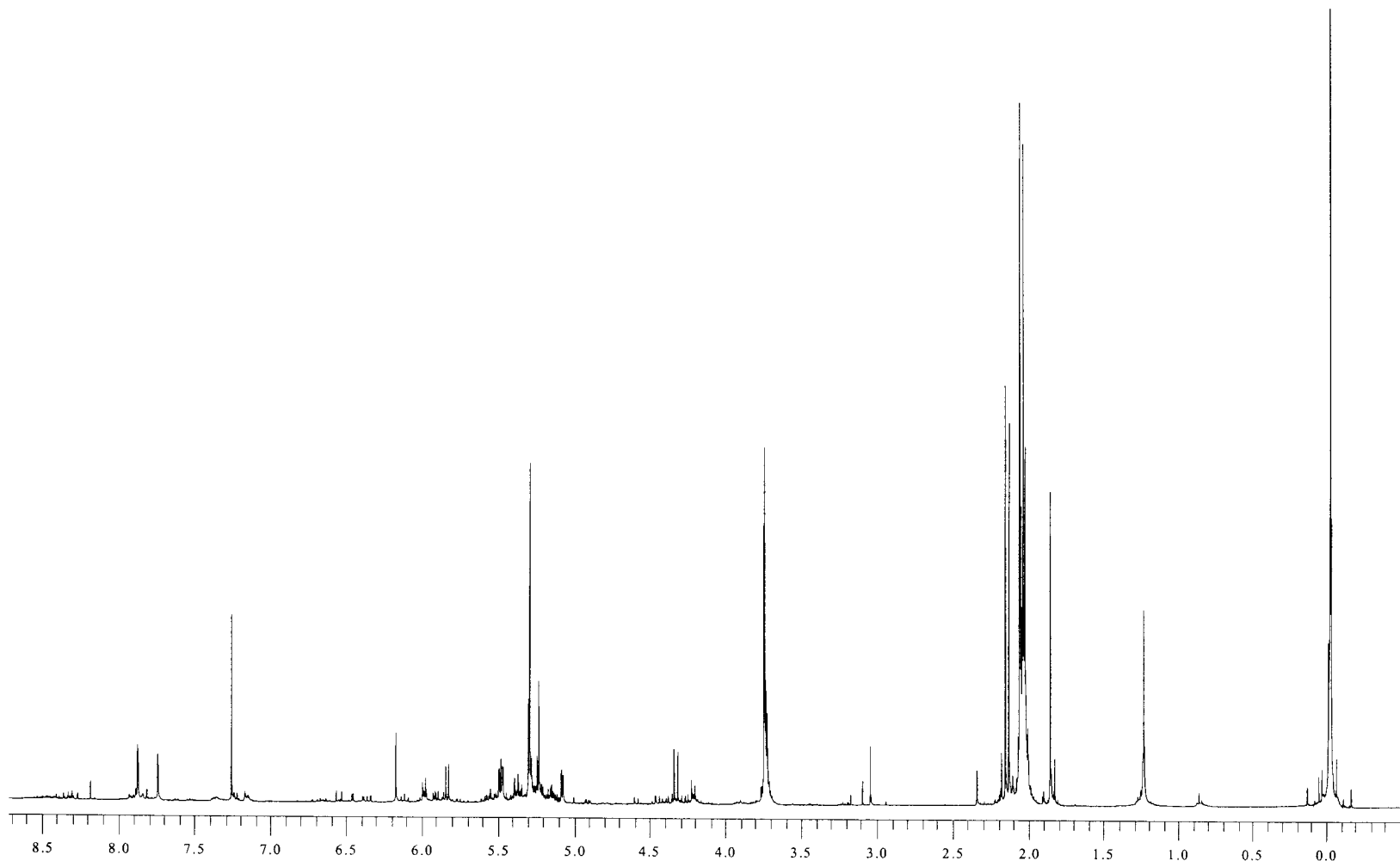
Figure 37: 400 MHz ^{1}H NMR spectrum of crude glucopyranuronosyl-1H-[1,2,3]triazol-4-(and 5-)carboxylic acids **18**.

Display Report

Analysis Info:
File: D:\DATA\YURI\5-063402.D   Printed: Mon Apr 28 17:15:17 2003
Date acquired:
Instrument: '   Operator :
Task   :
Method   :   Sample   :

Acquisition Parameter:
Source   :   Polarity :
Mode   :
CapExit   :   Skim 1   :
Scan Range: Trap Drive:
Accum.time: Summation :
MS/MS   :
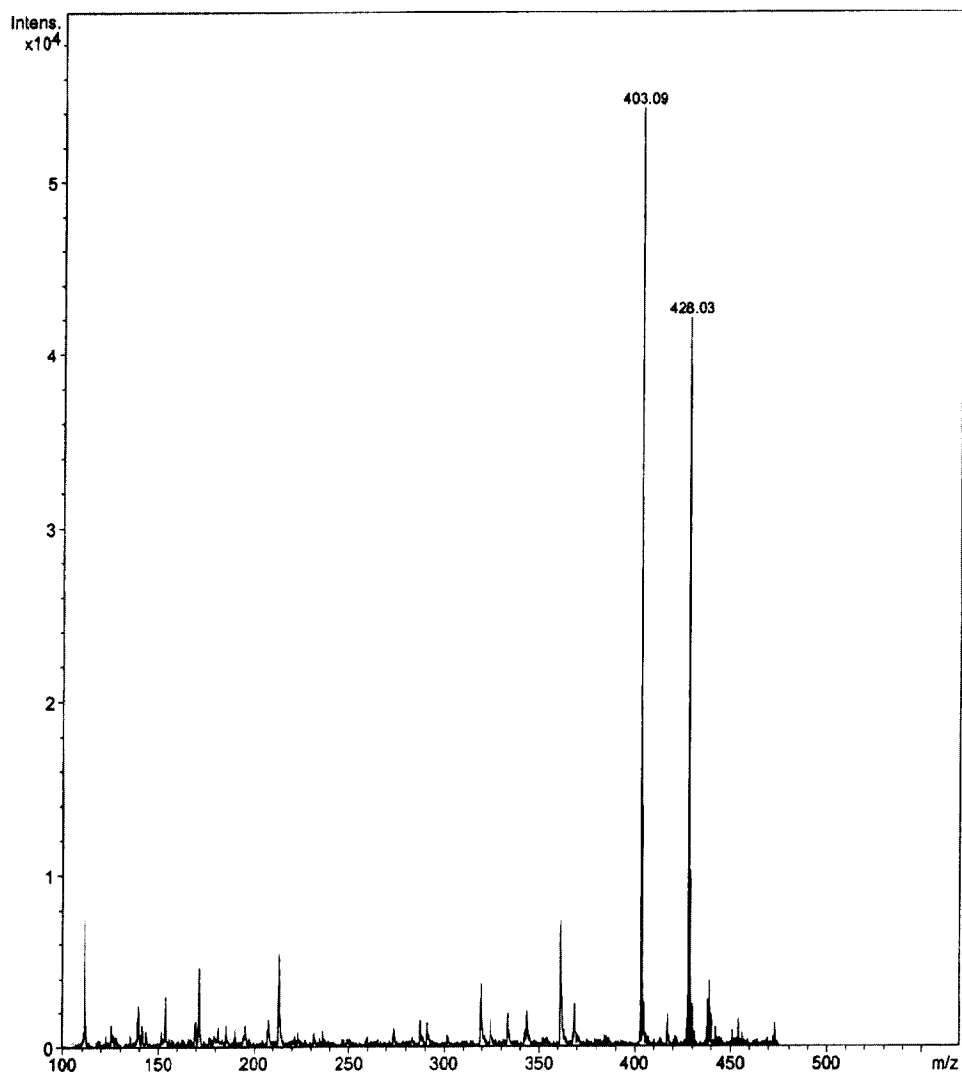
Figure 38: Mass spectrum of crude glucopyranuronosyl-1H-[1,2,3]triazol-4-(and 5-)carboxylic acids 18.
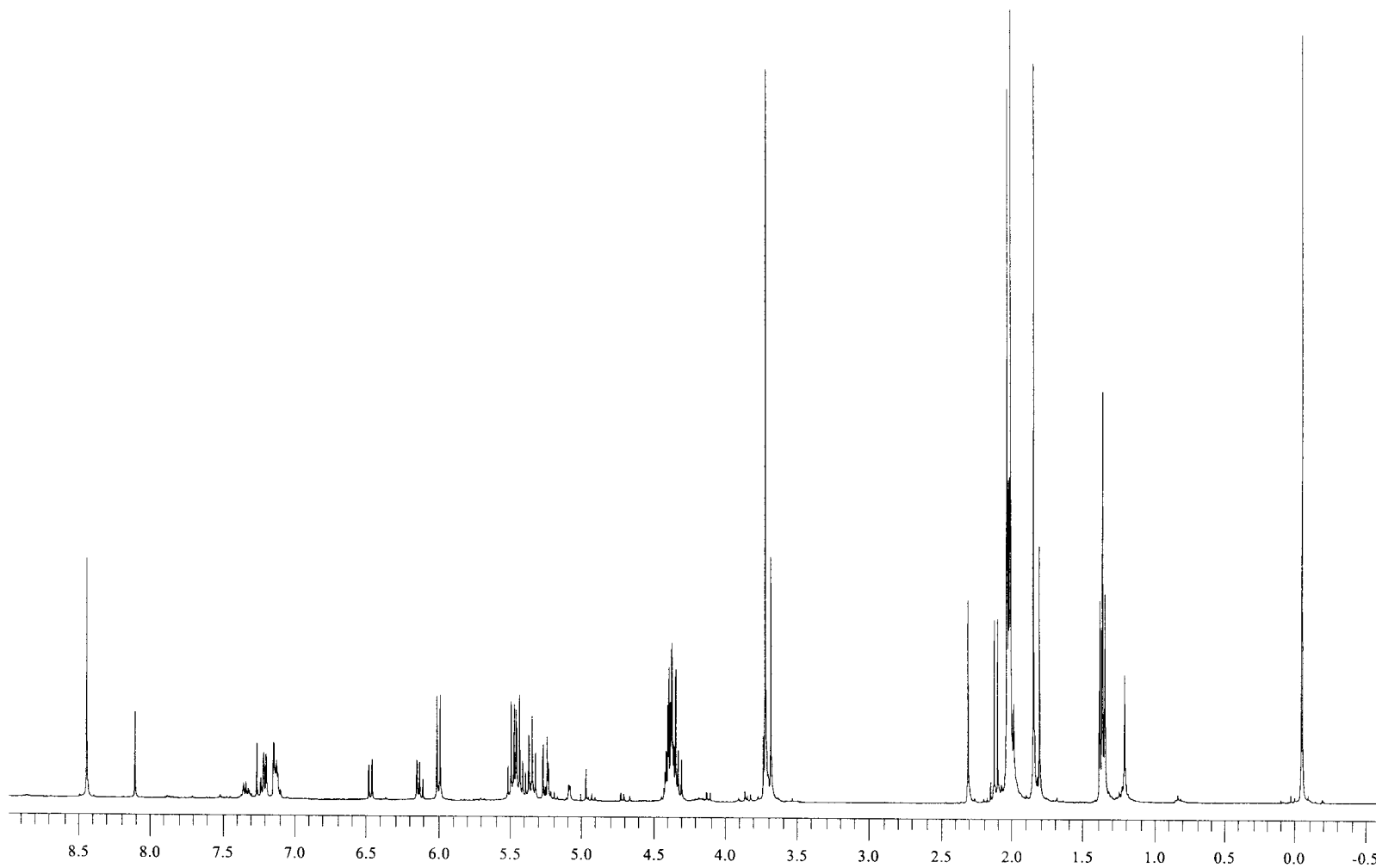
Figure 39: 400 MHz ^{1}H NMR spectrum of glucopyranuronosyl-1*H*-[1,2,3]triazol-4-(and 5-)carboxylic acid ethyl esters **19**.

Display Report
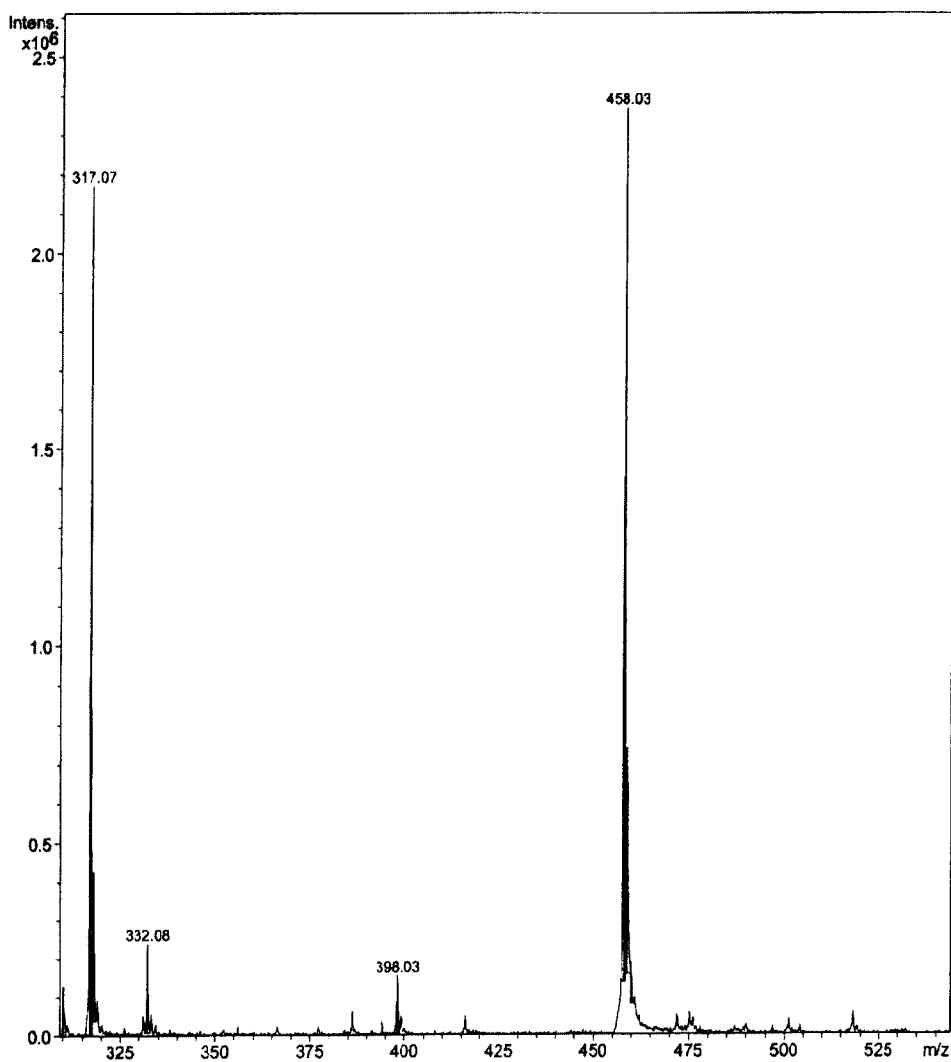
Figure 40: Mass spectrum of glucopyranuronosyl-1H-[1,2,3]triazol-4-(and 5-)carboxylic acid ethyl esters **19**.
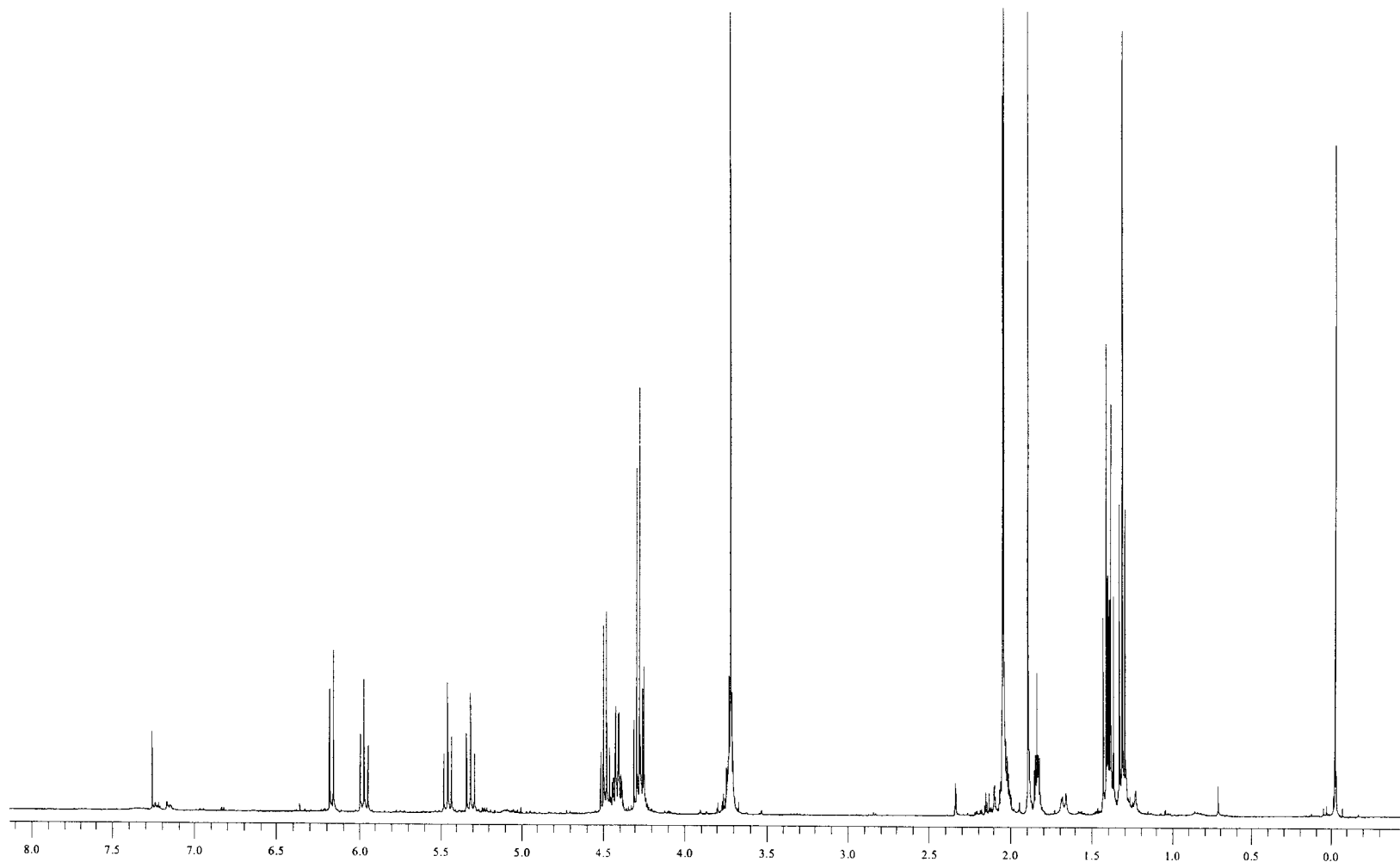
Figure 41: 400 MHz ^{1}H NMR spectrum of glucopyranuronosyl-1H-[1,2,3]triazol-4,5-dicarboxylic acid diethyl ester **20**.
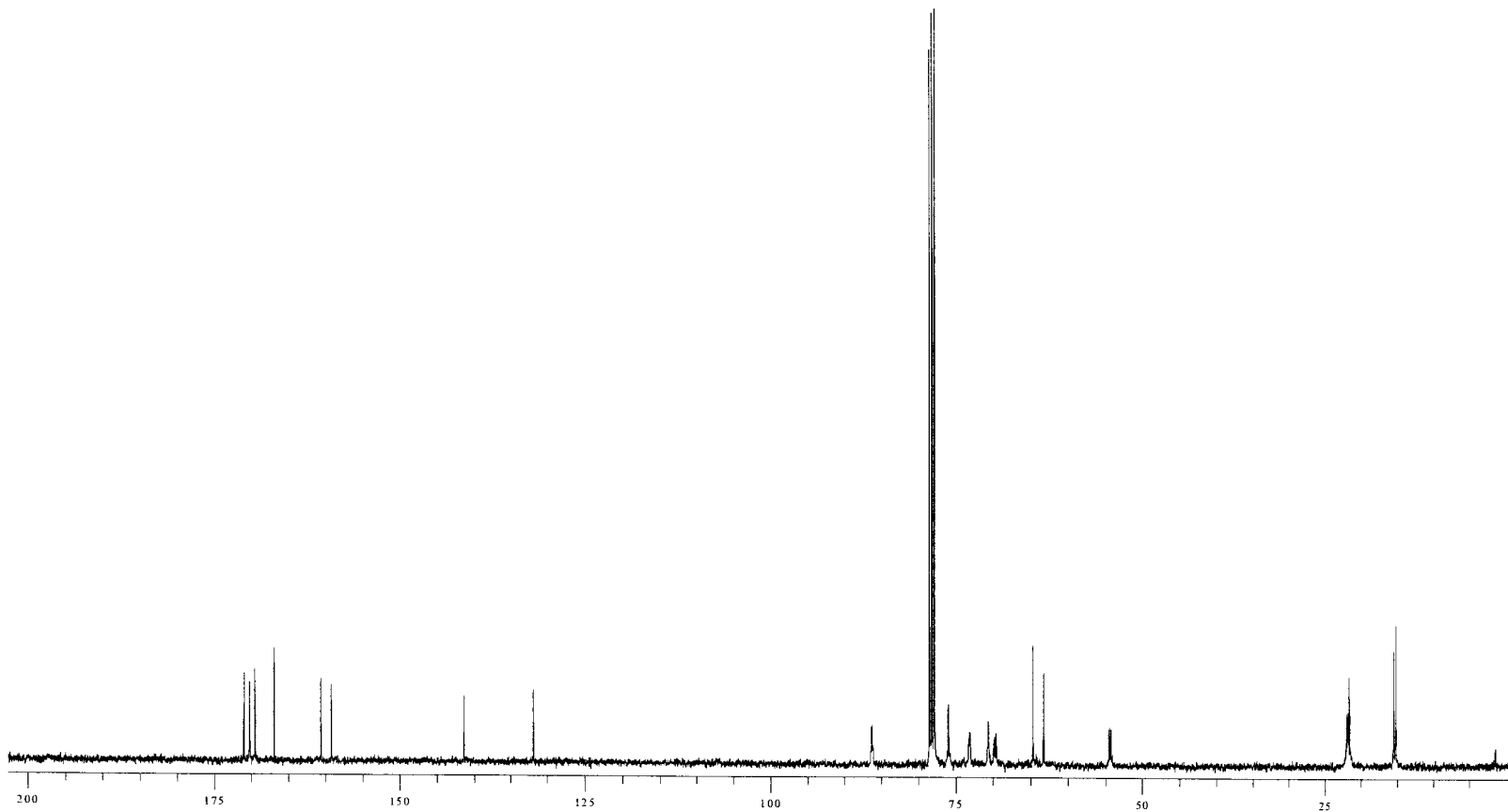
Figure 42: 100 MHz ^{13}C NMR spectrum of glucopyranuronosyl-1*H*-[1,2,3]triazol-4,5-dicarboxylic acid diethyl ester **20**.

Display Report
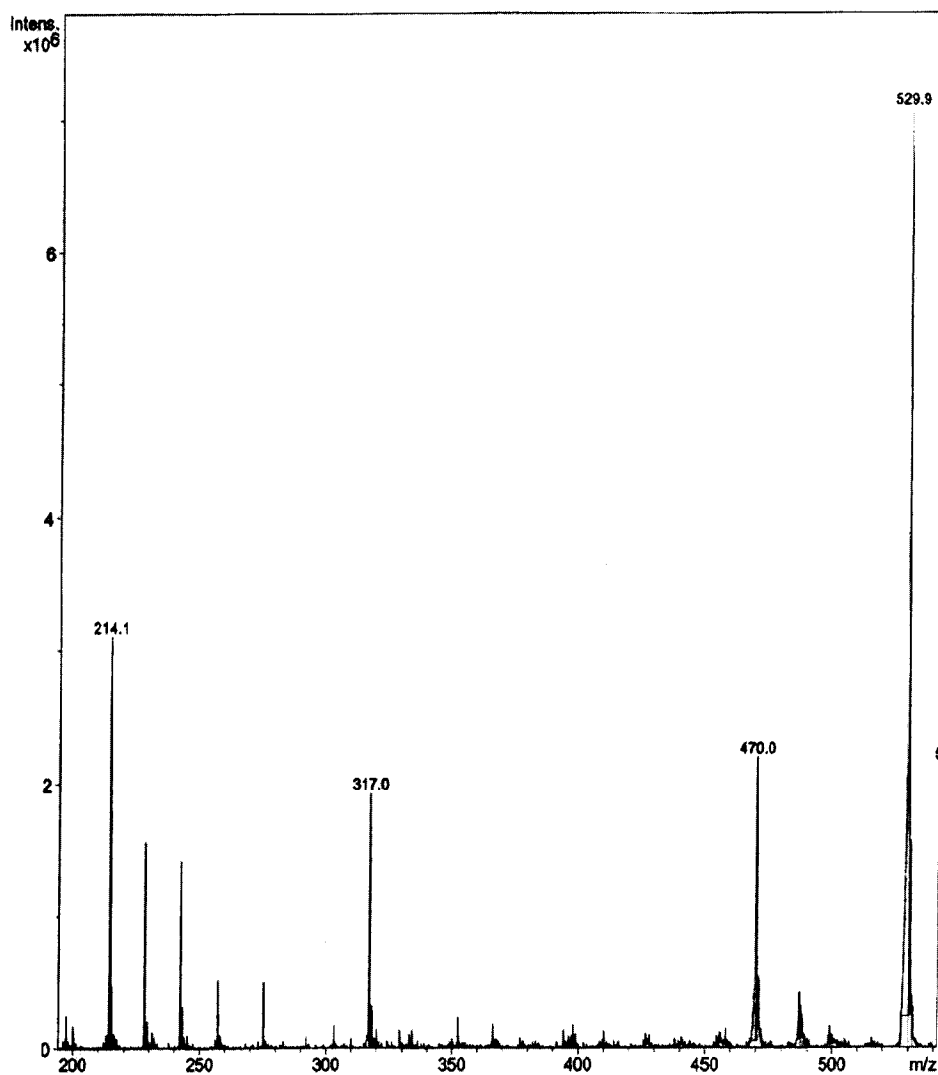
Figure 43: Mass spectrum of glucopyranuronosyl-1H-[1,2,3]triazol-4,5-dicarboxylic acid diethyl ester 20.
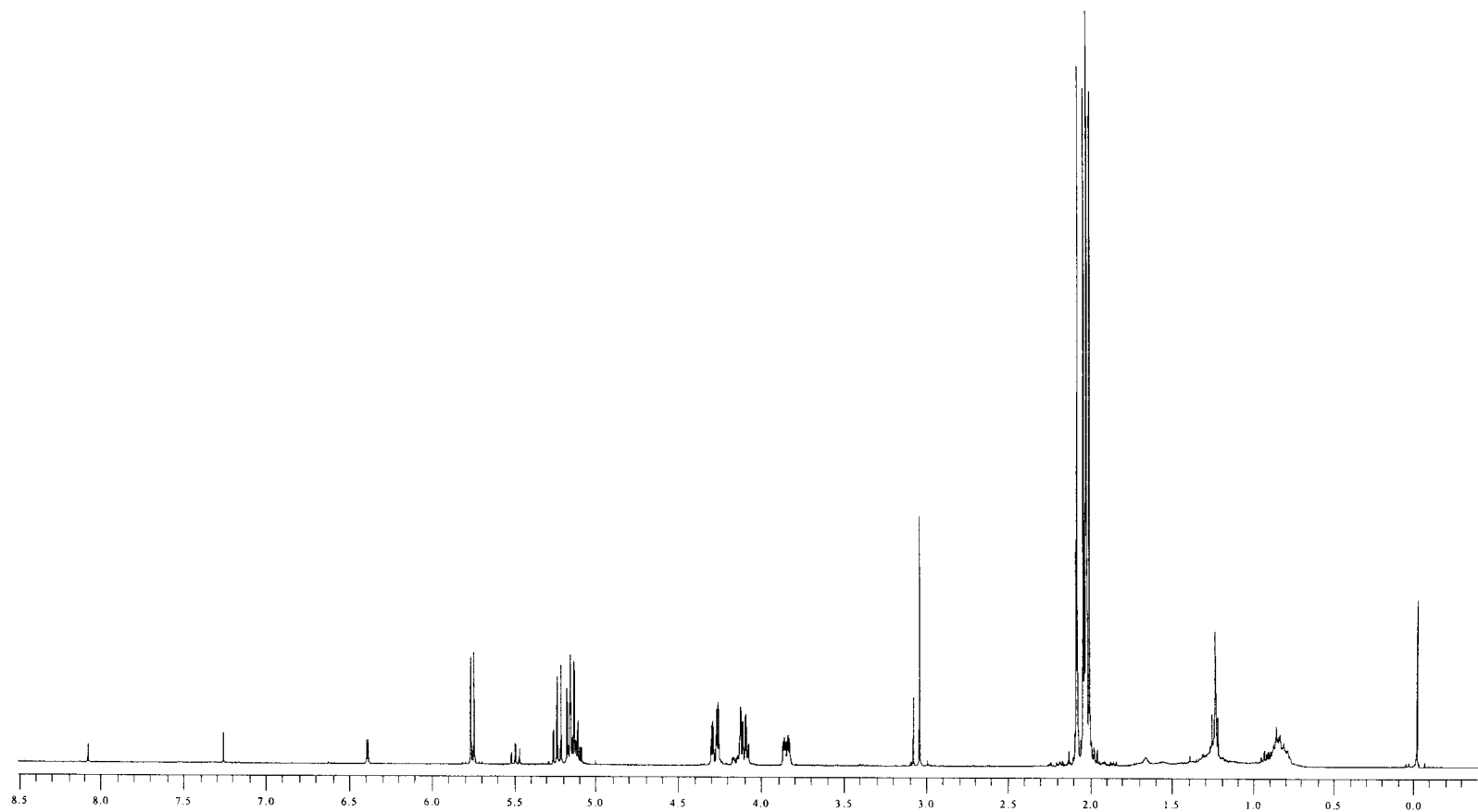
Figure 44: 400 MHz ^{1}H NMR spectrum of unknown product from treating glucosyl azide **17** with propiolic acid.

Display Report

Analysis Info:

File: D:\DATA\YURI\YR5061A0.D
Date acquired:
Instrument:
Task   :
Method   :

Printed: Thu Apr 17 10:20:17 2003

Operator :

Sample   :

Acquisition Parameter:

Source   :
Mode   :
CapExit   :
Scan Range:
Accum.time:
MS/MS   :

Polarity :

Skim 1   :
Trap Drive:
Summation :
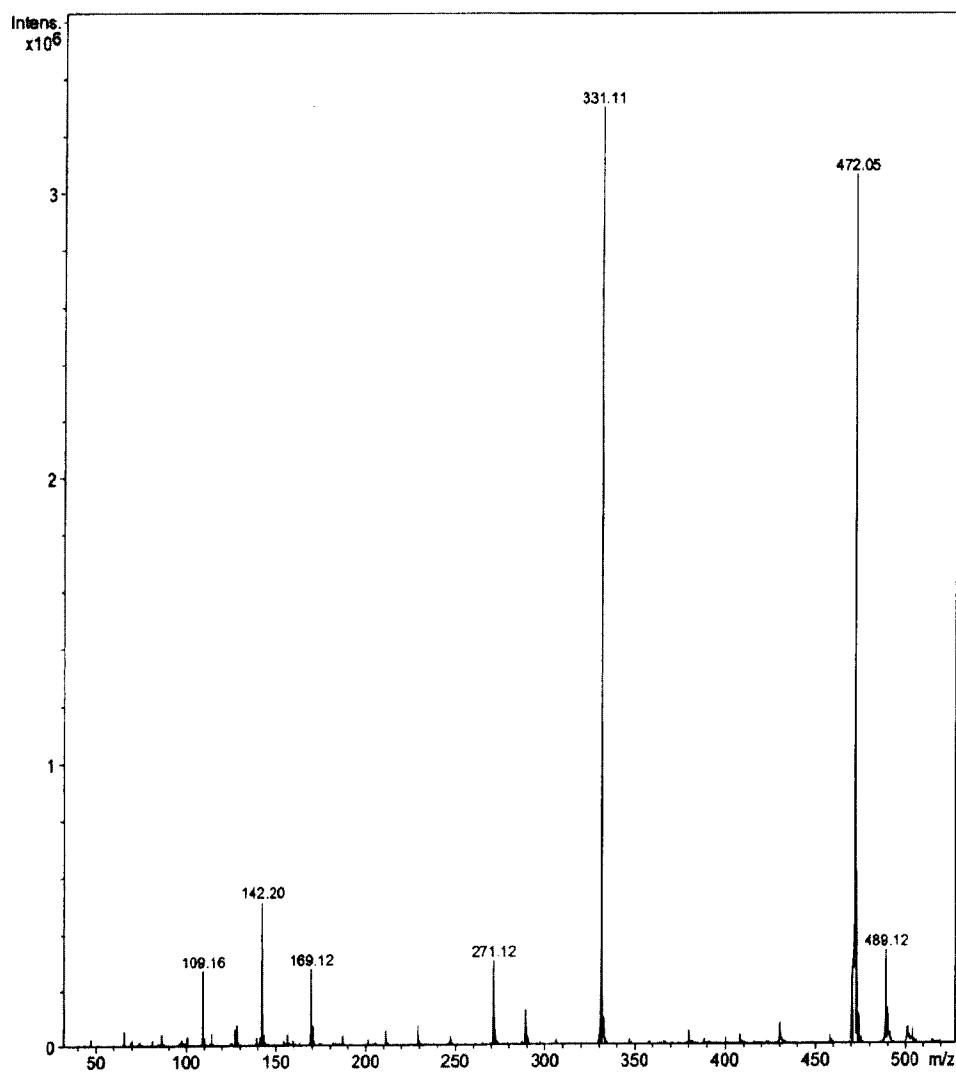
Figure 45: Mass spectrum of unknown product from treating glucosyl azide **17** with propiolic acid.
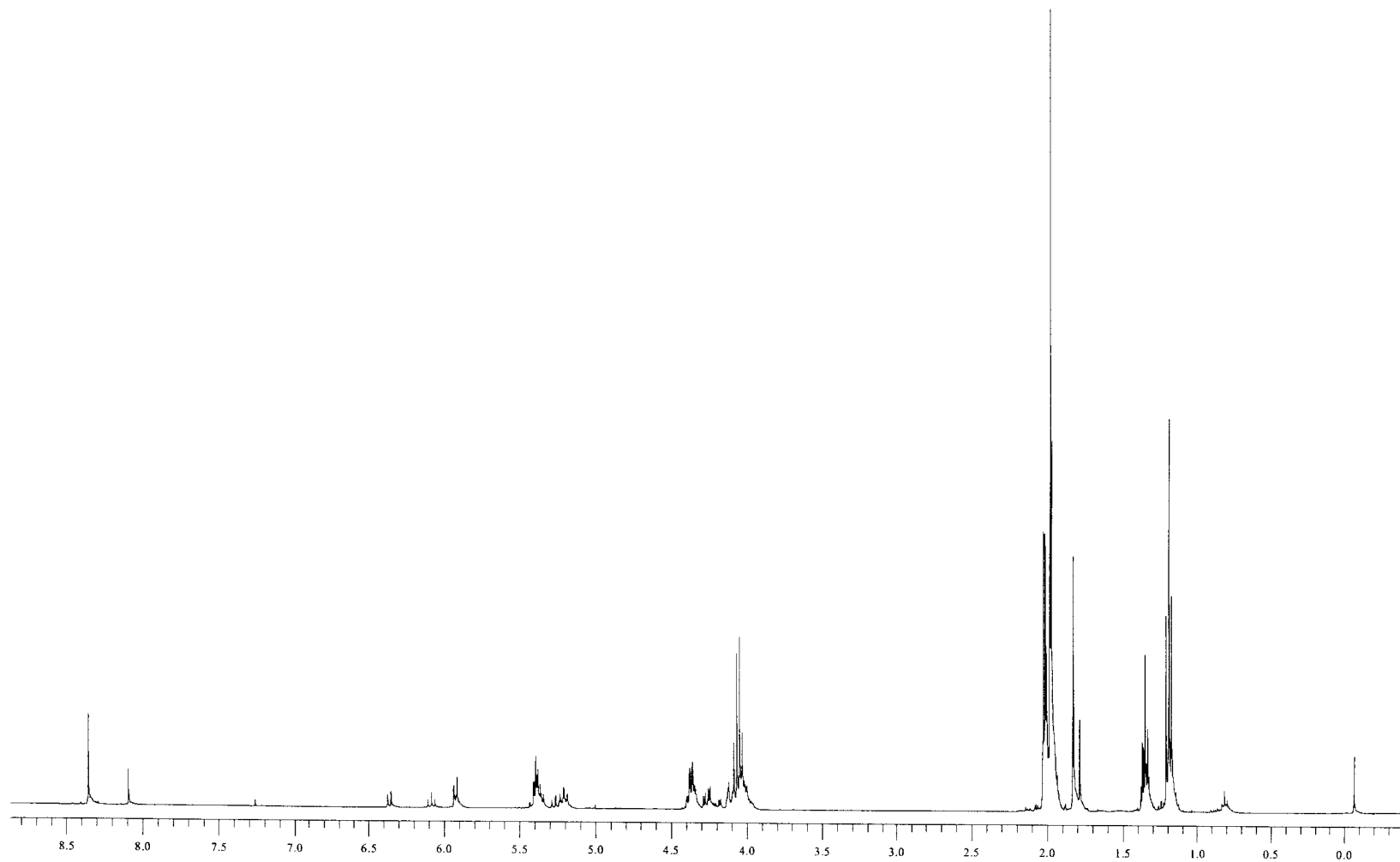
Figure 46: 400 MHz ^{1}H NMR spectrum of glucopyranosyl-1H-[1,2,3]triazol-4-(and 5-)-carboxylic acid ethyl esters **22**.
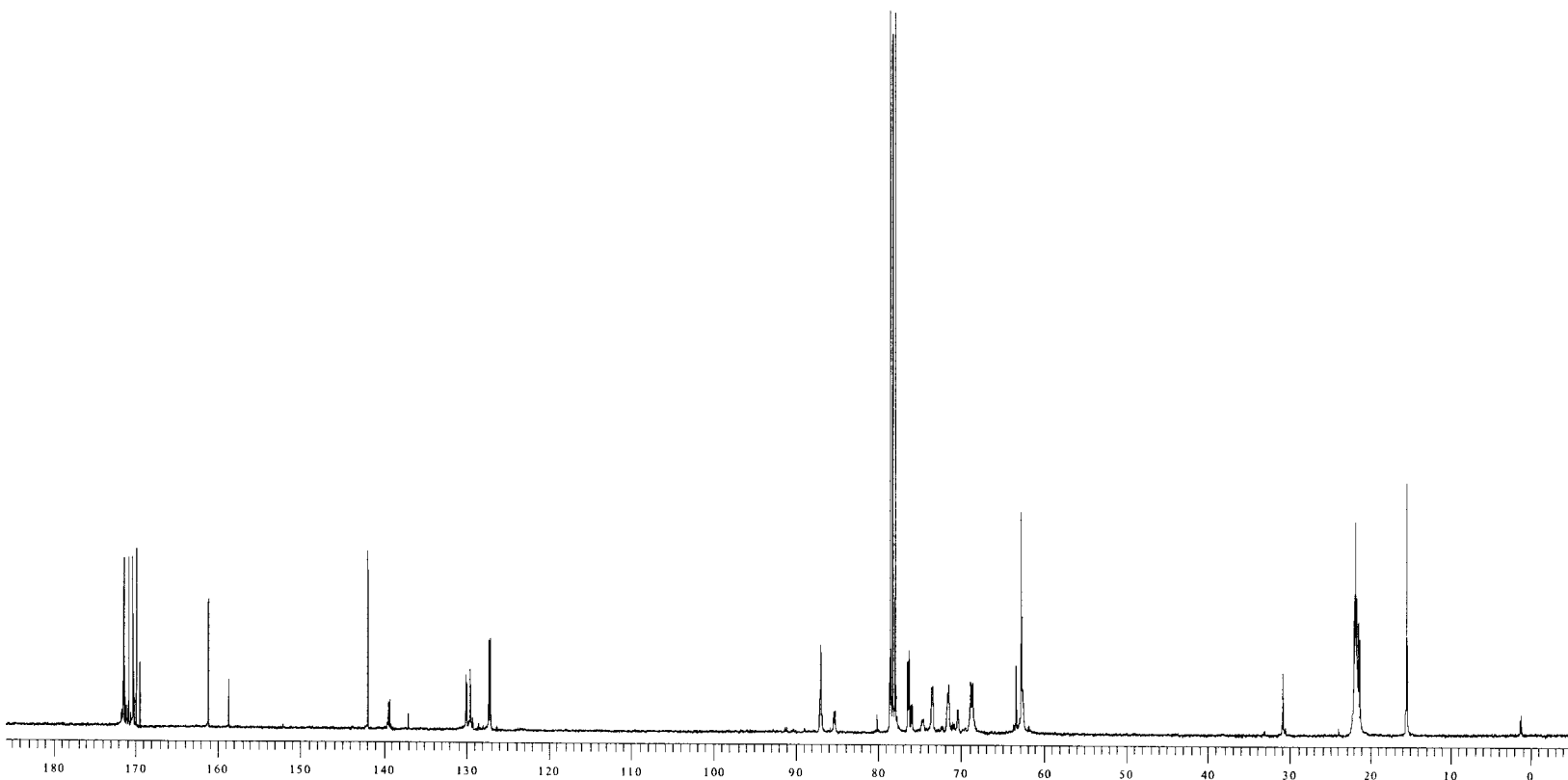
Figure 47: 100 MHz ^{13}C NMR spectrum of glucopyranosyl-1*H*-[1,2,3]triazol-4-(and 5-)-carboxylic acid ethyl esters **22**.

107

Display Report

Intens.
x10⁶

331.03

225.17
270.99
250.07
282.04
310.05
346.11 366.08
415.19 439.81
471.95
489.0

1.5
1.0
0.5
0.0

200   250   300   350   400   450   m/z
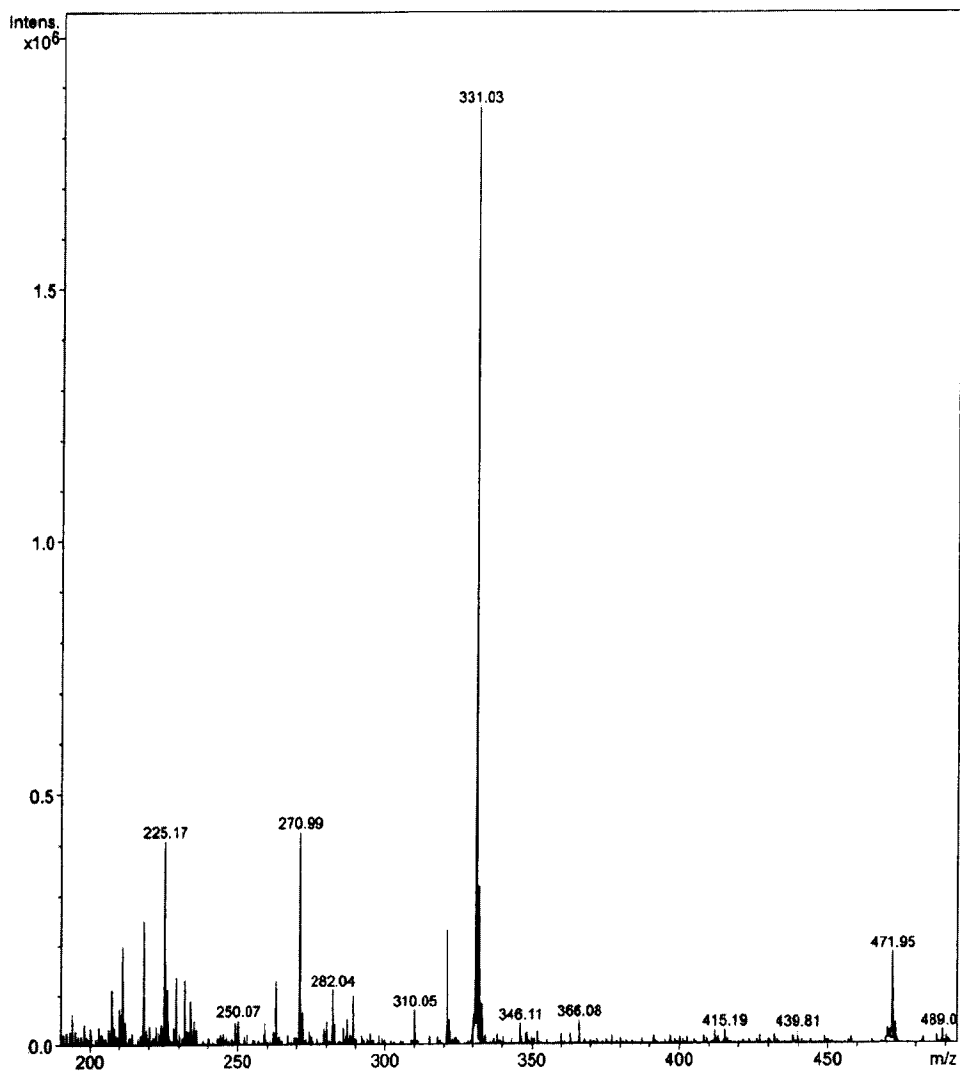
Figure 48: Mass spectrum of glucopyranosyl-1*H*-[1,2,3]triazol-4-(and 5-)-carboxylic acid ethyl esters **22.**
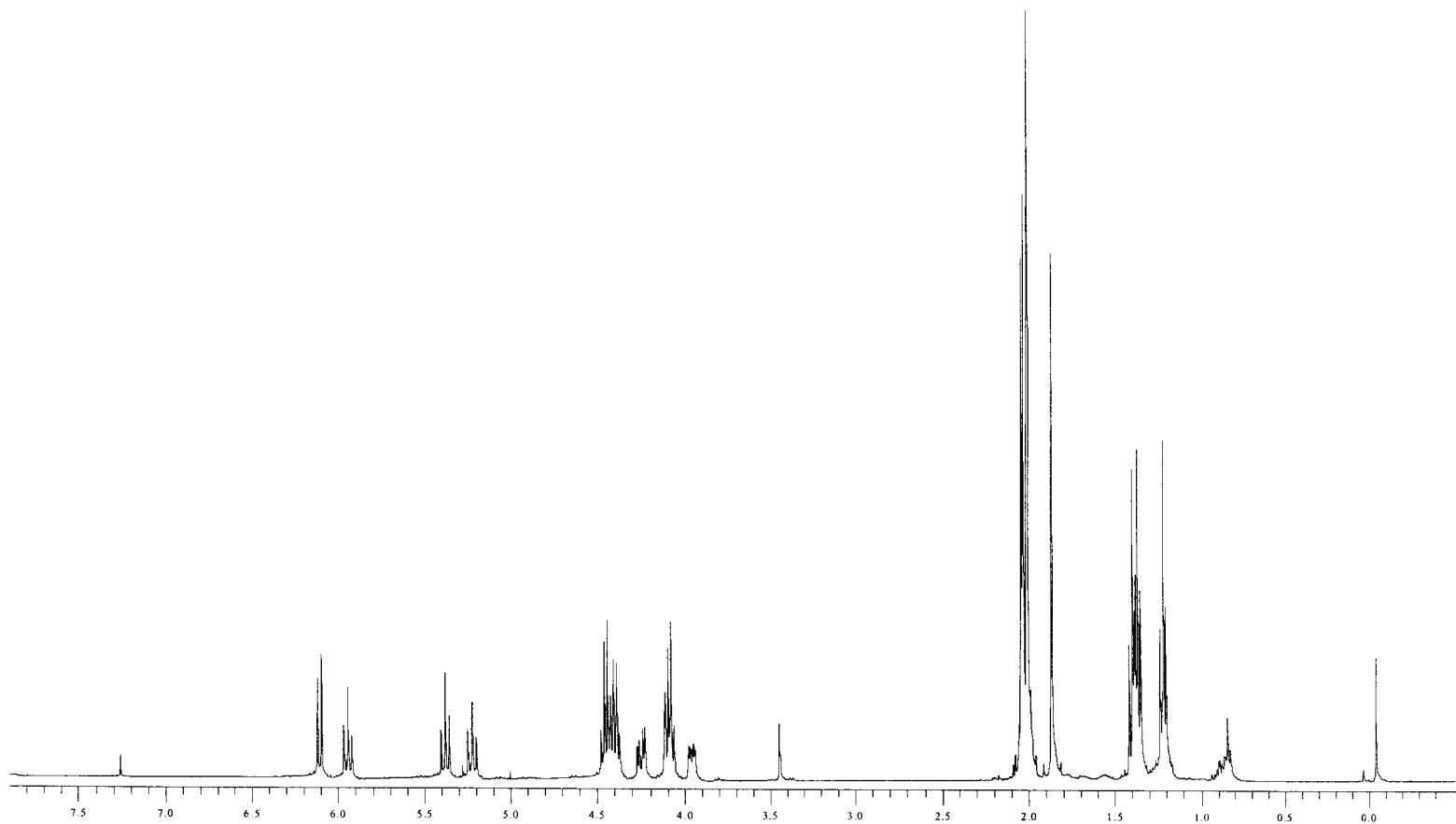
Figure 49: 400 MHz ^{1}H NMR spectrum of glucopyranosyl-1H-[1,2,3]triazol-4,5-dicarboxylic acid diethyl ester **23**.
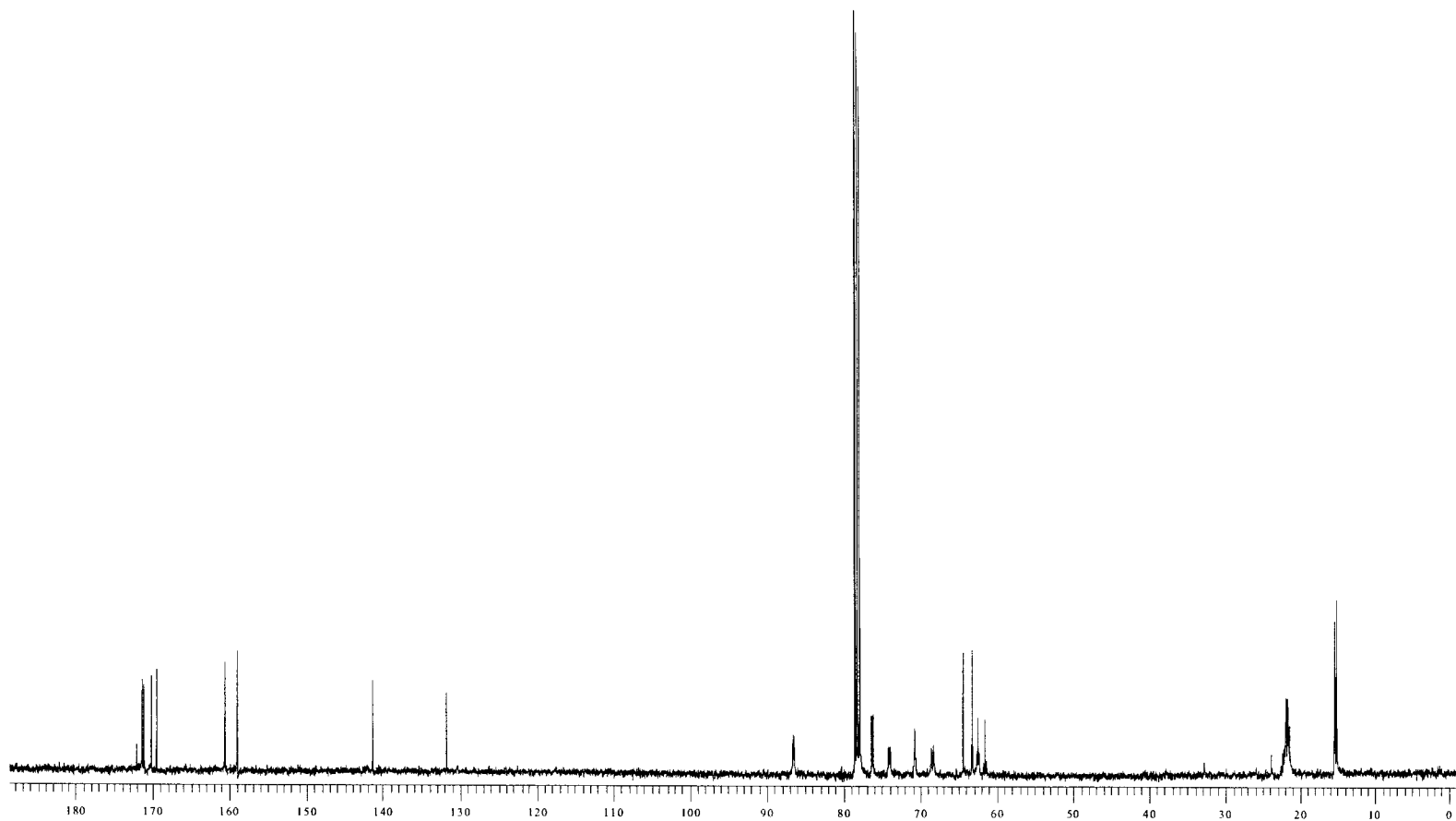
Figure 50: 100 MHz ^{13}C NMR spectrum of glucopyranosyl-1H-[1,2,3]triazol-4,5-dicarboxylic acid diethyl ester **23**.

Display Report
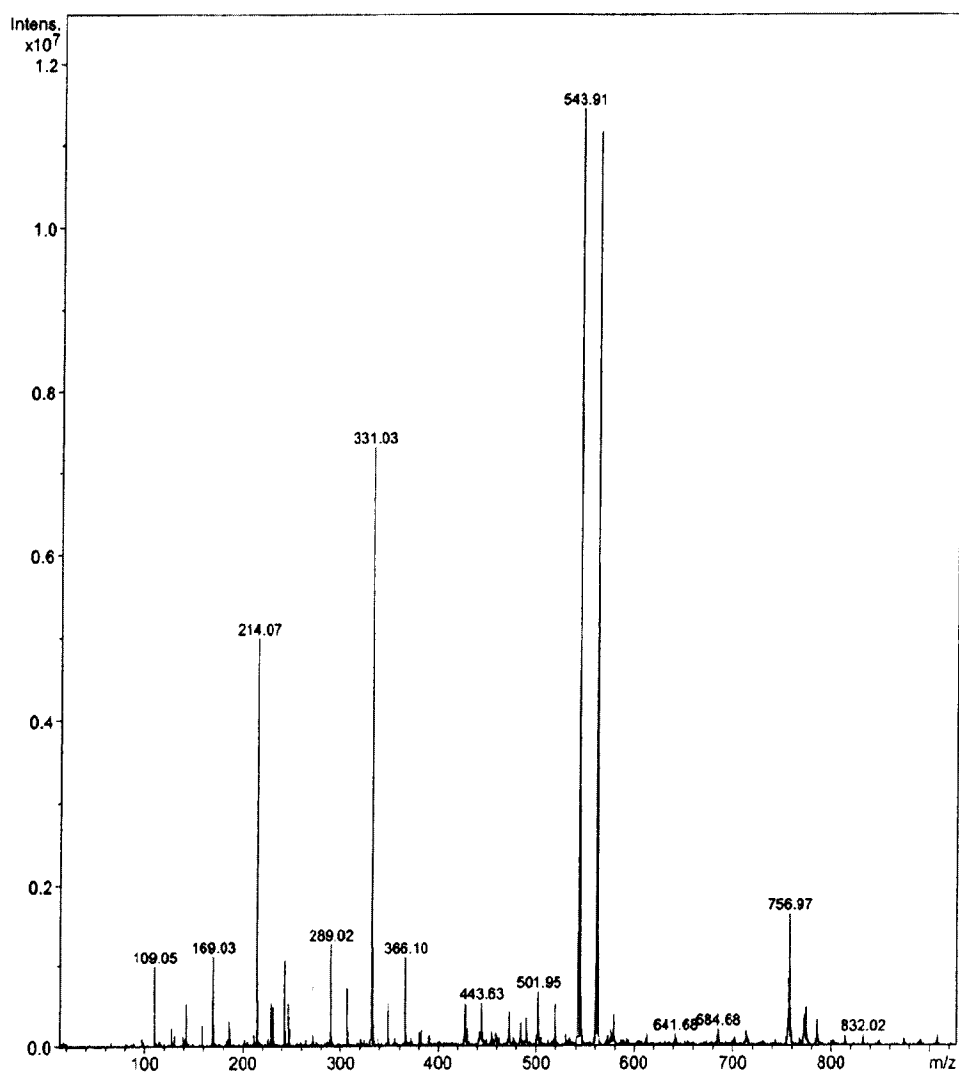
Figure 51: Mass spectrum of glucopyranosyl-1*H*-[1,2,3]triazol-4,5-dicarboxylic acid diethyl ester **23**.
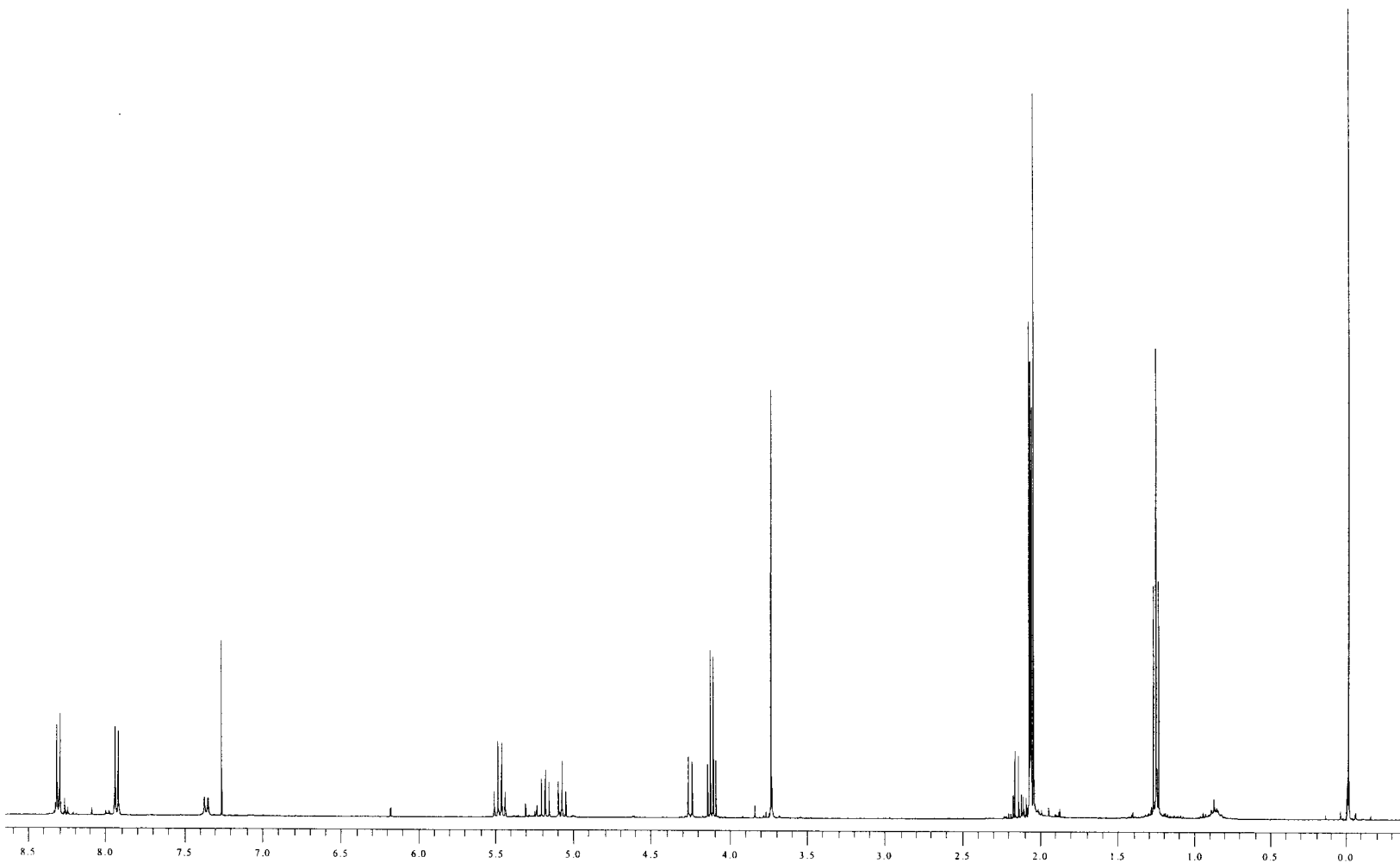
Figure 52: 400 MHz ^{1}H NMR spectrum of *p*-nitrobenzoic acid-β-D-glucopyranuronosyl amide **24**.
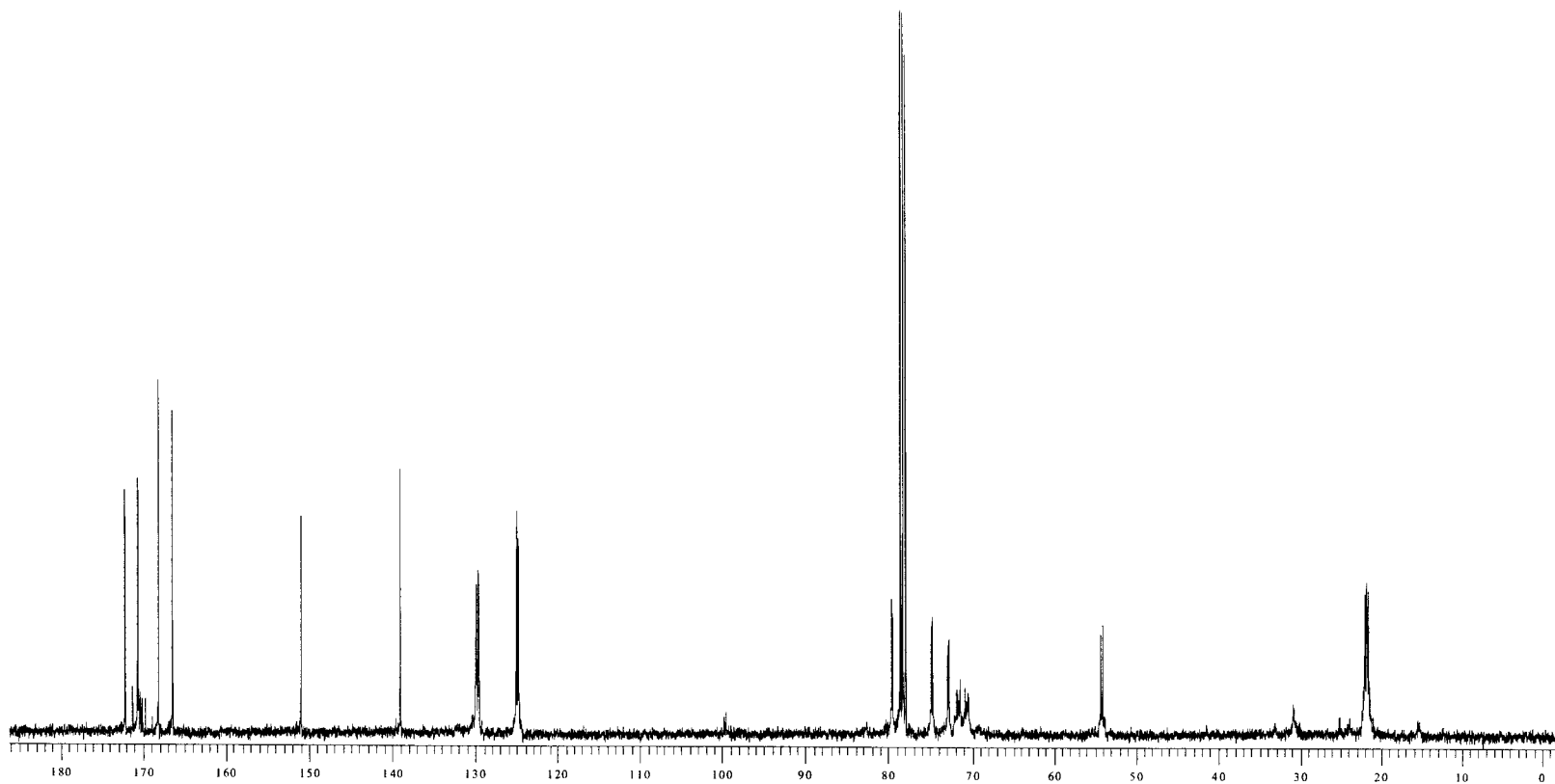
Figure 53: 100 MHz ^{13}C NMR spectrum of *p*-nitrobenzoic acid-β-D-glucopyranuronosyl amide **24**.

Display Report
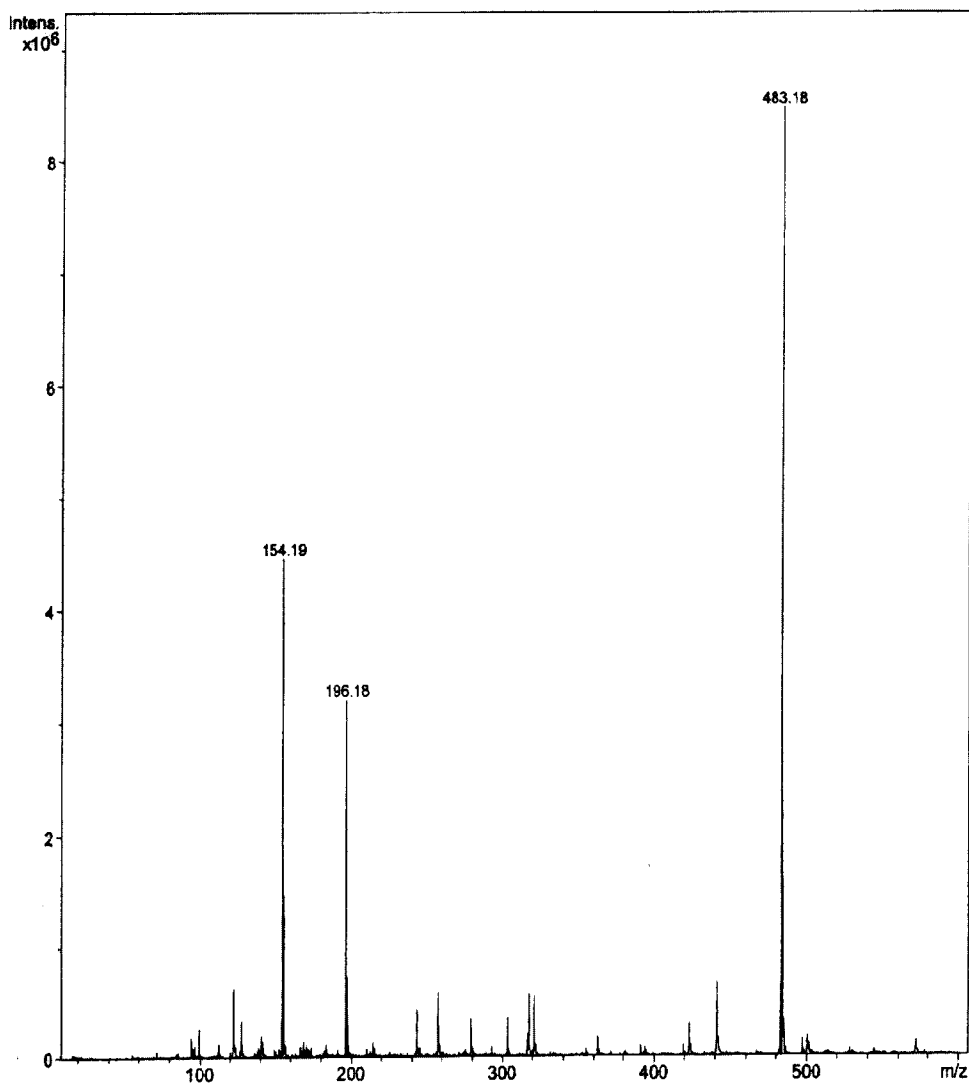
Figure 54: Mass spectrum of p-nitrobenzoic acid-β-D-glucopyranuronosyl amide 24.
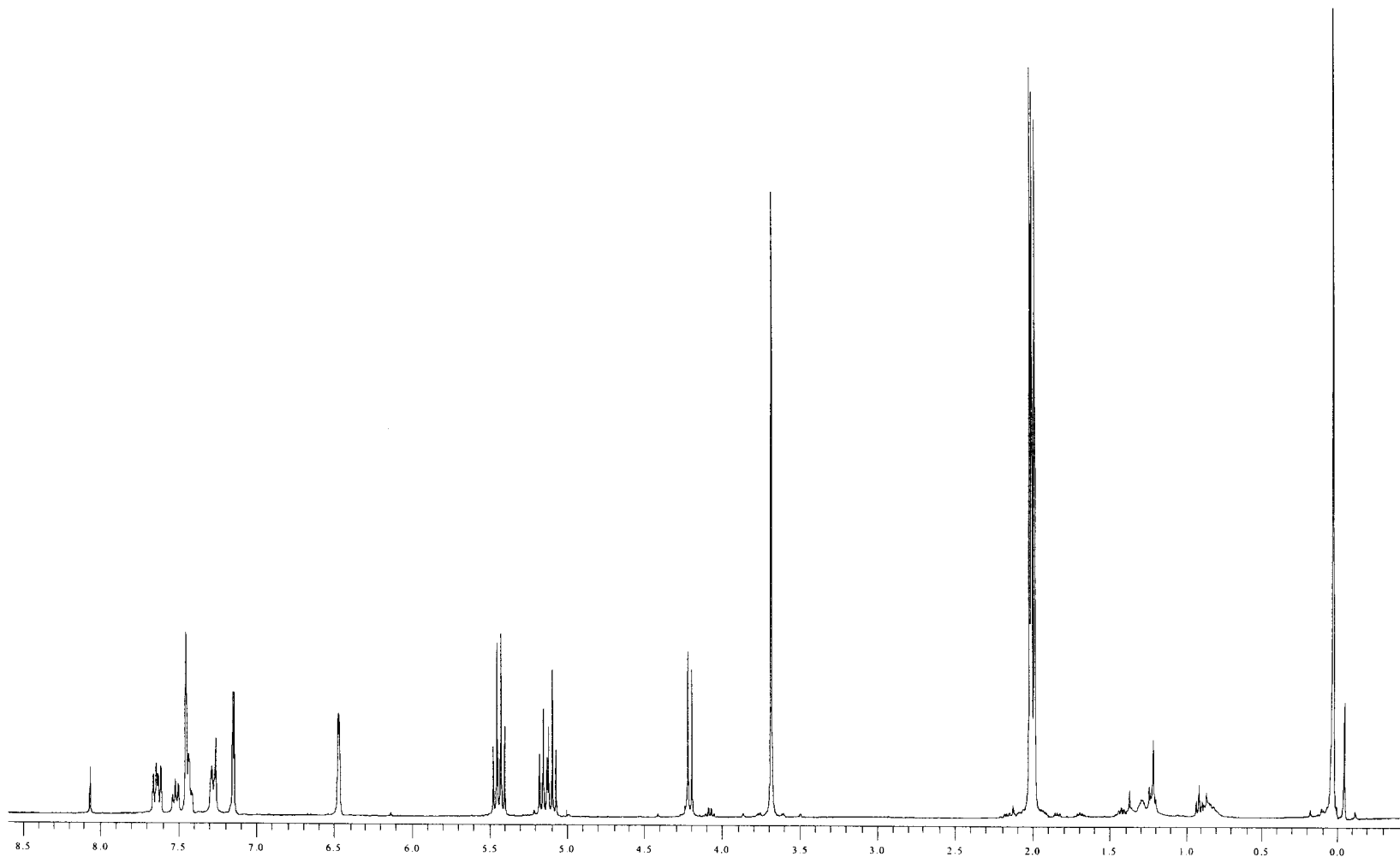
Figure 55: 400 MHz ^{1}H NMR spectrum of furan-2-carboxylic acid-β-D-glucopyranuronosyl amide **25**.
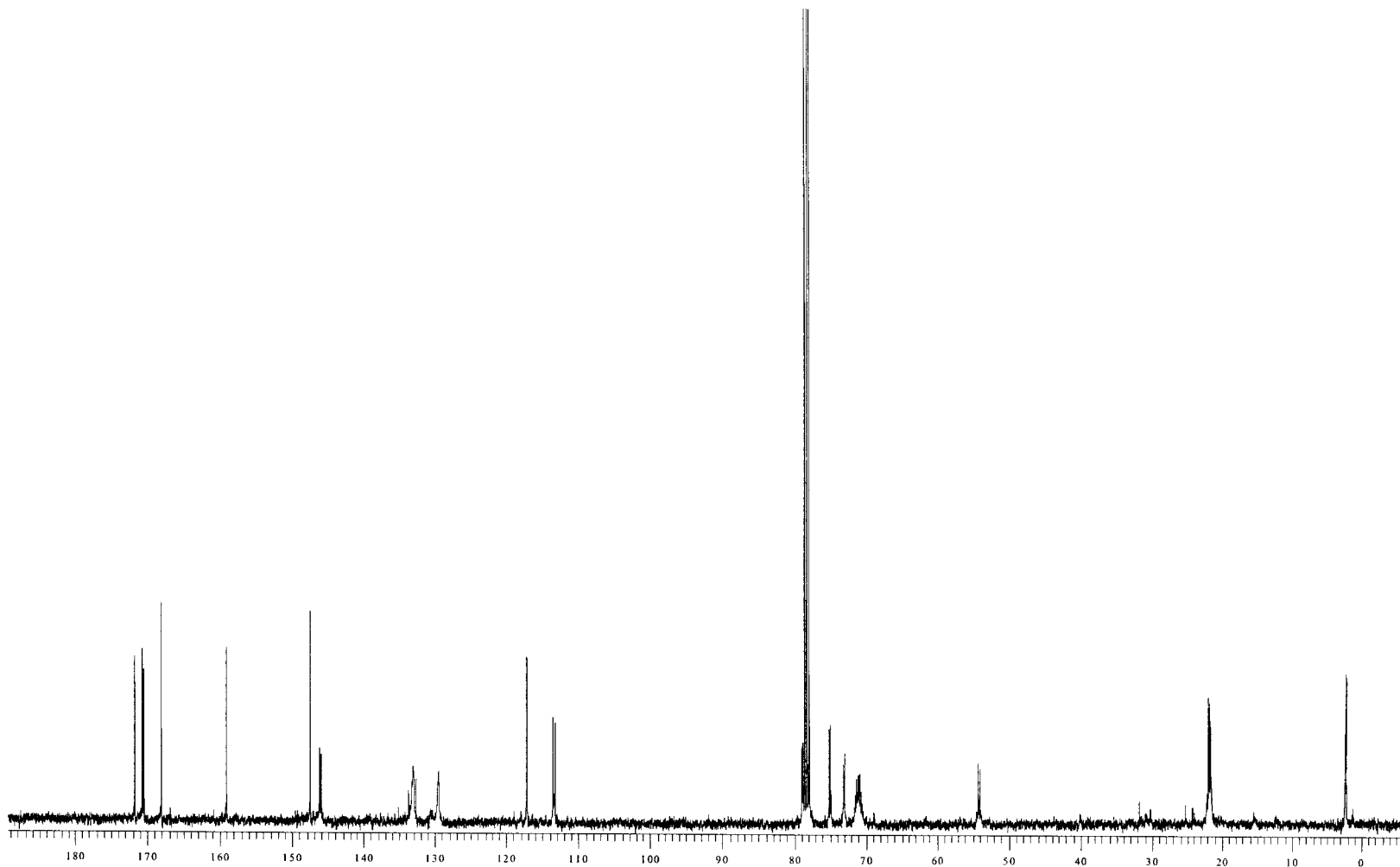
Figure 56: 100 MHz ^{13}C NMR spectrum of furan-2-carboxylic acid-β-D-glucopyranuronosyl amide **25**.

Display Report
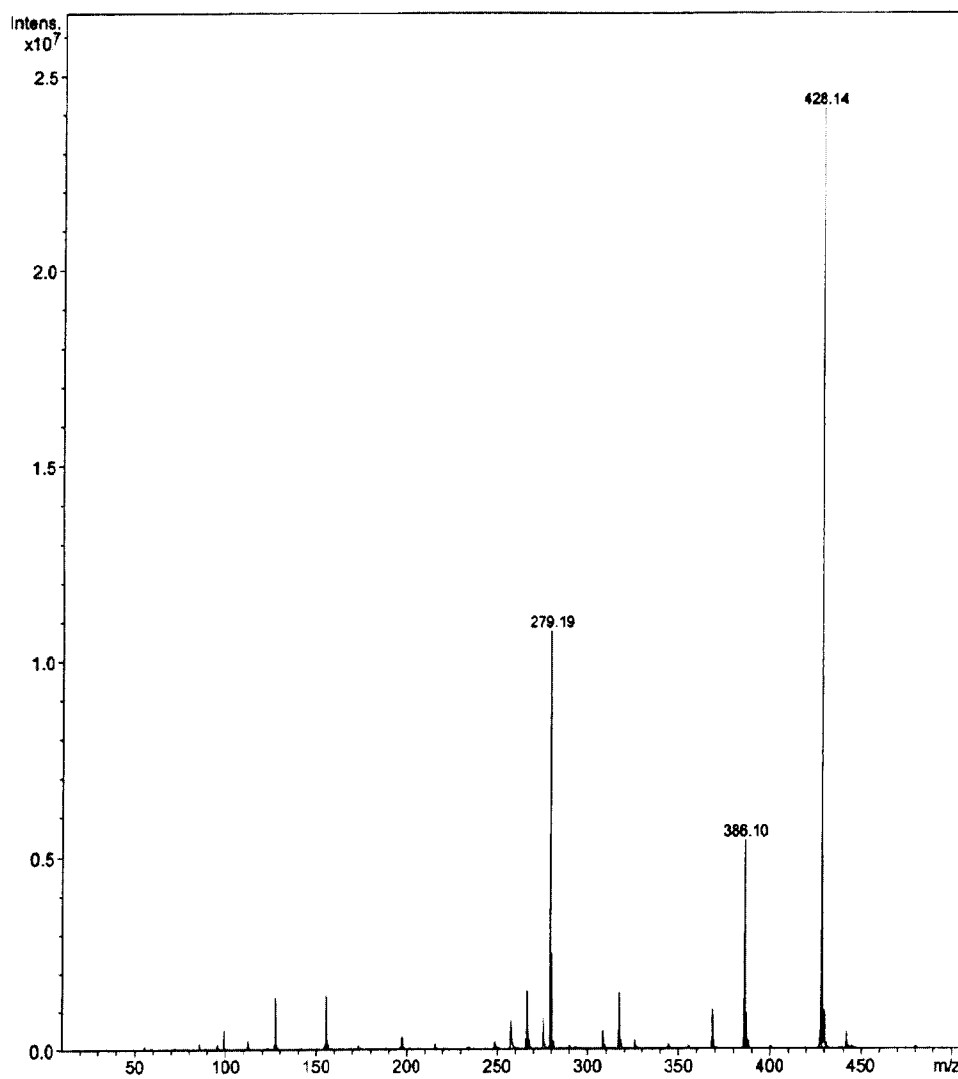
Figure 57: Mass spectrum of furan-2-carboxylic acid-β-D-glucopyranuronosyl amide **25**.
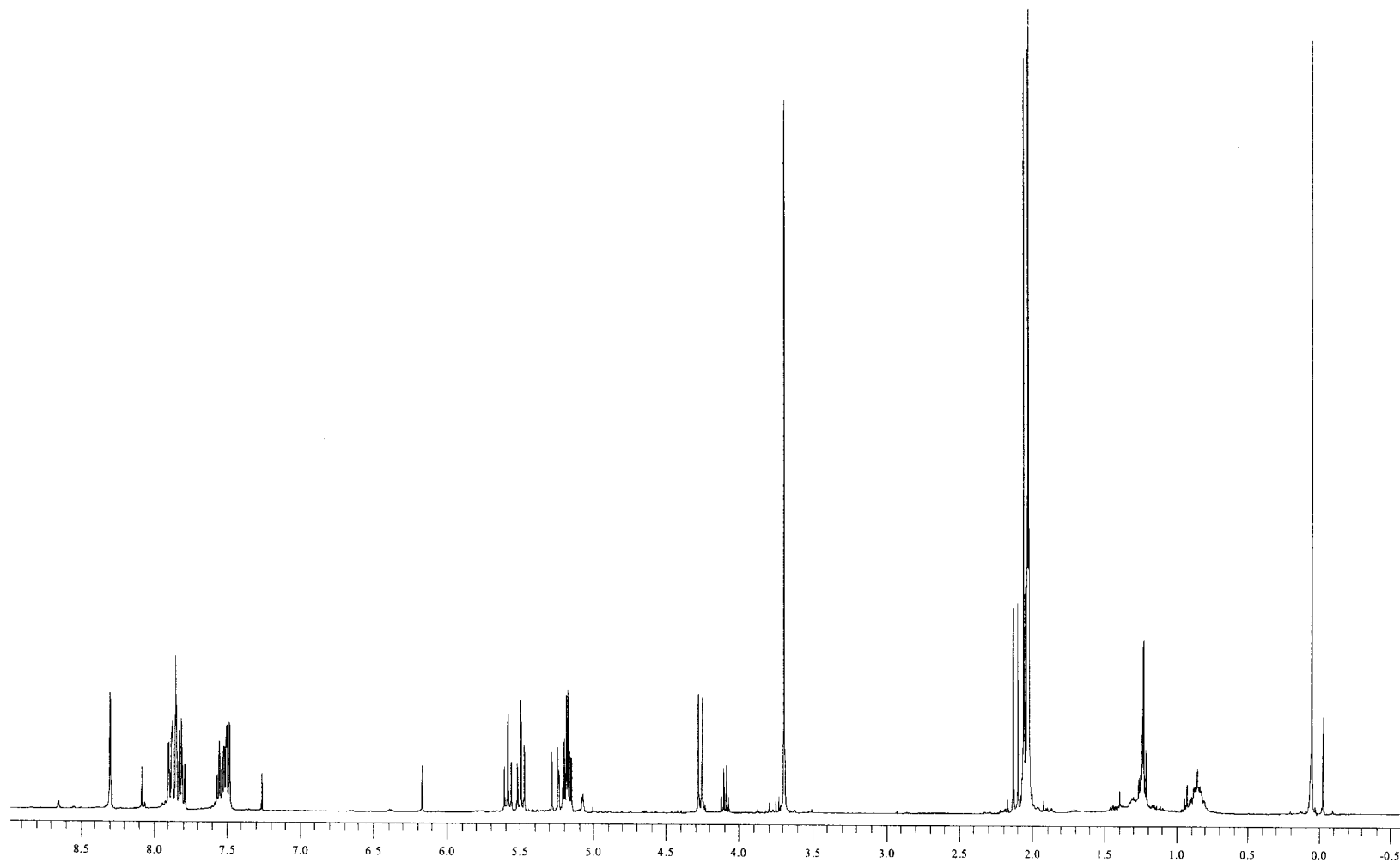
Figure 58: 400 MHz ^{1}H NMR spectrum of 2-naphthoic acid-β-D-glucopyranuronosyl amide **26**.
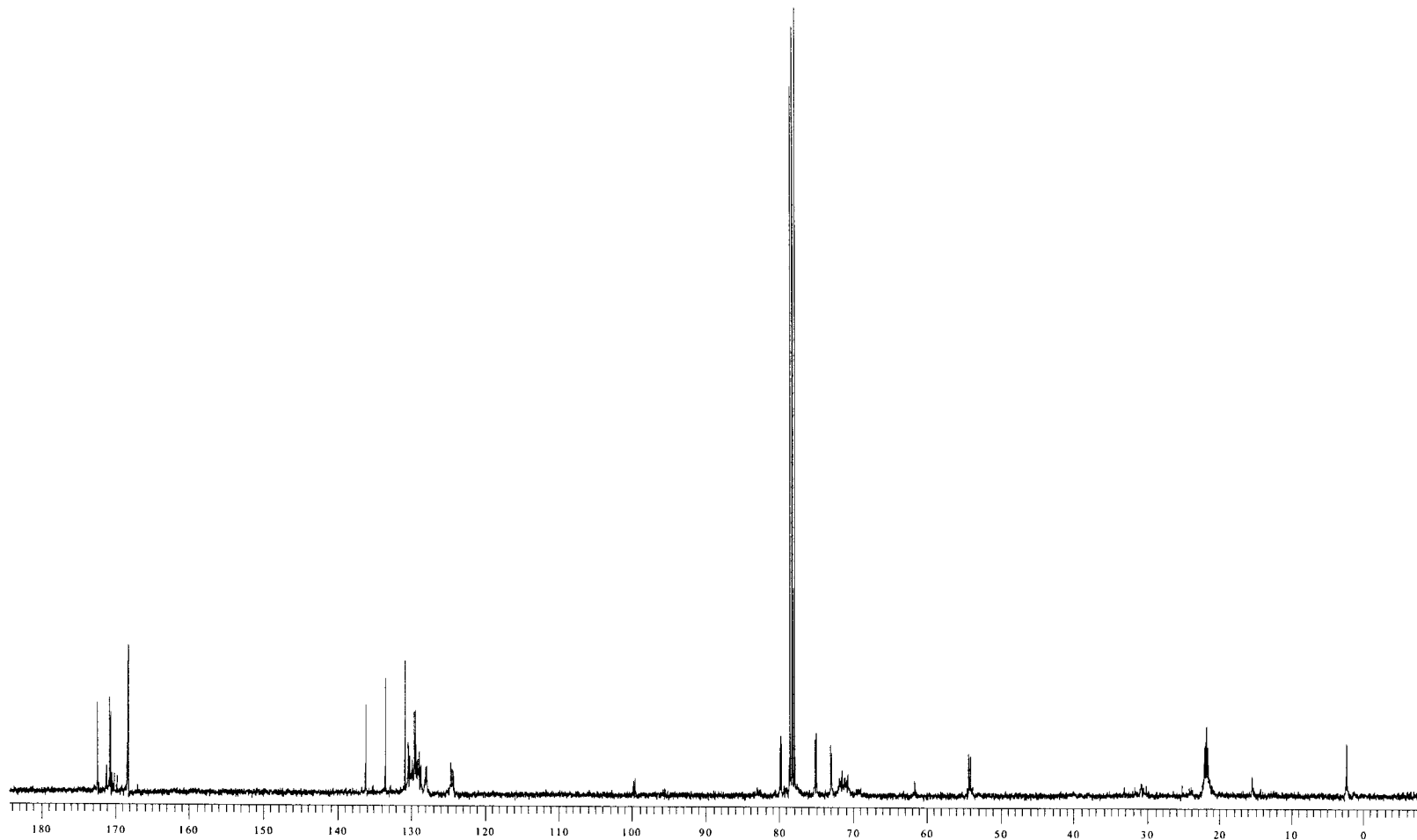
Figure 59: 100 MHz ^{13}C NMR spectrum of 2-naphthoic acid-β-D-glucopyranuronosyl amide **26**.
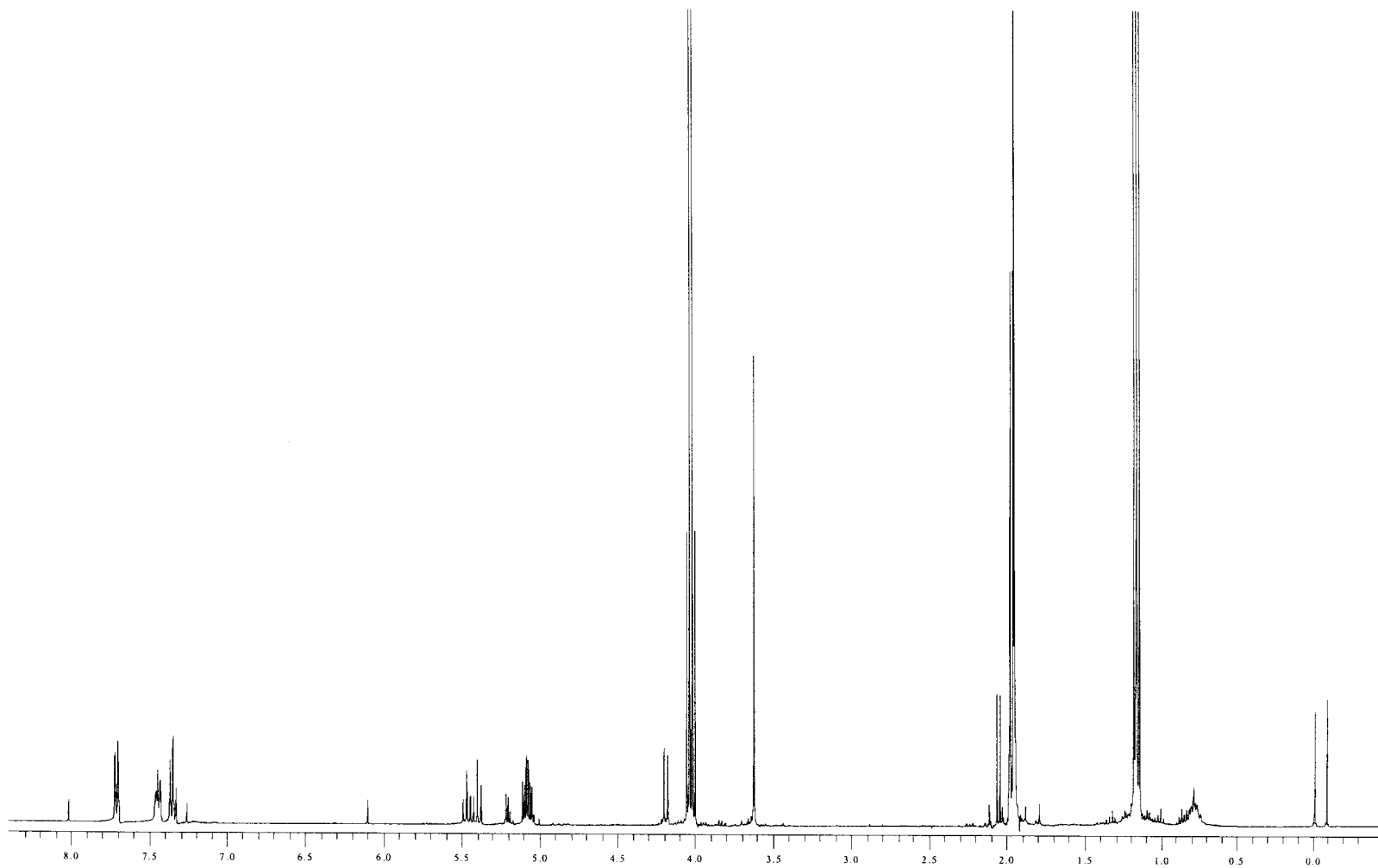
Figure 60: 400 MHz ^{1}H NMR spectrum of benzoic acid-β-D-glucopyranuronosyl amide **27** (contaminated with ethyl acetate).
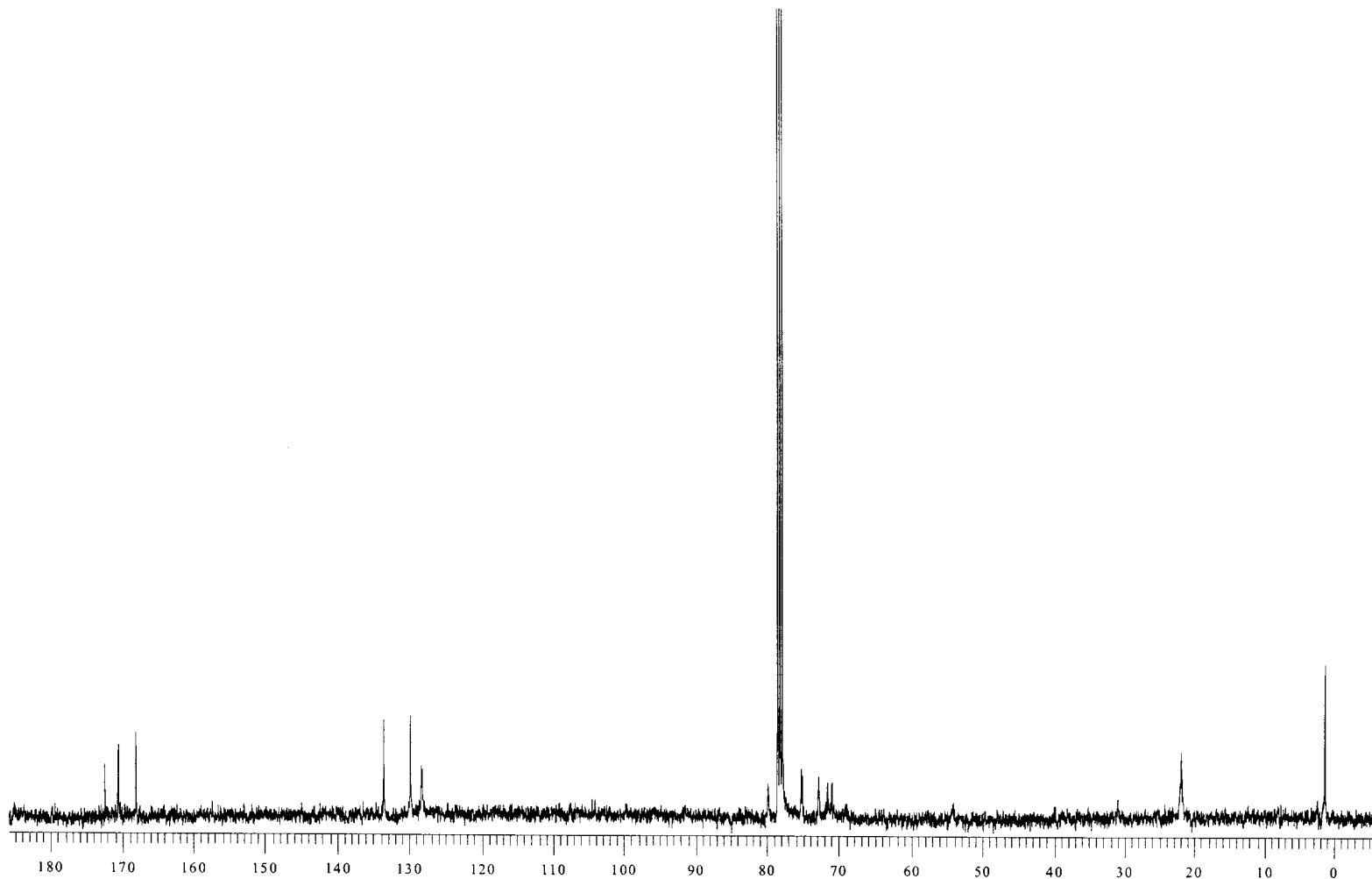
Figure 61: 100 MHz ^{13}C NMR spectrum of benzoic acid-β-D-glucopyranuronosyl amide **27**.

Display Report

Analysis Info:

File: D:\DATA\YURI\4-089400.D   Printed: Tue Apr 29 10:40:23 2003
Date acquired:
Instrument: Operator :
Task   :
Method   :   Sample   :

Acquisition Parameter:

Source   :   Polarity :
Mode   :
CapExit   :   Skim 1   :
Scan Range: Trap Drive:
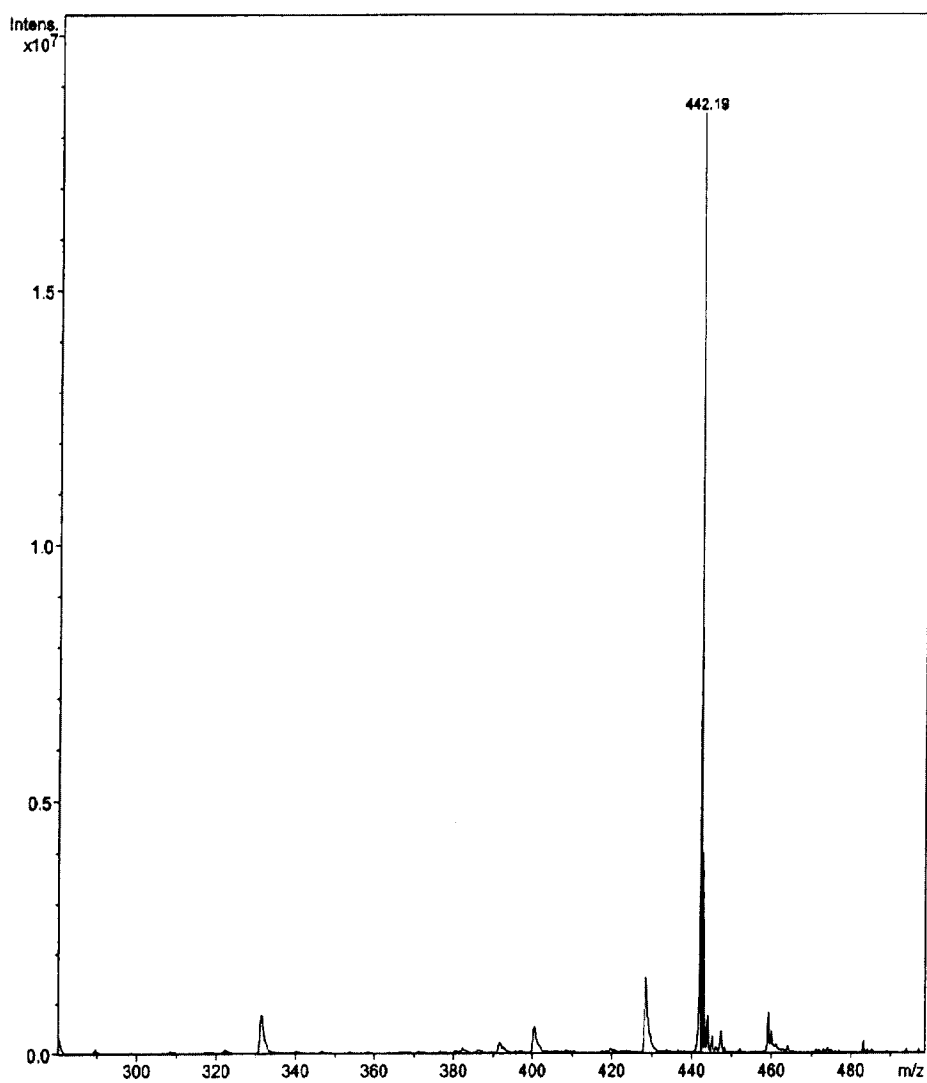Accum.time: Summation :
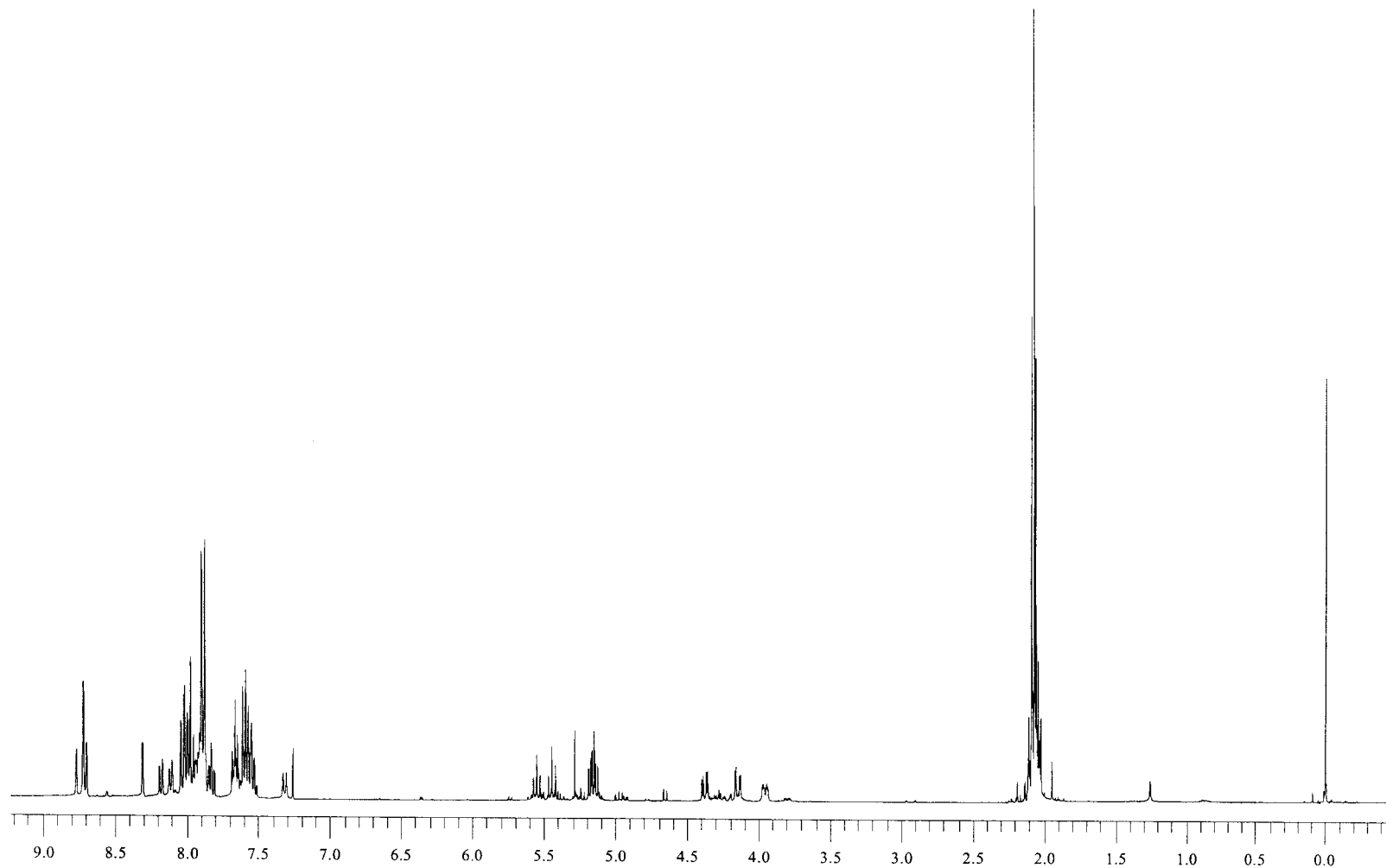MS/MS   :
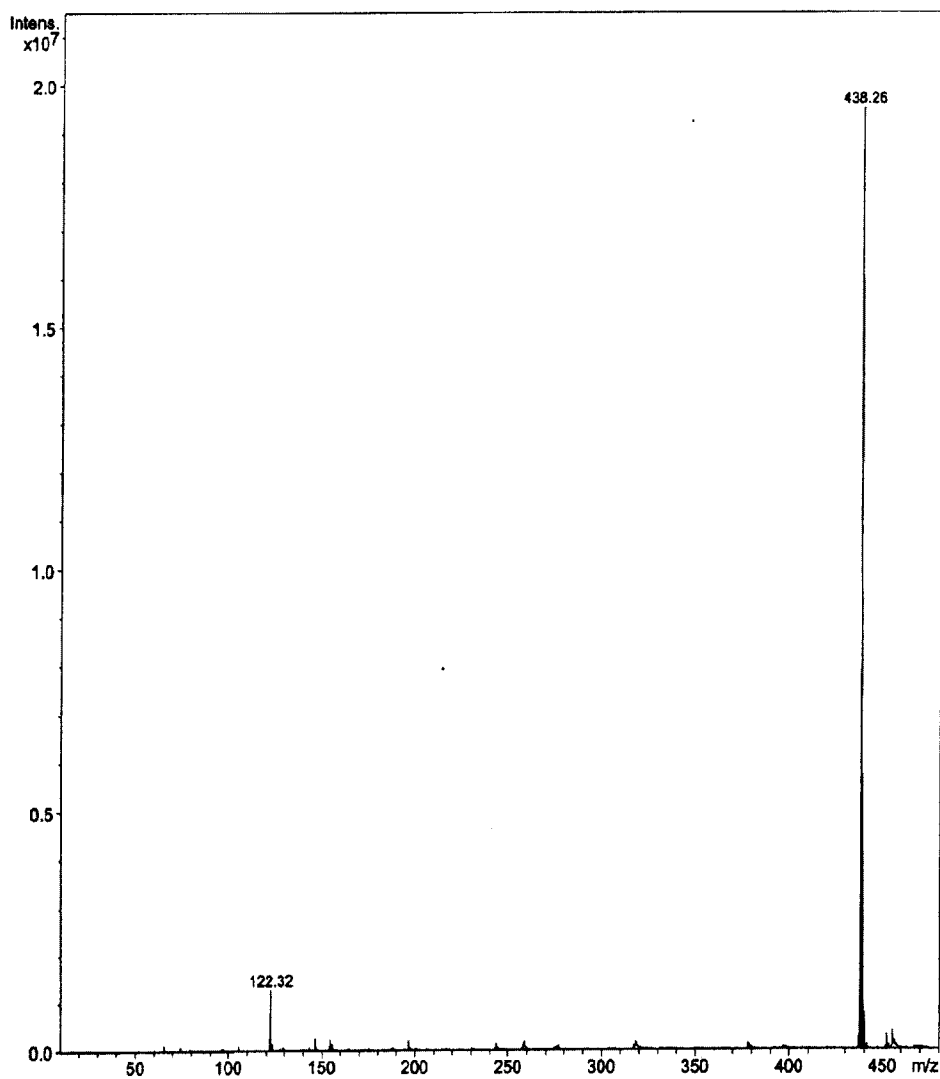
Figure 62: Mass spectrum of benzoic acid-β-D-glucopyranuronosyl amide 27.
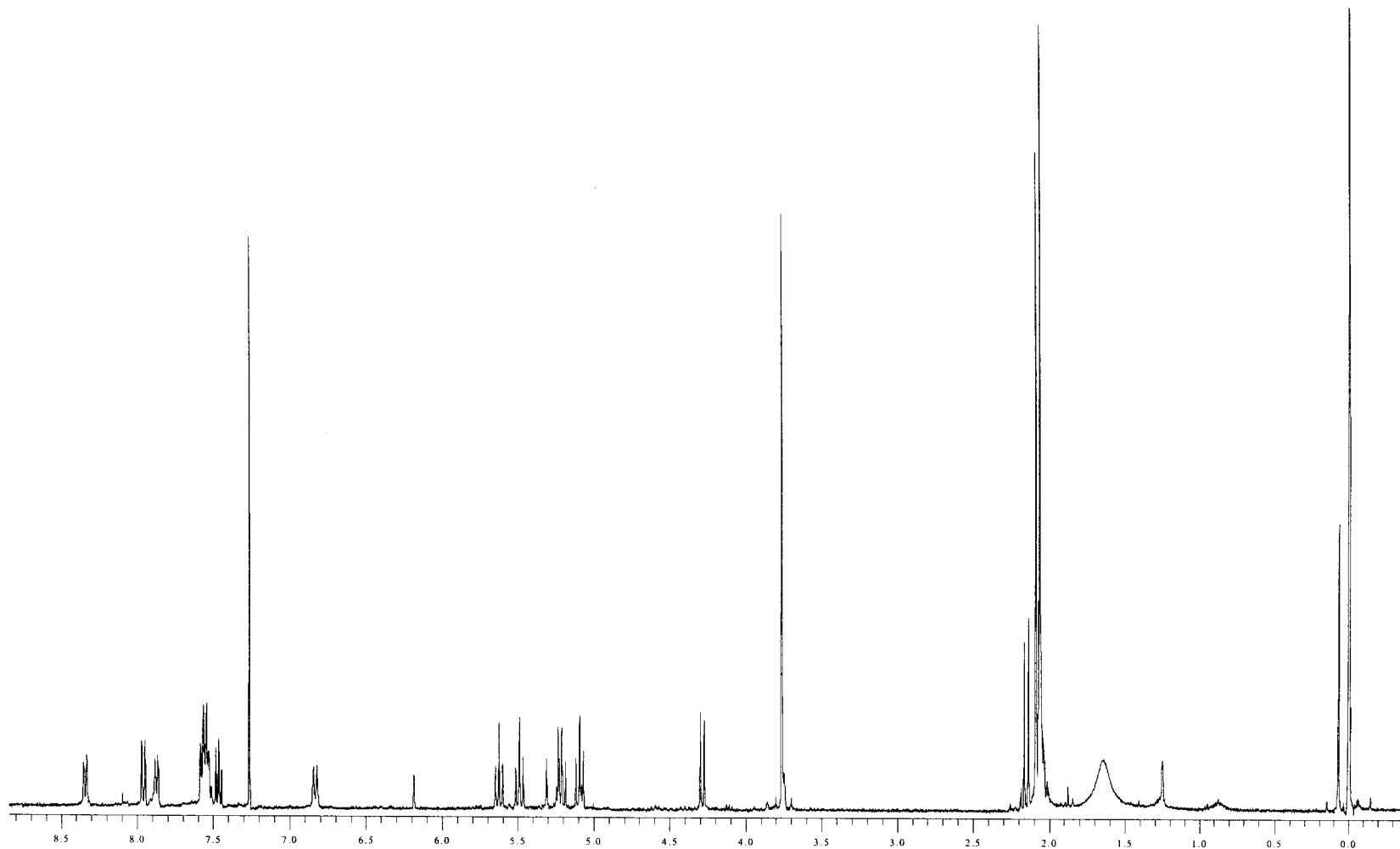
Figure 63: 400 MHz ^{1}H NMR spectrum of 1-naphthoic acid-β-D-glucopyranuronosyl amide **28**.
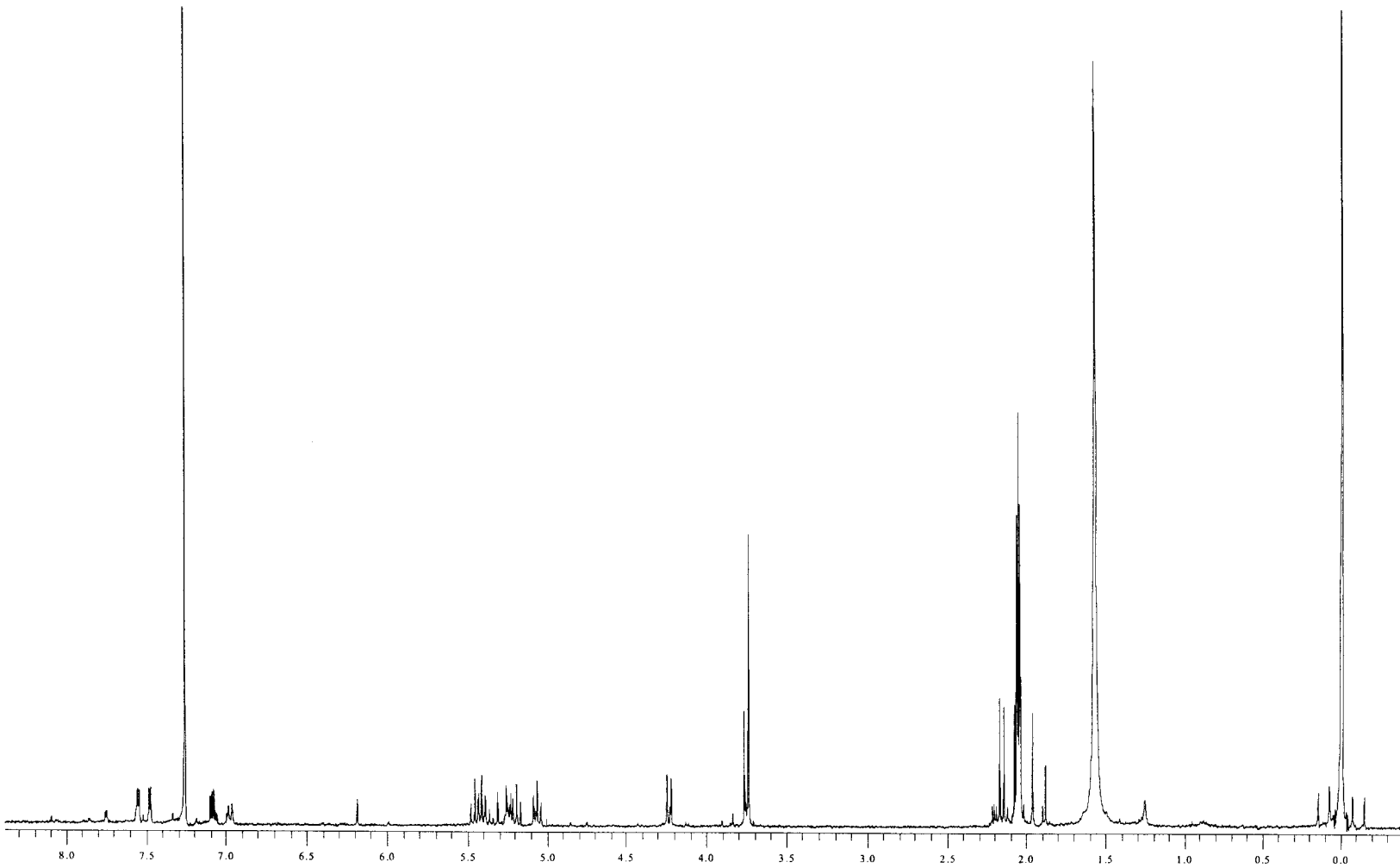
Figure 64: 400 MHz ^{1}H NMR spectrum of 2-thiophene carboxylic acid-β-D-glucopyranuronosyl amide **29**.
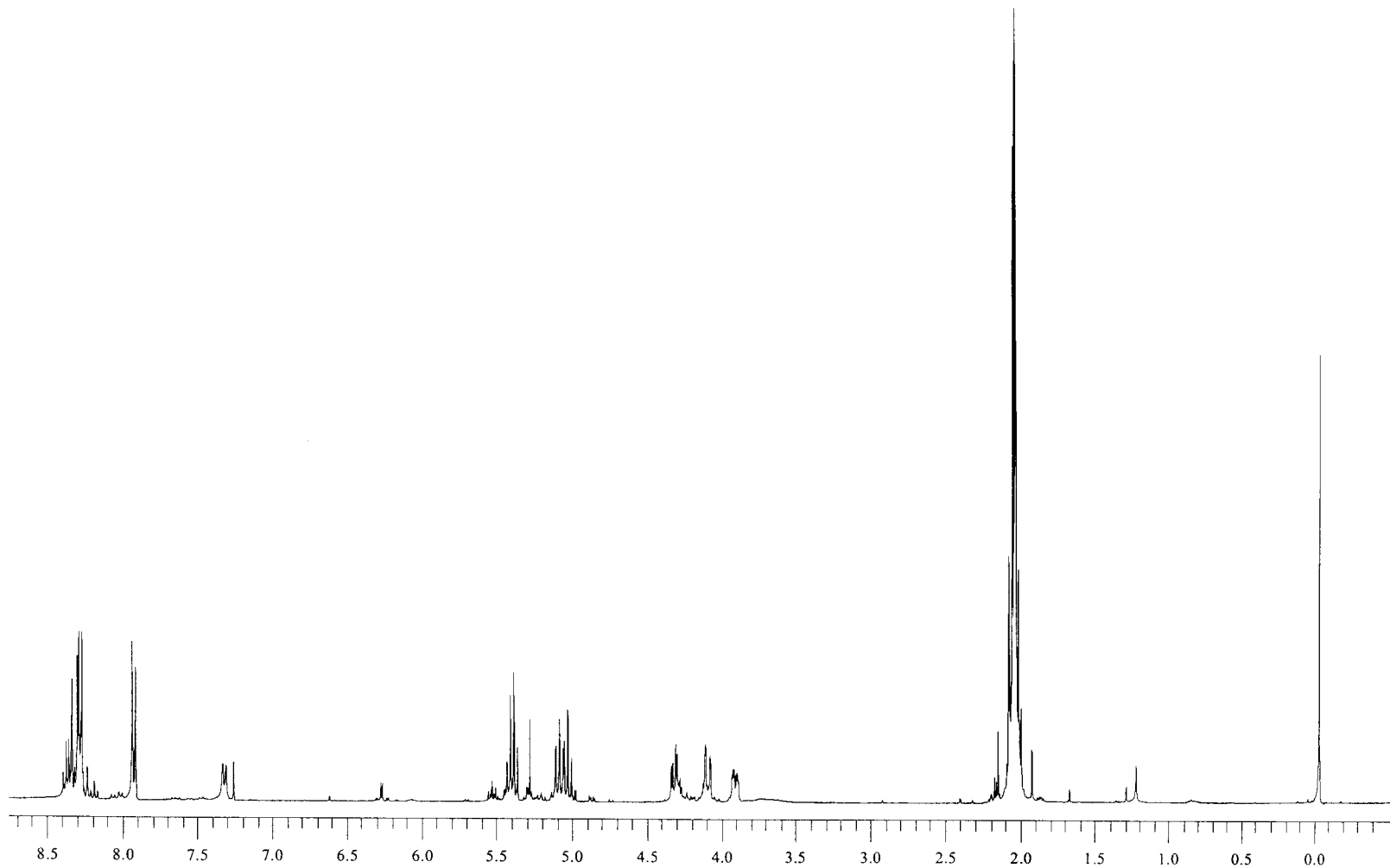
Figure 65: 400 MHz ^{1}H NMR spectrum of *p*-nitrobenzoic acid-β-D-glucopyranosyl amide **30**.

Display Report
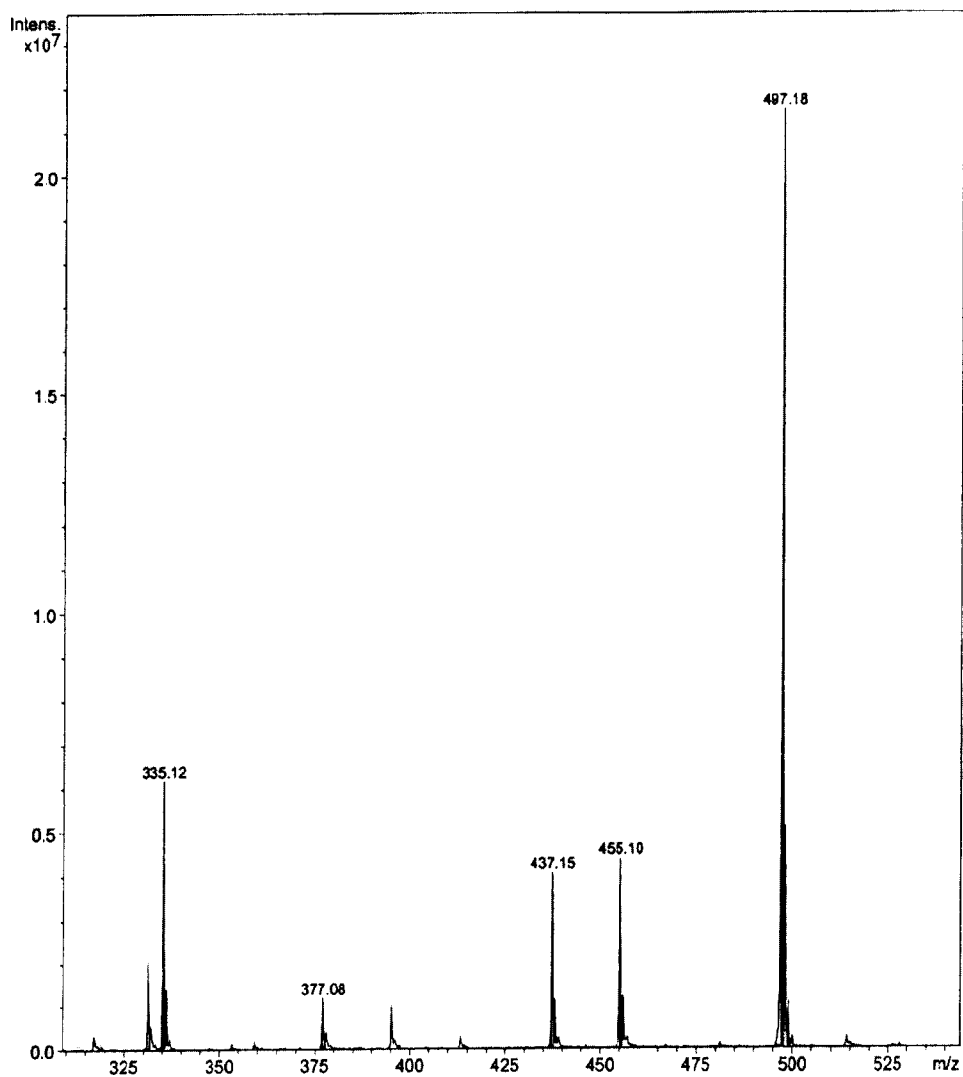
Figure 66: Mass spectrum of *p*-nitrobenzoic acid-β-D-glucopyranosyl amide **30**.
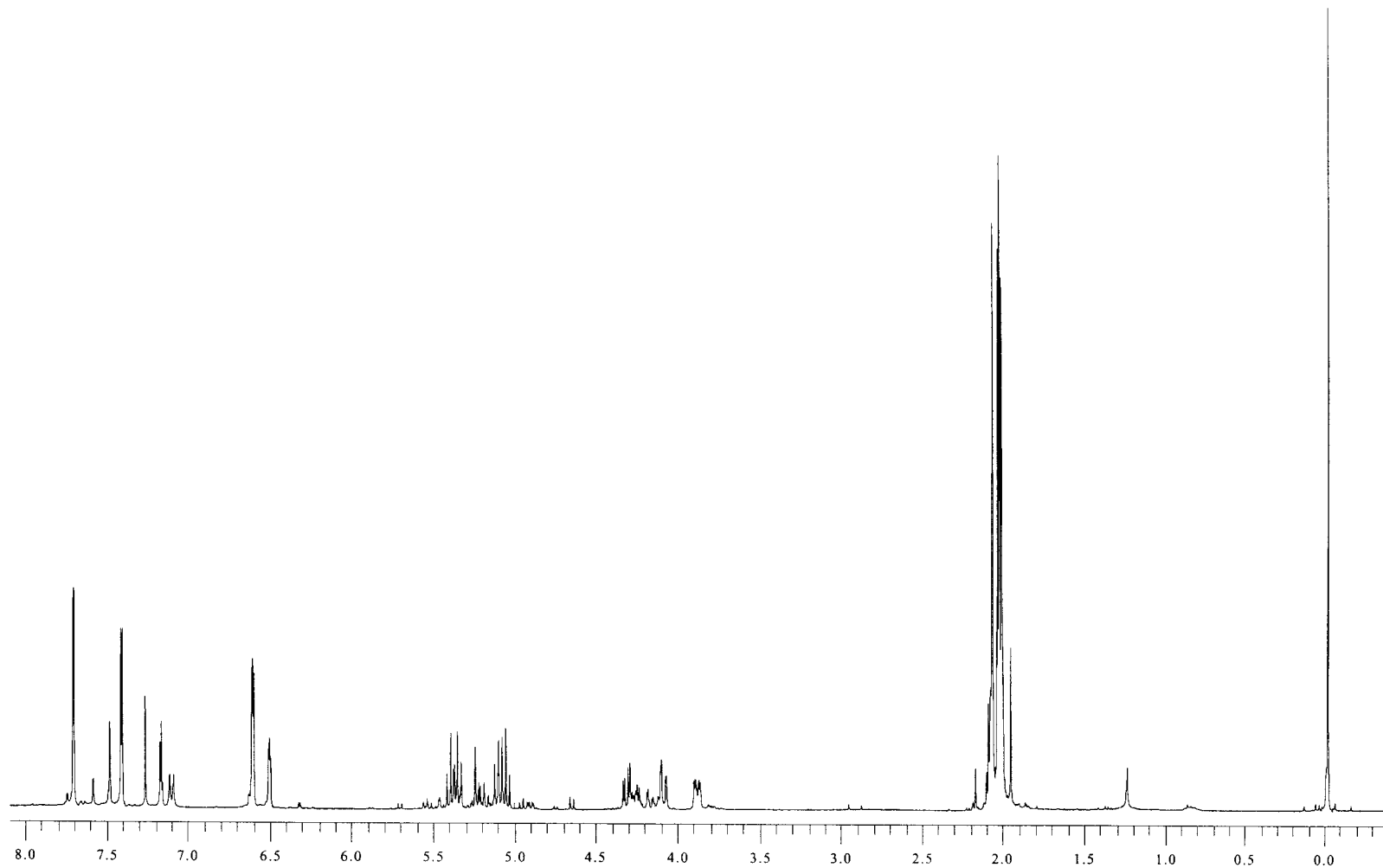
Figure 67: 400 MHz ^{1}H NMR spectrum of furan-2-carboxylic acid-β-D-glucopyranosyl amide **31**.

Display Report

Analysis Info:

File: D:\DATA\YURI\5-029200.D   Printed: Tue Apr 29 14:03:30 2003
Date acquired:
Instrument: Operator :
Task   :
Method   :   Sample   :

Acquisition Parameter:

Source   :   Polarity :
Mode   :
CapExit   :   Skim 1   :
Scan Range: Trap Drive:
Accum.time: Summation :
MS/MS   :

Intens.
x10⁷

442.19

1.5

1.0

0.5

0.0

300   320   340   360   380   400   420   440   460   480   m/z

Figure 68: Mass spectrum of furan-2-carboxylic acid-β-D-glucopyranosyl amide 31.

Figure 69: 400 MHz ^{1}H NMR spectrum of 2-naphthoic acid-β-D-glucopyranuronosyl amide **32**.
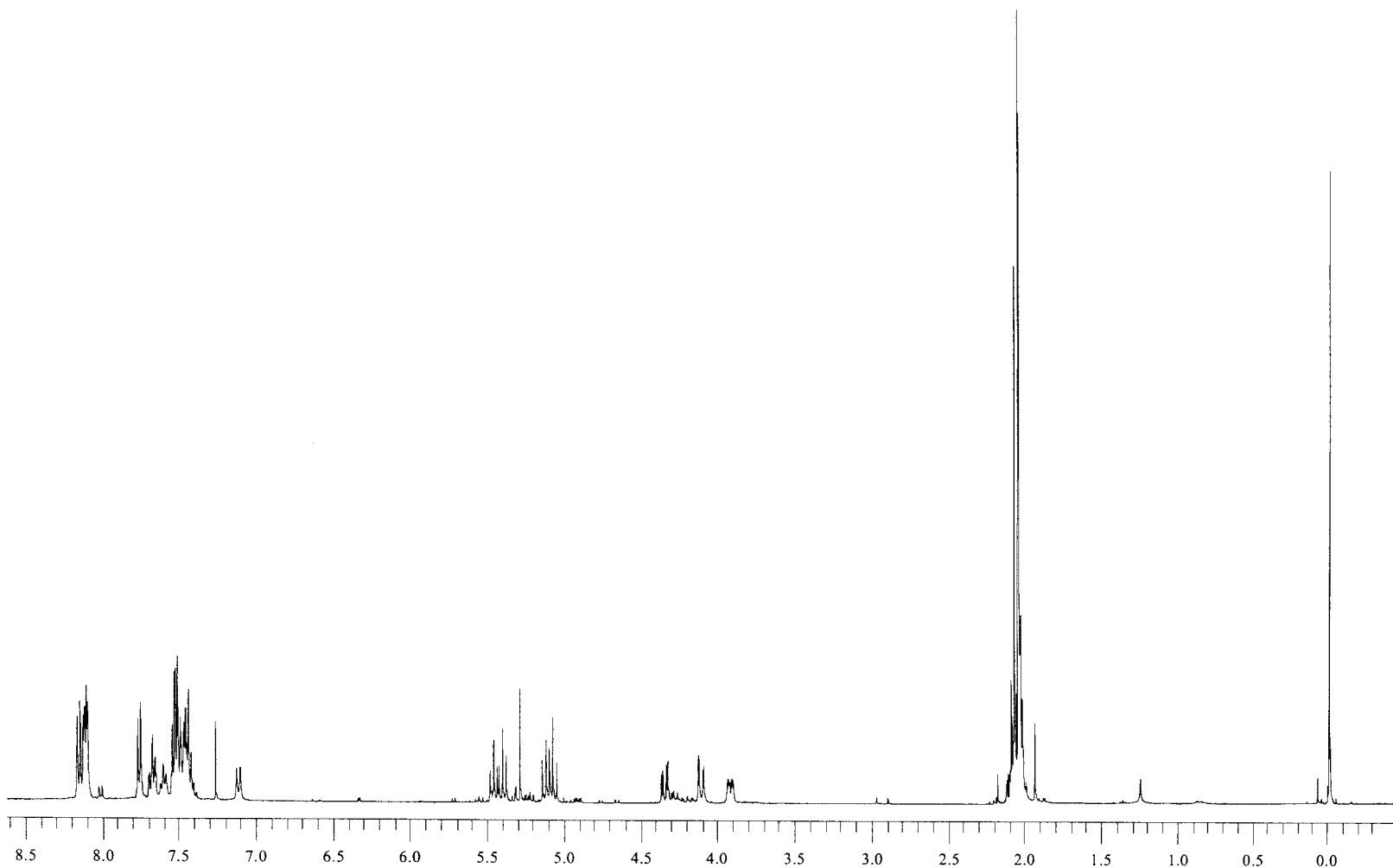
Figure 70: 400 MHz ^{1}H NMR spectrum of benzoic acid-β-D-glucopyranosyl amide **33**.

Display Report
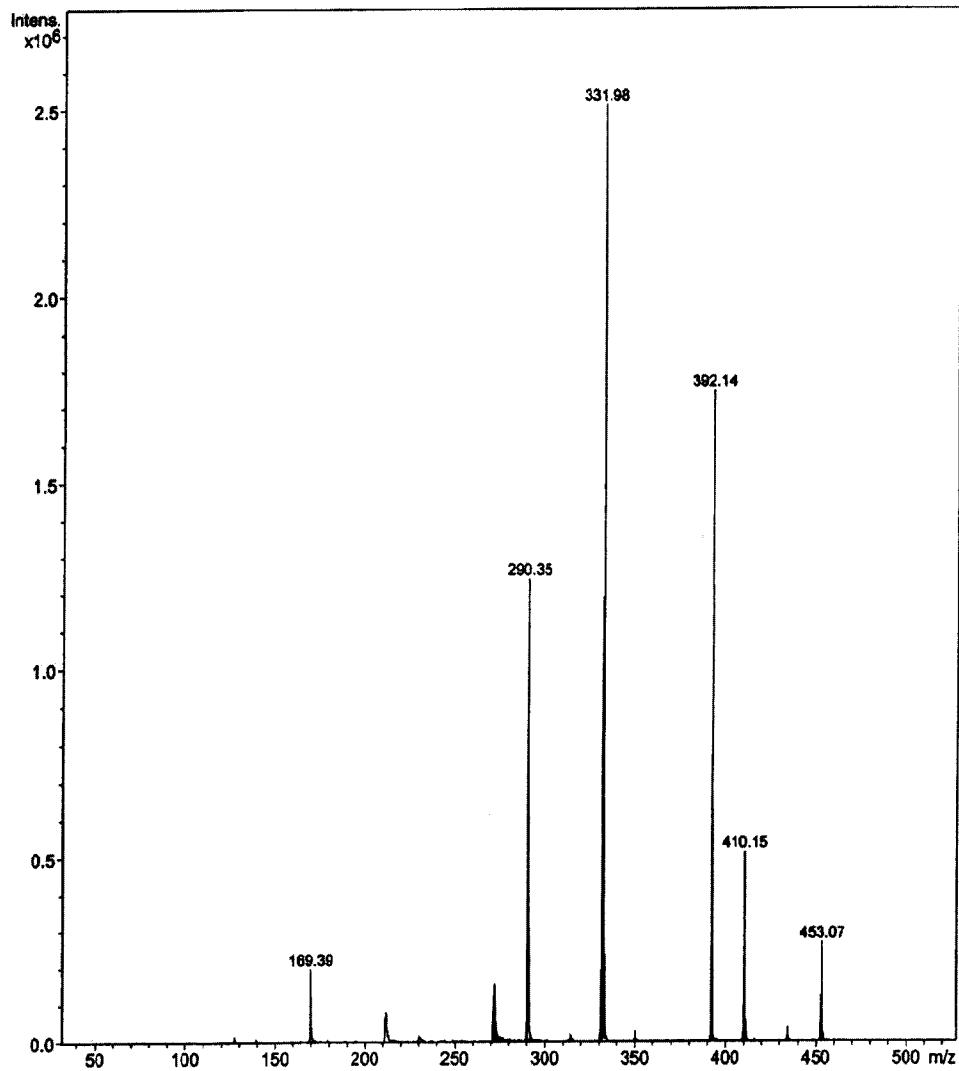
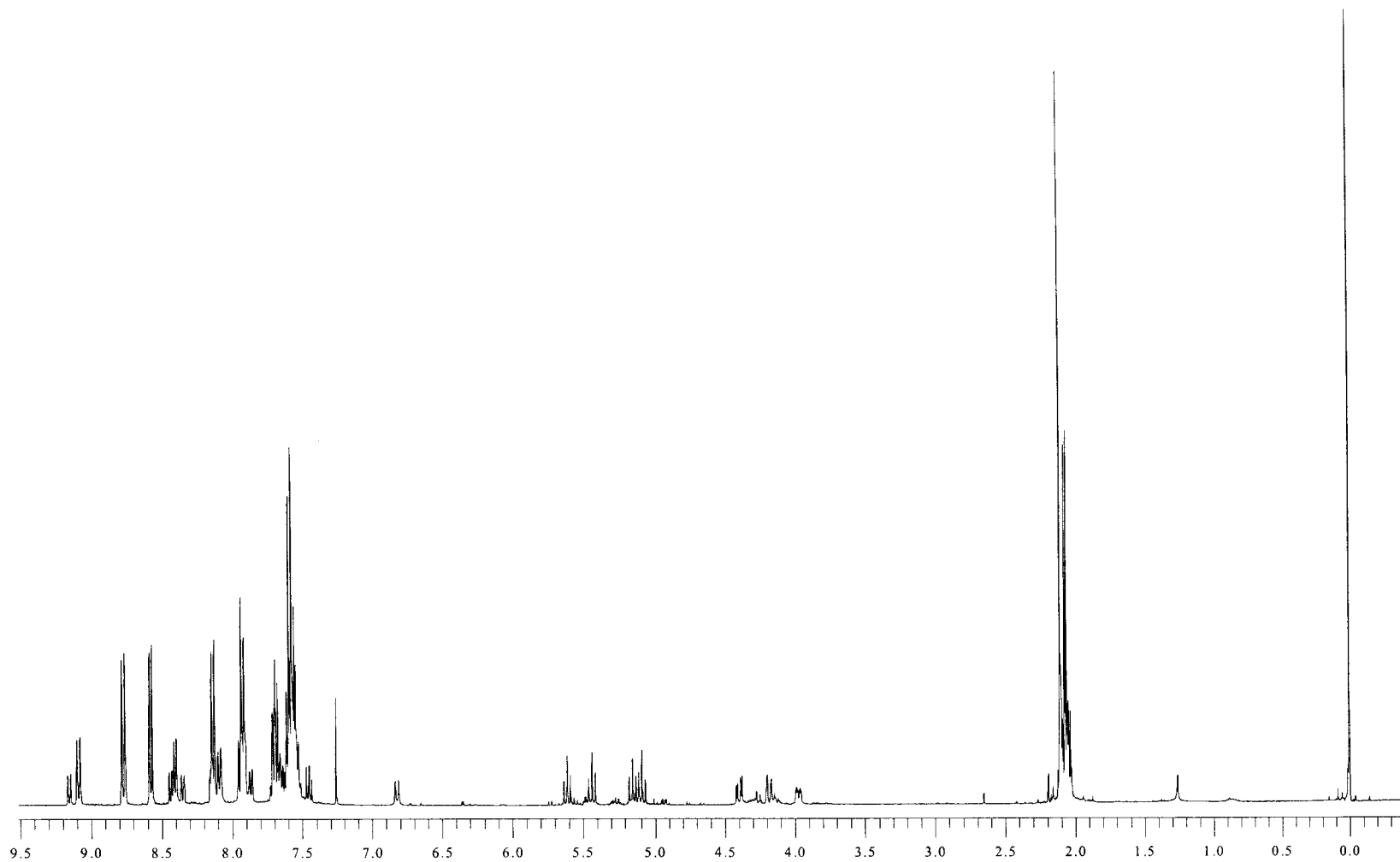Figure 71: Mass spectrum of benzoic acid-β-D-glucopyranosyl amide 33.

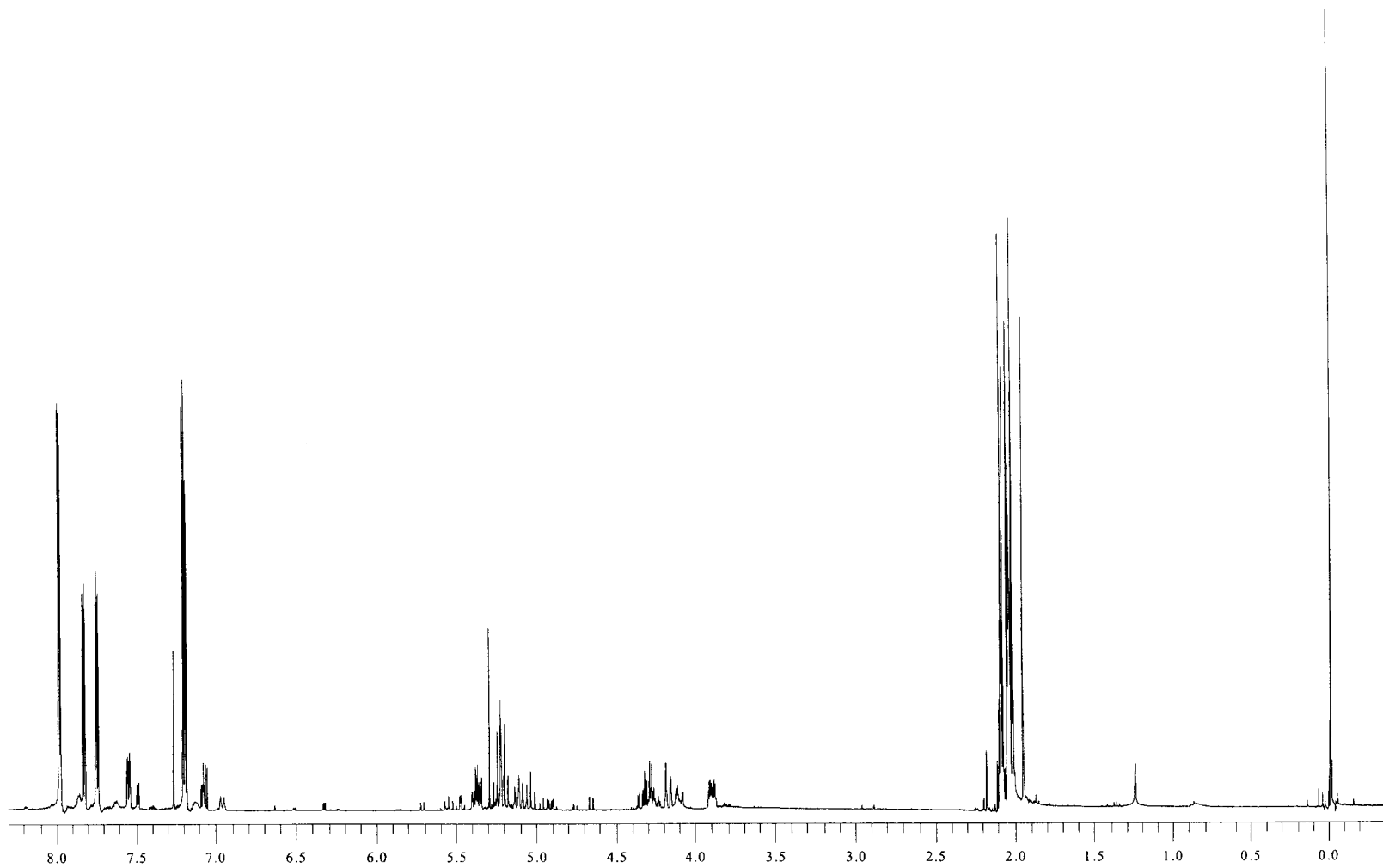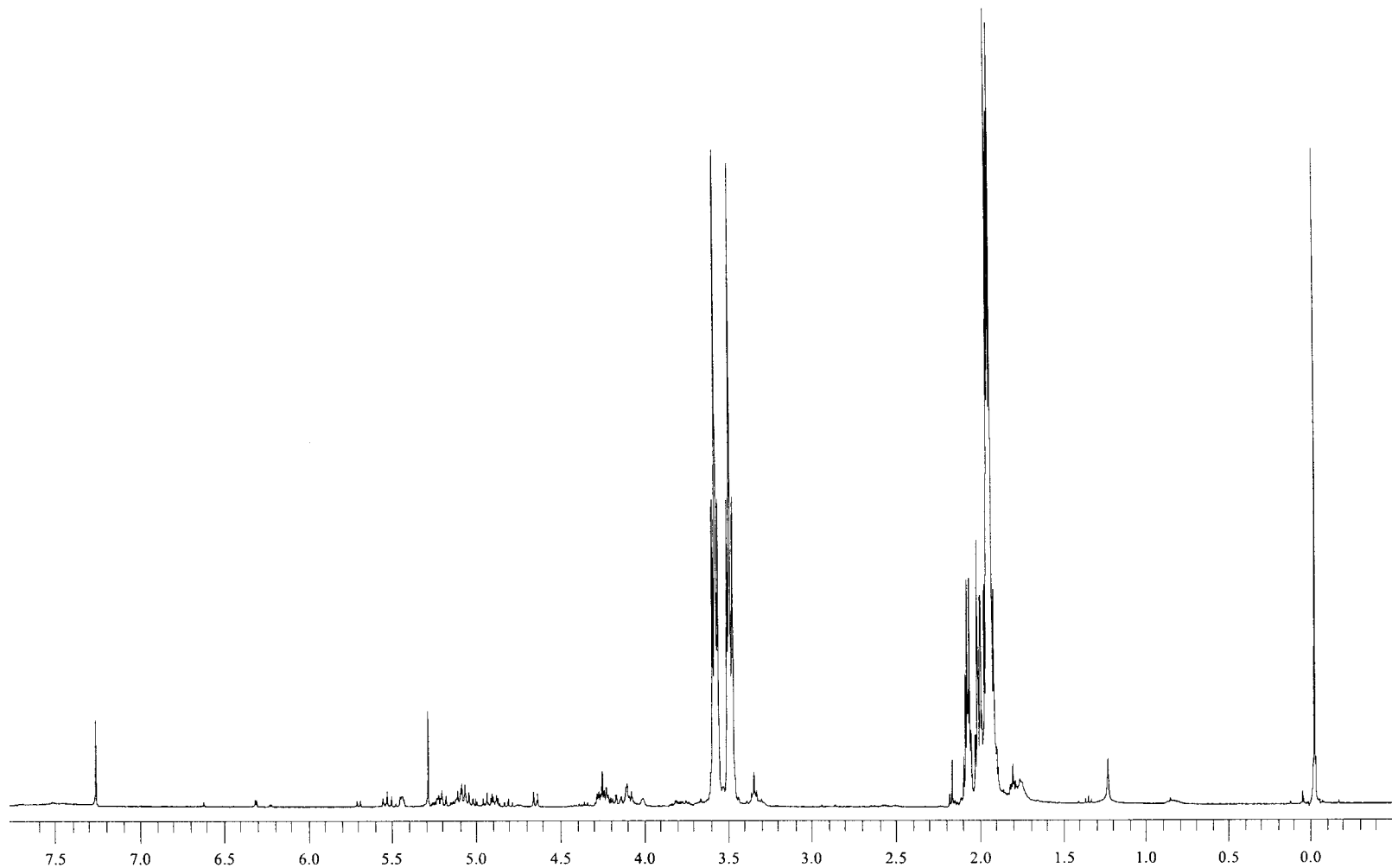**Figure 72:** 400 MHz ^{1}H NMR spectrum of 1-naphthoic acid-β-D-glucopyranosyl amide **34**.

Figure 73: 400 MHz ^{1}H NMR spectrum of thiophene-2-carboxylic acid-β-D-glucopyranosyl amide **35**.

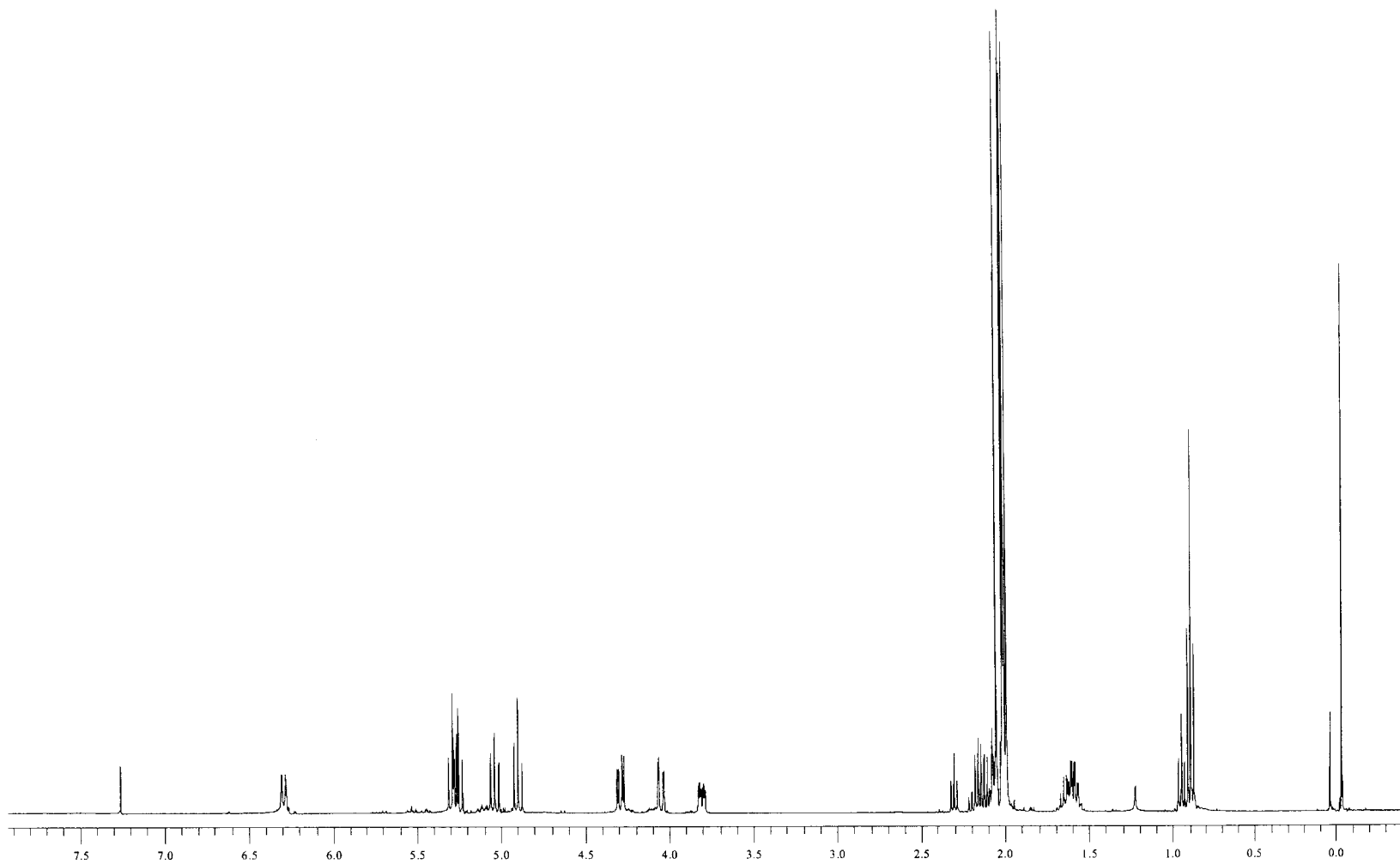**Figure 74:** 400 MHz ^{1}H NMR spectrum of crude reaction mixture from the attempted synthesis of amide **36**.

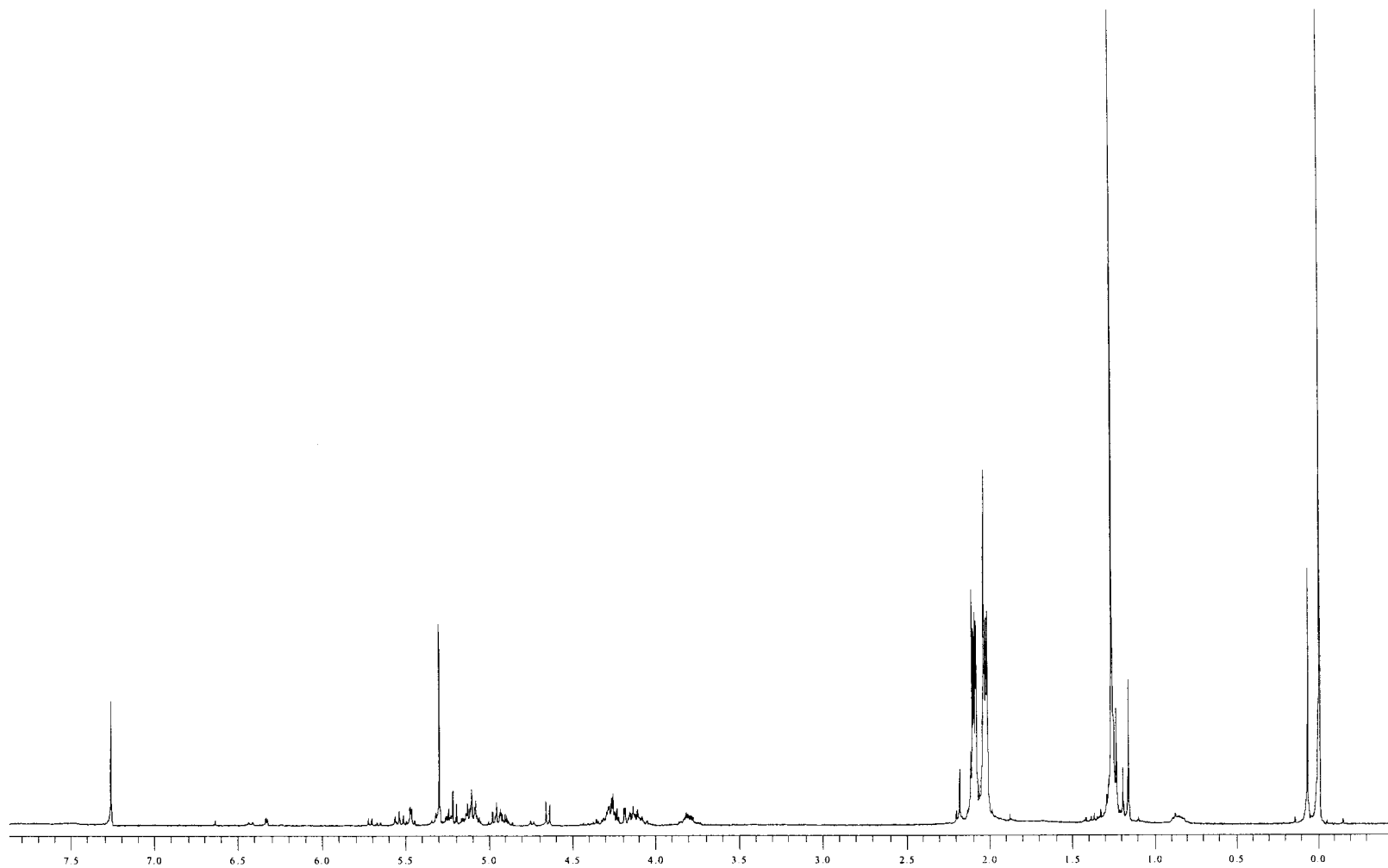**Figure 75:** 400 MHz ^{1}H NMR spectrum of butyric acid-β-D-glucopyranosyl amide **37**.

Figure 76: 400 MHz ^{1}H NMR spectrum of crude reaction mixture in the synthesis of β-D-glucopyranosyl amide **38**.
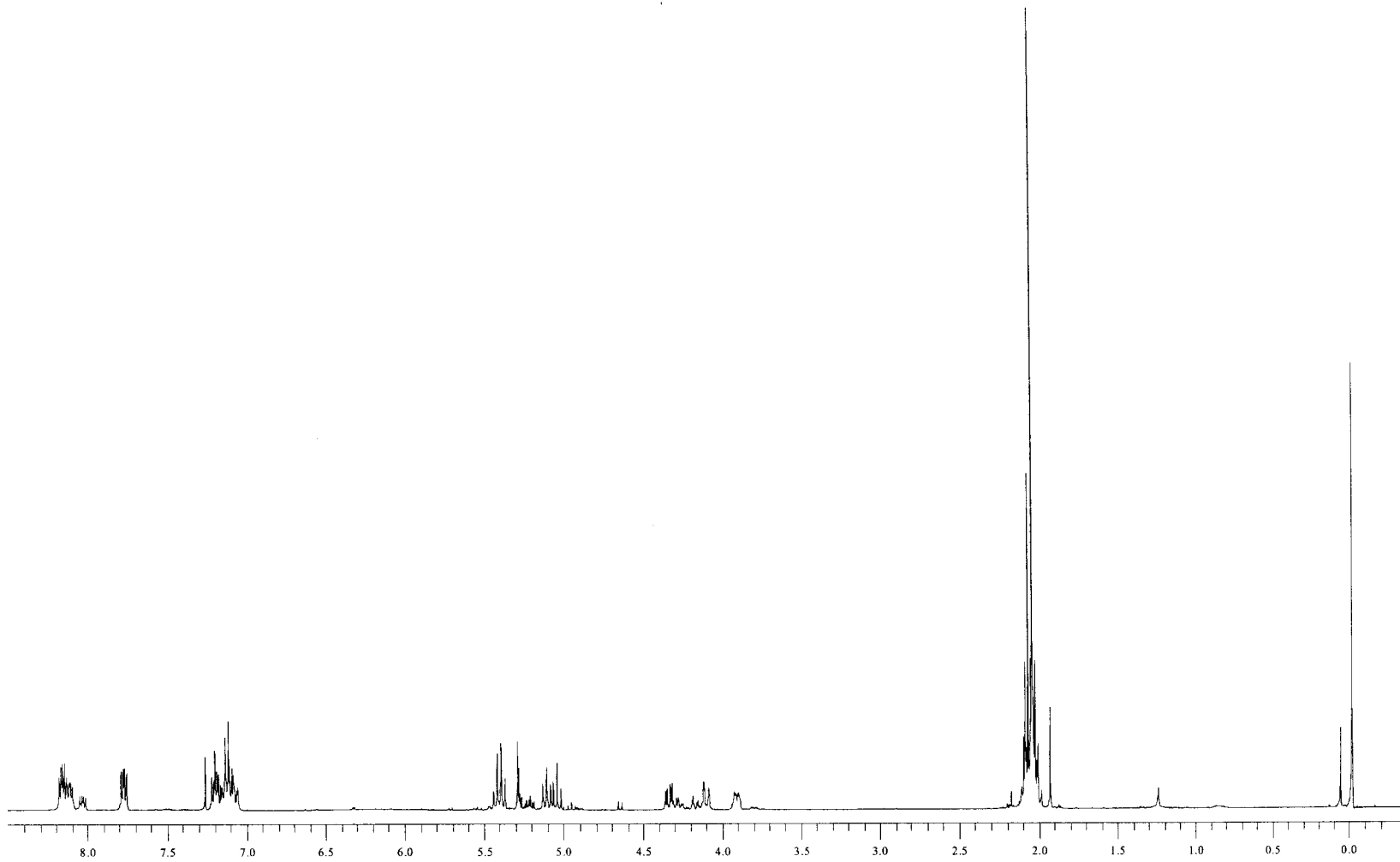
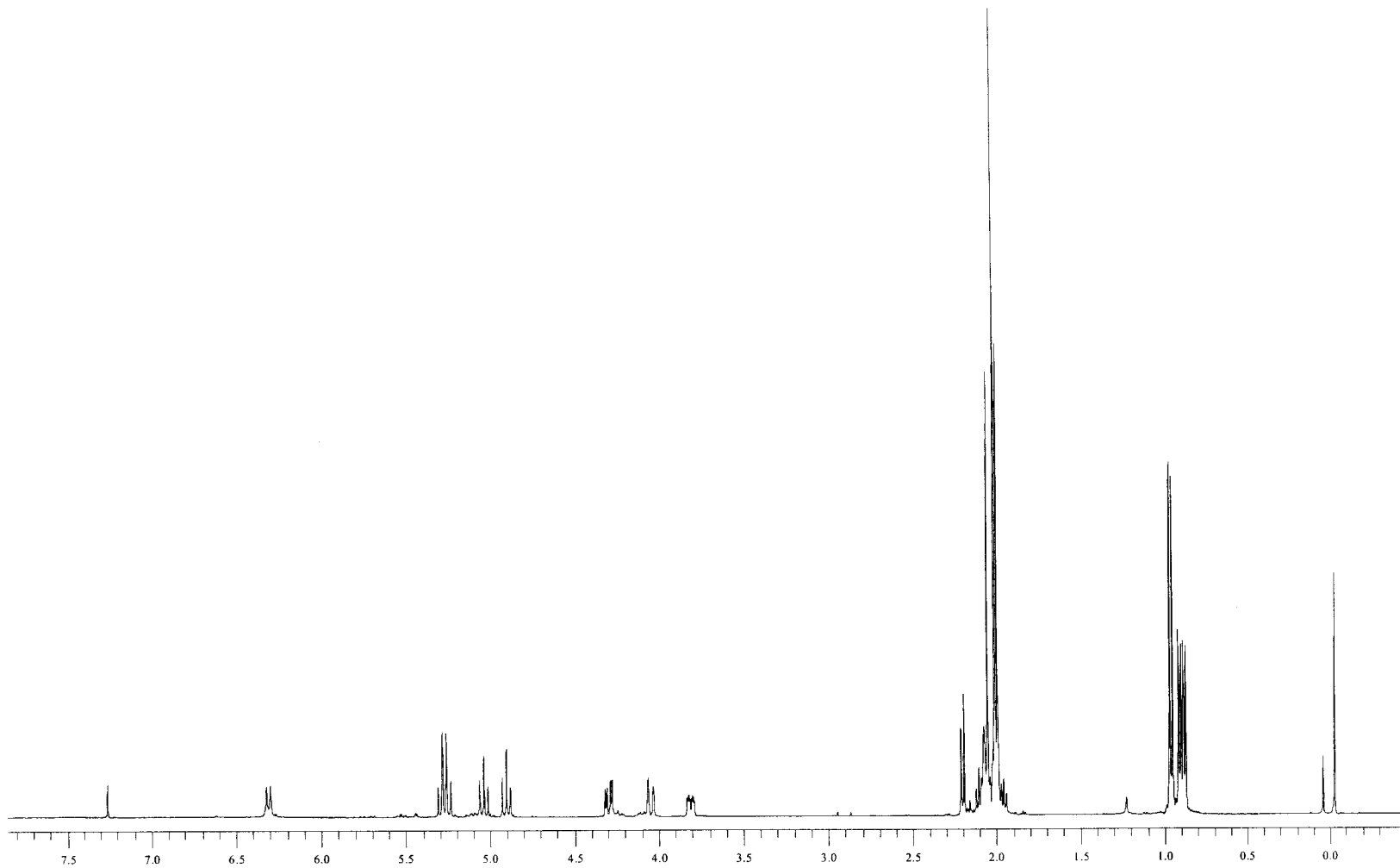**Figure 77:** 400 MHz ^{1}H NMR spectrum of 4-fluorobenzoic acid-β-D-glucopyranosyl amide **39**.

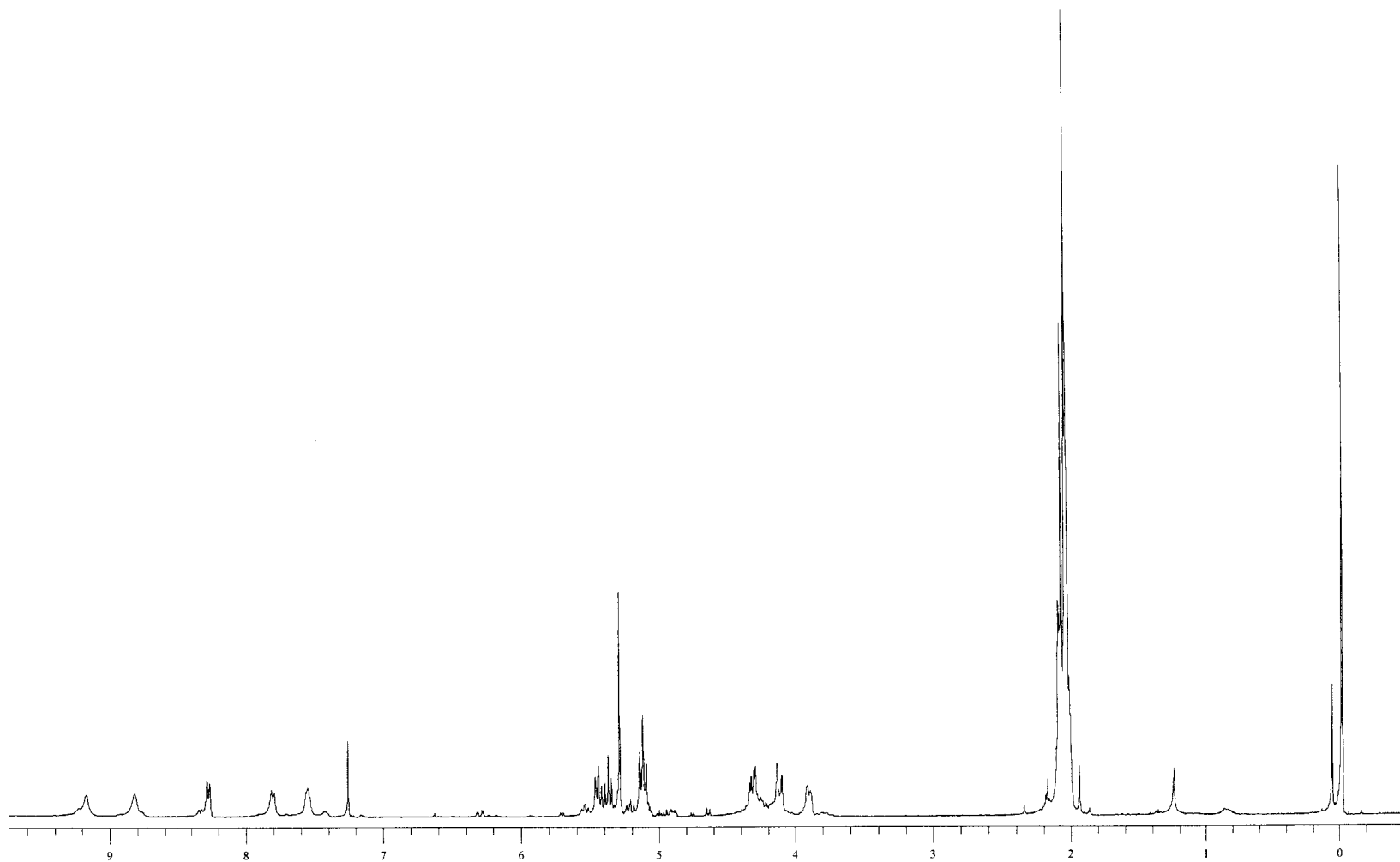**Figure 78:** 400 MHz ^{1}H NMR spectrum of isovaleroic acid-β-D-glucopyranosyl amide **40**.

Figure 79: 400 MHz ^{1}H NMR spectrum of nicotinic acid-β-D-glucopyranosyl amide **41**.